Microbially Induced Calcite Precipitation via Microbial Organic Acid Oxidation

Trent A. Shepherd

A thesis

submitted in partial fulfillment of the
requirements for the degree of

Master of Science in Civil Engineering

University of Washington

2023

Committee:
Michael G. Gomez
Brett W. Maurer

Program Authorized to Offer Degree:
Civil and Environmental Engineering

University of Washington

Abstract

Microbially Induced Calcite Precipitation via Microbial Organic Acid Oxidation

Trent A. Shepherd

Chair of the Supervisory Committee:

Michael G. Gomez

Civil and Environmental Engineering

Microbially Induced Calcite Precipitation (MICP) or biocementation can improve the engineering properties of granular soils through the precipitation of calcium carbonate minerals on particle contacts and surfaces. The process has received significant research attention for a variety of different geotechnical applications including the mitigation of earthquake-induced soil liquefaction and surficial soil stabilization. Although most commonly this process is accomplished using microbial urea hydrolysis, other microbial metabolic pathways can be used to enable biocementation with the potential to eliminate the generation of ammonium by-products. Microbial organic acid oxidation (MOAO) presents one alternative pathway by which increases in solution carbonate species can be generated to enable calcium carbonate mineral formation. While past studies have considered the potential of this particular microbial pathway to enable biocementation for surficial applications, to-date few studies have investigated the feasibility of this pathway towards addressing deeper subsurface geotechnical applications wherein oxygen is

more limited. In this study, small-scale batch and centimeter-scale column experiments were employed to explore the ability of microbial organic acid oxidation to enable biocementation soil improvement under conditions more representative of subsurface locations. Experiments investigated the potential of both microbial acetate and citrate oxidation to mediate biocementation as well as the effect of differences in treatment techniques including the methods used to supply dissolved oxygen, differences in solution compositions including the effect of supplied growth factors and bicarbonate salt additions, and differences treatment injection sequences. Results suggest that indigenous microorganisms can be enriched in natural sands to oxidize organic acids in the presence of calcium and bicarbonate salts under specific treatment conditions, thereby enabling the precipitation of calcium carbonate and other mineral by-products, with consequential increases in shear wave velocity. However, oxygen availability and solution bicarbonate additions may be a critical factor governing process success, with the contribution of abiotic precipitation mechanisms meriting further investigation.

ACKNOWLEDGEMENTS

First, I would like to thank my advisor, Dr. Michael G. Gomez. I consider myself very fortunate to have had such a thoughtful and diligent advisor. His knowledge and dedication to his field of study is truly inspiring to me and I am grateful to have the opportunity to be a member of his lab group. I would also like to thank Dr. Brett Maurer for his role in my thesis supervisory committee and for his guidance throughout my time here. In my search for a graduate school, he was my first point of contact from the school, and I owe him a debt of gratitude for introducing me to the University of Washington.

I would also like to thank Dr. Pedro Arduino for his mentorship. His passion and mastery of teaching will continue to inspire me for years to come. I am also grateful to all my professors in the geotechnical department for all their work and dedication in passing on their knowledge to students like me.

I would like to thank all my current and former lab colleagues and friends including Dellen Behrend, Andrea Mattson, Kelly Hillard, and Erick Martinez who have helped me immensely during my time here. I would like to especially thank Bruna Ribeiro and Dr. Minyong Lee for their daily guidance and patience as I learned the skills necessary to become an experimental researcher. I am forever grateful for their knowledge and friendship. I would also like to thank all the graduate and undergraduate students I have come to know for friendship. A special thank you to all the students whom I instructed during my time as a teaching assistant. I am grateful for their kindness and patience as I learned the skill and responsibility of passing on knowledge to others.

Lastly, I would like to thank all my friends and family for their love and support. Their emotional support gave me the strength to travel to the other side of the country and their pride in me inspires me every day to be the best engineer I can be.

Finally, I am grateful to the University of Washington and the National Science Foundation for the funding provided for this research. Specially funding and collaboration made possible by the National Science Foundation Grant ECI-2045058 and the Engineering Research Center Program of the National Science Foundation under NSF Cooperative Agreement No. EEC-1449501. Presented SEM images were made possible by the Molecular Analysis Facility, a National Nanotechnology Coordinated Infrastructure site at the University of Washington that is supported in part by the National Science Foundation Grants NNCI-1542101 and NNCI-2025489, the University of Washington, the Molecular Engineering & Science Institute, and the Clean Energy Institute. Any opinions, findings, conclusions, or recommendations expressed in this document are those of the author and do not necessarily reflect the views of the National Science Foundation or other funding sources.

TABLE OF CONTENTS

LIST OF FIGURES

LIST OF TABLES

Chapter 1: INTRODUCTION

While advancements in and diversification of ground improvement techniques has continued to advance over time, each strategy still presents unique advantages and disadvantages, including factors such as methodology, cost, environmental impact, and site accessibility (DeJong et. al. 2006). Growing awareness of the environmental impacts associated with traditional methods, including greenhouse gas emissions and the potential for subsurface groundwater and soil contamination, has encouraged research into innovative approaches that can improve soil with sustainable outcomes (DeJong et. al. 2013). Microbially induced calcite precipitation (MICP) or biocementation is one such strategy that can improve the properties of granular soils by utilizing native bacteria to precipitate calcium carbonate ($CaCO_3$) minerals (Stocks-Fisher et. al 1999). Biocementation can provide an alternative process for a wide range of geotechnical and structural applications including slope stability improvement, earthquake-induced liquefaction mitigation, self-healing concrete, dust control, and other many applications (Meyer et. al. 2011). The biocementation process is most typically mediated by ureolytic microorganisms that possess urease enzymes. In the presence of urea, these microorganisms can catalyze a hydrolysis reaction, resulting in the production of ammonia and carbonic acid, which serve as a precursor to calcium carbonate mineral formation. While urea hydrolysis is a well-studied process that significantly improves soil dynamic properties, the generation of ammonia raises environmental and human health concerns if left untreated in soils and groundwater (Lee et. al. 2019, 2023). Recent research has demonstrated that up to 98% of ammonia can be removed through the application of rinse solution injections following biocementation treatments (Lee et. al. 2019, 2023), however, alternative MICP approaches that eliminate ammonia production altogether have been more

sparsely examined, with the exception of microbial denitrification, and warrant further investigation.

This research explores the potential of an alternative biological pathway, namely the microbial oxidation of organic acids, to facilitate calcium carbonate precipitation without the generation of environmentally-concerning process byproducts such as ammonium. Similar to ureolysis, microbial organic acid oxidation (MOAO) can also produce aqueous carbonate species; however, instead of employing urea for carbonate ion production, weak organic acids like acetate or citrate are aerobically oxidized by heterotrophic bacteria. By eliminating the use of urea hydrolysis, related ammonium production can also be eliminated. While not exhaustive, this research provides insight into the feasibility of utilizing MOAO processes to mediate calcium carbonate mineral formation for subsurface geotechnical applications.

1.1 Overview of Ureolytic Biocementation

Microbially Induced Calcite Precipitation (MICP) via microbial ureolysis, or ureolytic biocementation, is an innovative ground improvement technique that utilizes ureolytic bacteria to precipitate calcium carbonate minerals and improve the mechanical properties of granular soils (Ferris et al. 1997). MICP provides an environmentally conscious alternative to traditional ground improvement strategies such as jet and permeation grouting, which oftentimes use energy-intensive materials and mechanical energy to improve soils. Fundamentally, MICP can be achieved using any biological process that can generate aqueous carbonate species in the presence of dissolved calcium (DeJong et al. 2022). While there are various microbial pathways that could be used for carbonate production, this has been most extensively mediated by microorganisms

containing the urease enzyme, which in the presence of urea, catalyze a hydrolysis reaction. This results in the production of ammonia as a byproduct and carbonic acid. When solution pH is near-neutral initially, generated ammonia can protonate to become ammonium, thereby producing hydroxide, which allows produced carbonic acid to become increasingly available as aqueous carbonate species. In the presence of sufficient aqueous calcium, aqueous carbonate production facilitates the precipitation of calcium carbonate minerals on soil particle surfaces and contacts (Lee et. al. 2019). This process has been well studied and investigations have shown that biocementation can significantly improve the engineering properties of soils through large increases in shear stiffness and shear strength (DeJong al. 2006; Gomez et. al. 2018; Gomez et. al. 201; Montoya et. al. 2015).

These improvements stem from various mechanisms, including (1) calcium carbonate bonding between particles, which can restrict soil particle movement and contractive behavior during shearing; (2) increased soil density due to the added mass of calcium carbonate precipitation, which enhances dilative behavior; and (3) calcium carbonate particle coatings, which can enhance particle surface roughness and increase interparticle frictional resistances (DeJong et al. 2010; El Kortbawi et al. 2022; and others). Biomediated calcium carbonate precipitation can be readily monitored by measuring both aqueous biogeochemical and soil mechanical and geophysical changes in treated soils (Lee et al. 2022). These measurements can include changes in aqueous calcium and urea concentrations, solution alkalinity, and solution pH in time, as well as shear wave velocity and calcium carbonate content measurements, among other metrics (DeJong et al. 2022). While ureolytic MICP is the most well-studied biological pathway and resulting improvements in engineering properties are well understood, the production of remains a significant practical

concern for the technology that should be addressed in order for MICP to offer a truly environmentally beneficial soil improvement alternative (Lee et. al. 2019).

1.2 Limitations of MICP Techniques

Researchers have made substantial progress towards further understanding various aspects of ureolytic MICP soil improvement, ranging from improving our understanding of the life cycle performance of MICP to quantifying the liquefaction behaviors of biocemented soils (Ribeiro et. al. 2023; and Lee et. al. 2023). However, the management of ammonia byproducts remains a persistent challenge hindering the widespread adoption of this technology (Lee et al. 2023). Recent research has demonstrated that up to 99.8% of ammonia can be removed from meter-scale soil specimens by rinsing ammonia out of the soil and collecting and treating the effluent *ex situ*. However, this approach requires additional materials and energy for ammonia removal and has yet to be employed under field-scale conditions (Lee et. al. 2019). Although not yet assessed, other strategies such as the use of microbial nitrification and denitrification may also provide alternative processes by which nitrogen byproducts can be transformed into more benign chemical species, such as dinitrogen gas. Moving forward, continued research is needed to further develop reliable processes which can manage produced ammonium by-products to meet site specific requirements as well as consider other alternative pathways which do not generate ammonium by-products.

1.3 Mediation of MICP by Microbial Organic Acid Oxidation (MOAO)

Over 10^9 microorganisms can exist within a single kilogram of soil near the ground surface (Mitchell and Santamarina 2005). This immense microbial diversity offers significant potential to identify other microbial processes that can be used for calcium carbonate precipitation without

generation of environmentally-compromising byproducts. Although many different microbial metabolic pathways can mediate calcium carbonate precipitation, it is important to consider the potential benefits and drawbacks of implementing these alternatives when compared to ureolytic MICP. Photosynthesis, methane oxidation, sulfate reduction, iron reduction, denitrification (MIDP), and microbial organic acid oxidation (MOAO) represent some possible alternative pathways to ureolysis (Fahimizadeh et al. 2022). While some of these pathways present immediate challenges, others hold promise for further investigation . For example, photosynthesis does not generate harmful byproducts, but would not be feasible to implement below the ground surface. Iron reduction requires insoluble iron (III) compounds. Sulfate reduction produces toxic hydrogen sulfide gases. Methane oxidation requires methane, a potent greenhouse gas. In addition to these challenges, many of these processes require specific redox conditions making their implementation practically challenging (DeJong 2022; Ganendra 2015). Denitrification is arguably the second most studied pathway to enable biocementation and has been shown to yield calcium carbonate contents comparable to that achievable with ureolytic MICP. However, the time required to complete denitrification-induced MICP can be orders of magnitude greater than ureolysis. For example, DeJong et al. (2022) compared precipitation magnitudes and found similar calcium carbonate contents between specimens receiving 100 days of denitrification-based treatments and only 4 days of ureolysis-based treatment. Moreover, nitrogen balance studies for denitrification-induced applications in natural soils remain needed to better understand the fate of supplied nitrate, which can be respired to produce ammonia or partially reduced to form other harmful intermediate byproducts such as nitrite (Rutting et al., 2021).

Microbial organic acid oxidation (MOAO), however, offers a viable alternative process to produce aqueous carbonate species, but requires oxygen availability. Previous studies have investigated the potential of MOAO to mediate biocementation for a range of *ex situ* surficial applications, including structural concrete repair (Ersan 2018; Fahimizadeh et al. 2022) and surficial erosion control (Hemayati et al. 2023). In these above ground applications, atmospheric oxygen is abundant and organic acids, calcium salts, growth factors, and specific cell strains can be supplied to material surfaces to enable the biocementation process. However, the feasibility of employing this pathway for subsurface applications, where oxygen may be limiting, has received less attention. Under these conditions, introducing sufficient dissolved oxygen into subsurface soils presents a significant implementation challenge.

This study explores the potential of two different organic acids, namely acetate and citrate, to be oxidized by native soil bacteria and enable the formation of calcium carbonate based biocementation. This process relies on heterotrophic bacteria, which can oxidize supplied organic acids such as acetate or citrate using oxygen. During this process, bacteria utilize dissolved oxygen as an electron acceptor and can generate an increase in aqueous carbonate species through the production of carbon dioxide. In addition to the generation of carbonate species, the presence of negatively-charged bacterial cells also serve as nucleation sites for precipitation (Hemayati et al. 2023). When sufficient carbonate and calcium is present in surrounding solutions, the afforded increase in solution alkalinity from organic acid oxidation can enable supersaturation of soil solutions with respect to calcium carbonate minerals and thereby enable calcium carbonate precipitation, while forgoing ammonium generation. Although other organic carbon sources such as lactate, gluconate, succinate, and formate could be used, acetate was chosen primarily because

it cannot be anaerobically fermented and it was not expected to enable the precipitation of minerals other than calcium carbonate. Citrate was also selected as this presented the possibility to generate other mineral phases such calcium citrate which may contribute to soil mechanical improvements in addition to calcium carbonate precipitation. In all experiments performed in this study, native bacteria were enriched to complete microbial organic acid oxidation, with the specific bacterial species active in these systems remain unknown. Similar augmented studies, however, have relied on various species of the genus *Bacillus* to complete MOAO including *Bacillus subtilis*, *Bacillus amyloliquefaciens*, *Bacillus pseudofirmus*, *Bacillus cohnii*, *Bacillus alkalinitrilicus*, *Bacillus thuringiensis*, and *Bacillus halo-duran*s (Fahimizadeh et. al. 2022, Hemayati et al. 2023), suggesting that similar species may have been enriched in the experiments performed in this study.

Although microbial oxidation of acetate and citrate were expected to enable calcium carbonate precipitation, specific solution compositions and treatment techniques needed to enable this process remained unknown. Experiments were designed to examine a wide range of treatment factors on both the enrichment of native bacteria and cementation success in order to identify feasible treatment techniques. These factors included: (1) differences in applied treatment solution compositions, (2) differences in treatment solution strategies including changes in solution application frequencies and concentration changes in time, (3) differences in oxygen availability mechanisms including the use of aeration and oxygen release compounds, (4) differences in supplied nutrients needed for microbial enrichment and growth, and (5) differences in supplied inorganic carbon including the addition of bicarbonate salts which may increase carbonate availability and alter microbial growth conditions through increased solution buffering.

1.4 Thesis Organization

The research performed and presented in this thesis was designed to examine the feasibility of using microbial organic acid oxidation to generate calcium carbonate biocementation. This work was performed in two sequences: (1) small-volume batch experiments to design solution compositions and preliminarily investigate process success and (2) centimeter-scale soil column experiments to assess these processes under conditions more representative of subsurface porous media. Chapter 2 presents results from the batch experiments which examined the use of both citrate and acetate oxidation as well as the effect of differences in treatment solution compositions and oxygen availability. Chapter 3 presents results from the soil column experiments that were intended to examine the success of similar solutions applied to porous media wherein the effects of oxygen availability, representative porosities, and repeated treatments could be further explored and understood . Finally, Chapter 4 summarizes the primary research findings from this work and recommends areas for possible future research.

Chapter 2: ACETATE & CITRATE OXIDATION BATCH EXPERIMENTS

2.1 Introduction

Microbially induced calcite precipitation (MICP) or biocementation is a bio-mediated process that can improve the engineering properties of granular soils through the precipitation of calcium carbonate minerals (Stocks-Fisher et al. 1999, DeJong et al. 2006, Gomez et al. 2018; DeJong et al. 2022). This process is most commonly achieved using microbial urea hydrolysis; however, the management of produced ammonium by-products has remained a persistent challenge with respect to field-scale deployment of the technology (Lee et al. 2019). Alternative microbial metabolic pathways offer the potential to mediate biocementation through the generation of carbonate species and pH increases while eliminating ammonium production. Such pathways include microbial methane oxidation, sulfate reduction, and denitrification, although many of these processes yield significantly slower precipitation rates than ureolysis as well as other process by-products that should be carefully considered (Graddy et al. 2018). Microbial organic acid oxidation is one potential alternative pathway that can mediate calcium carbonate mineral formation through the generation of aqueous carbonate species (Jonkers et al. 2010). In this process, heterotrophic bacteria can oxidize supplied organic acids while using dissolved oxygen as an electron acceptor, thereby generating increases in aqueous carbonate species. When sufficient calcium is present, this increase in solution alkalinity can enable supersaturation of soil solution with respect to calcium carbonate minerals, and thereby enable calcium carbonate precipitation while forgoing ammonium generation.

Previous studies have examined the ability of microbial organic acid oxidation to mediate biocementation for a variety of *ex situ* surficial applications including structural concrete repair (Ersan 2018, Fahimizadeh et al. 2022) and mitigation of soil surficial erosion (Hemayati et al. 2023). In these above ground applications, atmospheric oxygen is abundant and organic acids, calcium, growth factors, and specific cell strains can be supplied to material surfaces to initiate the process. The feasibility of using the pathway for subsurface applications wherein dissolved oxygen may be limiting, however, has received limited attention thus far. Under such conditions, supplying sufficient dissolved oxygen to subsurface soils will likely present new implementation challenges. In this study, eighteen small-scale batch experiments were performed to investigate the ability of microbial acetate and citrate oxidation to enable the biocementation process. Six experiments were performed to examine acetate oxidation and twelve experiments were performed to examine citrate oxidation. The performed experiments examined: (i) the effect of techniques used to supply dissolved oxygen through both sealed flask experiments containing oxygen-releasing compounds (i.e., calcium peroxide) and fully aerobic experiments maintained by continuously-shaking open flasks, (ii) the effect of biological activity through experiments with and without supplied yeast extract, (iii) the effect of initial carbonate species through experiments with varying sodium bicarbonate additions, and (iv) the impact of solution sampling frequency for sealed flasks receiving oxygen-releasing compounds, for which oxygen intrusion was of concern. Although not exhaustive, the performed experiments provide new insights regarding the feasibility of using microbial organic acid oxidation to mediate the formation of calcium carbonate minerals for subsurface geotechnical applications.

2.2 Materials and Methods

Batch Experiments

Eighteen batch experiments were conducted to examine the feasibility of using microbial organic acid oxidation to enable calcium carbonate precipitation. All batch experiments were performed in 500 mL glass Erlenmeyer flasks containing 250 mL of treatment solutions of various chemical compositions and 30 grams of a poorly-graded clean Monterey Sand (D_{10} of 0.55 mm, D_{30} of 0.85 mm, D_{60} of 1.4 mm) intended to introduce soil microorganisms to experiments. Six batch experiments were performed to examine microbial acetate oxidation using solutions with 50 mM sodium acetate, 25 mM calcium chloride, 100 mM sodium bicarbonate, varying concentrations of supplied yeast extract (0 or 0.2 g/L), varying techniques to supply dissolved oxygen (1 mM calcium peroxide for sealed flasks or continuous shaking for open flasks), and differences in solution sampling frequencies. Twelve batch experiments were also performed to examine microbial citrate oxidation using solutions with 50 mM sodium citrate, 25 mM calcium chloride, varying concentrations of sodium bicarbonate (0 mM or 100 mM), varying concentrations of supplied yeast extract (0 or 0.2 g/L), similar differences in techniques to supply dissolved oxygen, and differences in solution sampling frequencies. All flasks receiving calcium peroxide additions were isolated from atmospheric oxygen by placing a 2 cm thick layer of heavy mineral oil on the surface of flask solutions and a rubber stopper with an airlock at the flask closures, which allowed for gases to exit experiments while limiting oxygen intrusion. All shaken flasks had closures that were covered loosely with aluminum foil to avoid evaporation and potential biological contamination, while allowing for oxygen transfer, and were shaken continuously at 150 rpm using a double orbital shaker. All experiments had solutions that were prepared to an initial pH value of 7.5 obtained through pH adjustment with either 1 M NaOH or 1 M HCl. During all experiments,

a temperature near 25°C was maintained. A summary of all acetate and citrate oxidation experiments are provided in **Tables 2.1 and 2.2**, respectively. As shown, all experiments were named according to the following convention: (i) the first term describes either the inclusion of either acetate (A) or citrate (C), (ii) the second term describes the sodium bicarbonate (BC) concentration, (iii) the third term describes the presence (Biotic) or absence (Abiotic) of yeast extract intended to promote cell growth, (iv) the fourth term describes the supply of oxygen via either peroxide additions (P) or aeration via continuous shaking (A), and (v) high and low sampling frequencies are noted with and without an asterisk, respectively. All batch experiments were monitored for 16 days to allow for microbial enrichment and precipitation activity.

Monitoring & Characterization Methods

All batch experiments were monitored either once daily (high sampling frequency) or solely at the beginning and end of experiments (low sampling frequency) to assess the impact of potential oxygen intrusion during sampling on sealed experiments receiving oxygen-releasing compounds. During sampling, 1.0 mL of solutions were removed from experiments for solution pH and electrical conductivity measurements. An additional 0.5 mL sample was also obtained from the center of all flasks and used for OD_{600} measurements to assess changes in solution cell densities in time. Other solution samples (~0.75 mL) were also obtained and clarified using a 0.45-µm cellulose acetate centrifuge spin-filter and 0.5 mL of this sample was stabilized using 1 M HCl for calcium assay measurements performed using a microplate spectrophotometer and a calcium assay kit (Bioassay Systems). Following the 16-day monitoring period, magnitudes of added solids and calcium carbonate minerals formed during the monitoring period were characterized for all experiments. In order to mitigate potential precipitation of salts during the sample drying process, all samples were filtered using large volume 0.45-µm filters and solids that were retained on filters and within the flasks were dried at 90°C with final masses measured to assess total mass changes. Following these measurements, solid samples were removed from flasks, homogenized, and calcium carbonate content measurements were performed on samples following the acid chamber process outlined in ASTM D4373-21 (ASTM, 2014). A minimum of three calcium carbonate content measurements were performed for each experiment with average values reported.

2.3 Results and Discussion

Figure 2.1 presents aqueous OD_{600} measurements in time for all batch experiments. As shown, increases in OD_{600} values were indicative of aqueous cell growth and were expected to increase

most rapidly in experiments containing 0.2 g/L yeast extract (biotic), sufficient oxygen, and a respirable organic acid source (citrate or acetate). As shown in **Figure 2.1a**, no detectable cell growth was observed in any of the abiotic acetate experiments, as expected. However, when yeast extract was supplied, significant cell growth was detected in the shaken experiment, while the other two peroxide containing experiments had no detectable cell growth. When examining OD_{600} measurements in citrate containing experiments (**Figure 2.1b**), detectable increases in cell densities were observed in both biotic shaken experiments with and without added sodium bicarbonate. In contrast, in the peroxide containing experiments, OD_{600} increases were lower but detectable in both experiments without sodium bicarbonate but were negligible in peroxide experiments containing 100 mM sodium bicarbonate. Interestingly, in the shaken abiotic citrate experiment containing no added sodium bicarbonate, increases in OD_{600} were observed suggesting that some cell growth may have occurred solely in the presence of citrate, without yeast extract. Such growth although unexpected, may have been enabled by trace nutrients provided by the Monterey Sand. When comparing similar acetate and citrate peroxide containing experiments, both low and high sampling frequency trends were similar, suggesting that oxygen intrusion during sampling likely had a minimal impact on observed cell growth. Even though increases in OD_{600} values observed in select experiments were promising, such measurements provided only an indicator of total cell growth and thus did not provide a direct measurement of acetate or citrate oxidation activity.

Figure 2.2 presents solution pH trends in time for all batch experiments. As shown in **Figure 2.2a**, both shaken acetate experiments achieved large increases in pH values from 7.5 to near 8.0 and 9.0 in experiments without and with yeast extract, respectively. Despite these large pH increases

in the shaken experiments, all peroxide containing acetate experiments exhibited minimal pH changes throughout the monitoring period. When considering the citrate experiments shown in **Figure 2.2b**, a wide variety of pH responses were observed. Although all biotic peroxide containing citrate experiments experienced pH reductions in time to values near 6.5, the majority of these experiments had minimal pH changes. Conversely, in both of the shaken citrate experiments with 100 mM sodium bicarbonate and in the biotic experiment without sodium bicarbonate, large pH increases were observed to values between 9.0 and 9.5. While pH increases were expected in the biotic experiments, the large pH increase observed in the abiotic shaken 100 mM sodium bicarbonate experiment and the small pH increase observed in the abiotic shaken 0 mM sodium bicarbonate experiment coupled with small OD_{600} increases observed earlier, suggested that biological activity may have been present in these experiments despite the absence of yeast extract. Even though pH responses were reflective of both pH increases from organic acid oxidation and pH decreases from calcium carbonate precipitation, specimens experiencing increases in pH were expected to have a higher likelihood of calcium carbonate precipitation, due to the higher abundance of aqueous carbonate (CO_3^{2-}) at more alkaline pH values.

Figure 2.3 presents aqueous calcium trends in time for all batch experiments. In all experiments, calcium degradation in time was expected to be indicative of calcium carbonate mineral formation. As shown in **Figure 2.3a**, large differences in calcium degradation behaviors were observed between the acetate experiments. In all three abiotic experiments, which did not contain yeast extract, minimal calcium degradation was observed over time, although lower initial calcium concentrations near 10 mM were observed in both abiotic peroxide containing experiments likely due to chemically-induced calcium carbonate precipitation that was observed during the solution

mixing process. Minimal calcium concentration changes in time were observed in all abiotic experiments, however, suggested that little calcium carbonate precipitation occurred after initial mixing, as expected. In the biotic experiments, both peroxide containing experiments had elevated calcium concentrations likely owing to the added calcium supplied by calcium peroxide. Modest calcium decreases in time were observed in the biotic peroxide containing acetate experiments likely reflective of some biomediated precipitation occurring in time. Finally, when examining the shaken biotic acetate experiment, a large reduction in calcium was observed with near full consumption of the supplied 25 mM calcium within 4 days. When examining the citrate experiments (**Figure 2.3b**), almost all experiments exhibited minimal decreases in calcium in time. In the two shaken experiments containing 100 mM sodium bicarbonate, however, gradual and significant calcium consumption was observed over time with near full consumption of the supplied calcium observed after 12 days in both the abiotic and biotic experiments. Although such trends might suggest that calcium consumption in these experiments was largely due to abiotic precipitation, both of these experiments exhibited significant pH increases in time as well as modest OD_{600} increases, which may instead suggest that some cell growth may have occurred in both experiments despite the lack of supplied yeast extract in the abiotic variation. Collectively, the observed trends from both experiments suggested that calcium carbonate precipitation was initiated in all shaken aerobic experiments, with some albeit minor biotic precipitation also occurring in the peroxide containing acetate experiments, but very limited biotic precipitation occurring in all peroxide containing citrate experiments. Again, low and high sampling frequency experiments from both sets demonstrated similar behaviors, suggesting that sampling frequency likely had minimal impacts on observed precipitation behaviors.

Figure 2.4 presents a comparison of added solids after the 16-day monitoring period in percent by mass versus yeast extract concentration for all acetate and citrate oxidation experiments. As shown in **Figure 2.4a**, all abiotic acetate experiments without added yeast extract achieved added solids by mass between 1% and 2.5%. Although unexpected, these results suggested that some amount of abiotic precipitation of insoluble matter occurred in all acetate experiments likely due the presence of added sodium bicarbonate. Once yeast extract was supplied, however, increases in added solids were observed for all conditions with values near 3.5% by mass observed for both peroxide containing acetate experiments and a slightly higher value near 4.2% observed in the shaken biotic acetate experiment. When considering similar trends for citrate experiments in **Figure 2.4b**, higher added solid percentages were observed in most cases with values up to near 12.5% by mass. In some experiments, including the peroxide 100 mM sodium bicarbonate added experiments and the shaken experiment without added sodium bicarbonate, solid percentages increased with added yeast extract indicating the possibility of biomediated mineral formation. In other experiments, including the peroxide 0 mM sodium bicarbonate added experiments, added solids decreased with the addition of yeast extract, however, likely due to the interference of abiotic precipitation processes. It should be noted that added solids measurements did not differentiate between generated calcium carbonate and other insoluble matter, thus subsequent calcium carbonate content measurements were used to provide further insights regarding process success and the impact of biological activity.

Figure 2.5 presents a comparison of calcium carbonate contents measured after the 16-day monitoring period in percent by mass versus yeast extract concentration for all acetate and citrate oxidation experiments. As shown in **Figure 2.5a**, acetate specimens without yeast extract had

calcium carbonate contents near 0% by mass when shaken and near 0.5% by mass when calcium peroxide was added. This outcome suggested that some fraction of precipitation observed in the peroxide containing experiments likely resulted from alkalinity provided from the calcium peroxide additive and that despite the high added solids contents measured previously, most of these added solids were not calcium carbonate minerals. When yeast extract was provided, however, small but detectable increases in calcium carbonate contents were observed in the peroxide containing experiments and a significantly larger calcium carbonate content was observed in the biotic shaken acetate experiment with a calcium carbonate content near 2.5% by mass. Despite much larger added solids contents in the citrate experiments, calcium carbonate content measurements in these same experiments (**Figure 2.5b**) indicated very few experiments had appreciable calcium carbonate precipitation. Almost all calcium carbonate contents were below 0.25% by mass with both of the shaken citrate experiments with 100 mM sodium bicarbonate (without and with yeast extract) achieving calcium carbonate contents between 1% and 1.5% by mass. This was consistent with earlier calcium measurements and coupled with insights from OD_{600} and pH measurements, again suggested that significant microbial citrate oxidation may have occurred in the shaken citrate experiments both with and without supplied yeast extract.

2.4 Conclusions

Eighteen different batch experiments were conducted to investigate the feasibility of using microbial organic acid oxidation to enable calcium carbonate biocementation for geotechnical soil improvement. Batch experiments included differences in supplied organic carbon sources, oxygen supply techniques, supplied yeast extract, and sodium bicarbonate additions. Experiments were

monitored over 16 days during which changes in bacterial growth, solution chemistry, and inorganic mineral formation were characterized using measurements of solution OD_{600}, pH, and calcium concentrations along with measurements of added solids and calcium carbonate contents. Experiments included solutions with 25 mM calcium chloride, 50 mM sodium acetate or sodium citrate,0- or 100-mM sodium bicarbonate, with and without yeast extract, and continuously shaken or sealed peroxide-containing experiments. In acetate-containing experiments, calcium reductions were observed in time in all biotic experiments while experiments without added yeast extract had no detectable calcium reductions. Added solids and calcium carbonate content measurements indicated the presence of some inorganic solid precipitation in all acetate experiments while the shaken biotic experiment exhibited a significant OD_{600} increase, pH increase, near complete calcium consumption after 4 days, and a much larger final calcium carbonate content of 2.5% by mass when compared to its abiotic counterpart that had no detectable calcium carbonate. In citrate-containing experiments detectable OD_{600} increases were observed in almost all biotic experiments. Calcium degradation trends indicated that minimal calcium consumption occurred in almost all experiments aside from the shaken experiments without sodium bicarbonate. While added solid contents increased to near 12.5% in the abiotic citrate experiments, calcium carbonate content analyses were consistent with calcium measurements and again indicated minimal calcium carbonate was precipitated in all experiments aside from the shaken experiments without sodium bicarbonate. The presence of significant calcium degradation and an OD_{600} increase in the abiotic shaken citrate experiment suggested that microbial activity may have been present despite no supplied yeast extract. While the obtained results are promising, continued research remains needed to investigate the feasibility of using microbial organic acid oxidation for biocementation soil improvement under conditions more representative of porous media.

Table 2.1. Summary of acetate oxidation batch experiments including solution chemical compositions, presence or absence biological activity, oxygen source, and solution sampling frequency.

	Solution Chemical Composition							
Specimen Name[1]	**Sodium Acetate (mM)**	**Calcium Chloride (mM)**	**Sodium Bicarbonate (mM)**	**Yeast Extract (g/L)**	**Calcium Peroxide (mM)**	**Biotic/ Abiotic**	**Oxygen Source**	**Solution Sampling Frequency**
A_100 mM BC BC_Biotic_P*	50	25	100	0.2	1	Biotic	Peroxide	High (Once Daily)
A_100 mM BC_Abiotic_P*	50	25	100	0	1	Abiotic	Peroxide	High (Once Daily)
A_100 mM BC_Biotic_P	50	25	100	0.2	1	Biotic	Peroxide	Low (First & Last Days Only)
A_100 mM BC_Abiotic_P	50	25	100	0	1	Abiotic	Peroxide	Low (First & Last Days Only)
A_100 mM BC_Biotic_A*	50	25	100	0.2	0	Biotic	Aerated (Shaken)	High (Once Daily)
A_100 mM BC_Abiotic_A*	50	25	100	0	0	Abiotic	Aerated (Shaken)	High (Once Daily)

[1] "*" denotes highly sampled experiments.

Table 2.2. Summary of citrate oxidation batch experiments including solution chemical compositions, presence or absence biological activity, oxygen source, and solution sampling frequency.

	Solution Chemical Composition							
Specimen Name[1]	**Sodium Citrate (mM)**	**Calcium Chloride (mM)**	**Sodium Bicarbonate (mM)**	**Yeast Extract (g/L)**	**Calcium Peroxide (mM)**	**Biotic/Abiotic**	**Oxygen Source**	**Solution Sampling Frequency**
C_0 mM BC_Biotic_P*	50	25	0	0.2	1	Biotic	Peroxide	High (Once Daily)
C_0 mM BC_Abiotic_P*	50	25	0	0	1	Abiotic	Peroxide	High (Once Daily)
C_0 mM BC_Biotic_P	50	25	0	0.2	1	Biotic	Peroxide	Low (First & Last Days Only)
C_0 mM BC_Abiotic_P	50	25	0	0	1	Abiotic	Peroxide	Low (First & Last Days Only)
C_0 mM BC_Biotic_A*	50	25	0	0.2	0	Biotic	Aerated (Shaken)	High (Once Daily)
C_0 mM BC_Abiotic_A*	50	25	0	0	0	Abiotic	Aerated (Shaken)	High (Once Daily)
C_100 mM BC_Biotic_P*	50	25	100	0.2	1	Biotic	Peroxide	High (Once Daily)
C_100 mM BC_Abiotic_P*	50	25	100	0	1	Abiotic	Peroxide	High (Once Daily)
C_100 mM BC_Biotic_P	50	25	100	0.2	1	Biotic	Peroxide	Low (First & Last Days Only)
C_100 mM BC_Abiotic_P	50	25	100	0	1	Abiotic	Peroxide	Low (First & Last Days Only)
C_100 mM BC_Biotic_A*	50	25	100	0.2	0	Biotic	Aerated (Shaken)	High (Once Daily)
C_100 mM BC_Abiotic_A*	50	25	100	0	0	Abiotic	Aerated (Shaken)	High (Once Daily)

[1] "*" denotes highly sampled experiments.

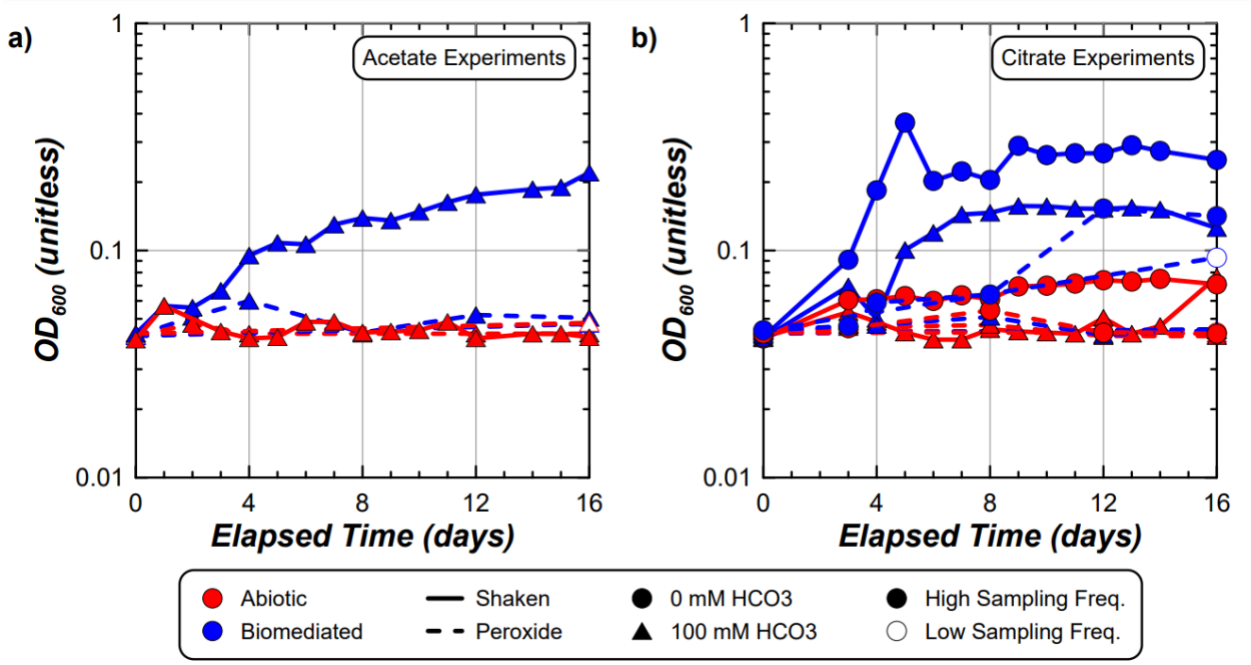

Figure 2.1. OD600 measurements in time for all **(a)** acetate and **(b)** citrate oxidation batch experiments.

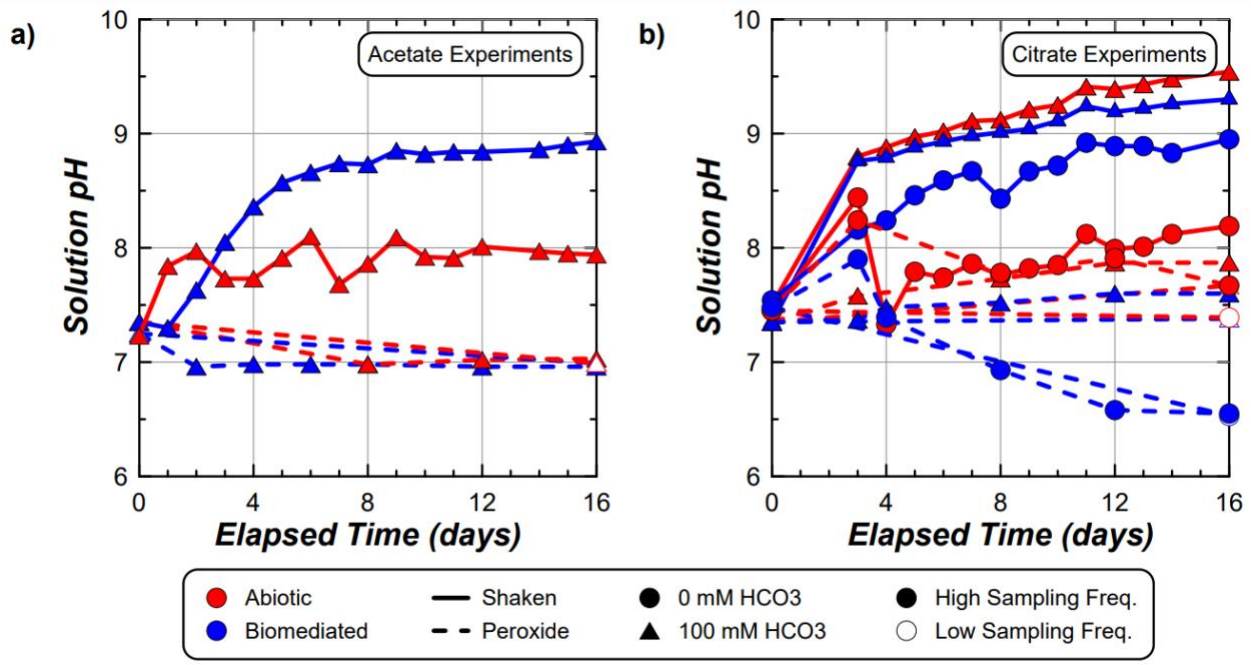

Figure 2.2. Solution pH measurements in time for all **(a)** acetate and **(b)** citrate oxidation batch experiments.

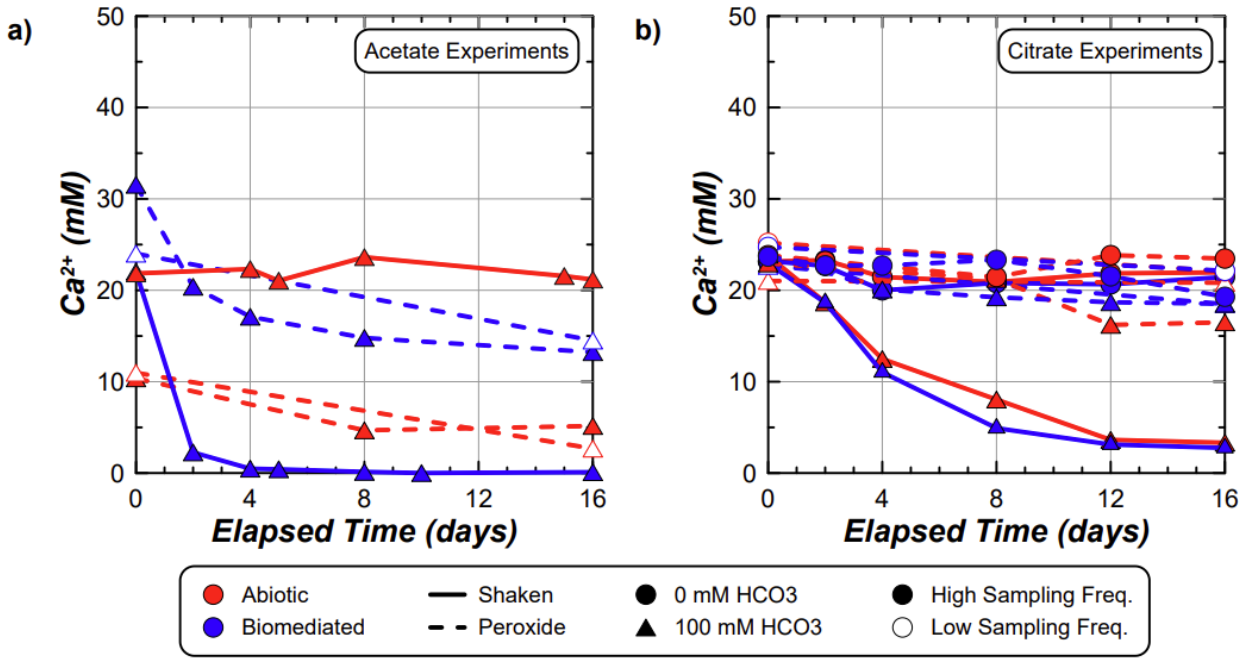

Figure 2.3. Aqueous calcium measurements in time for all **(a)** acetate and **(b)** citrate oxidation batch experiments.

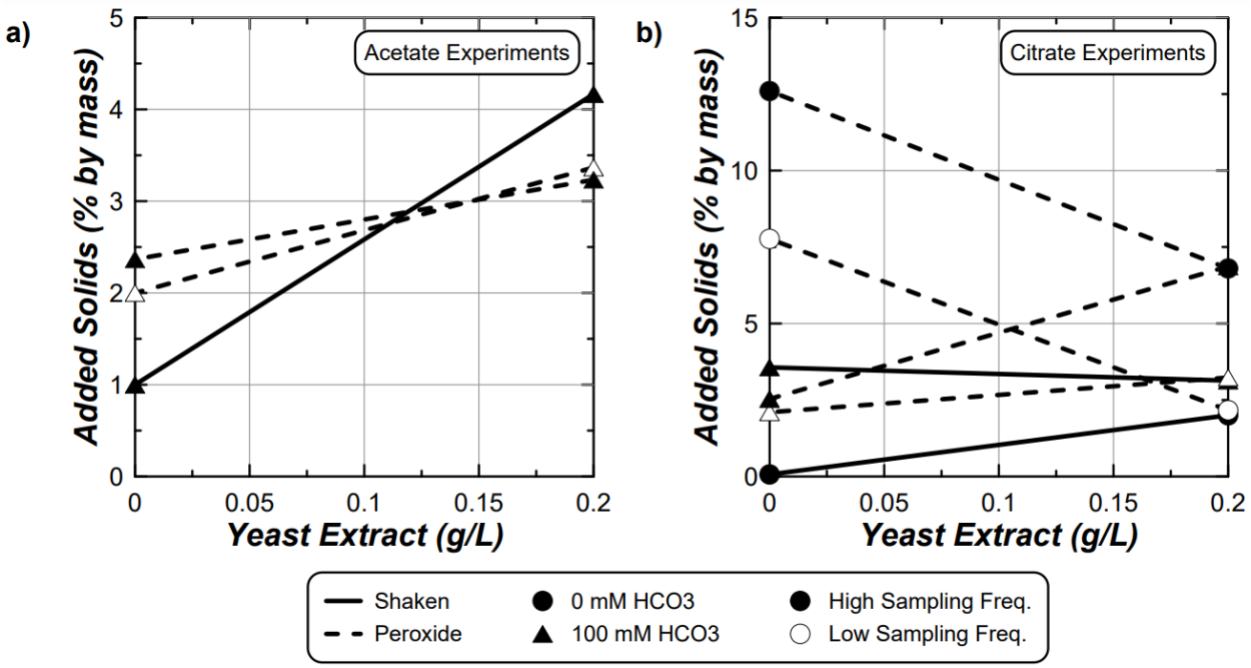

Figure 2.4. Comparisons of added solids (in % by mass) versus supplied yeast extract concentrations for all **(a)** acetate and **(b)** citrate oxidation batch experiments.

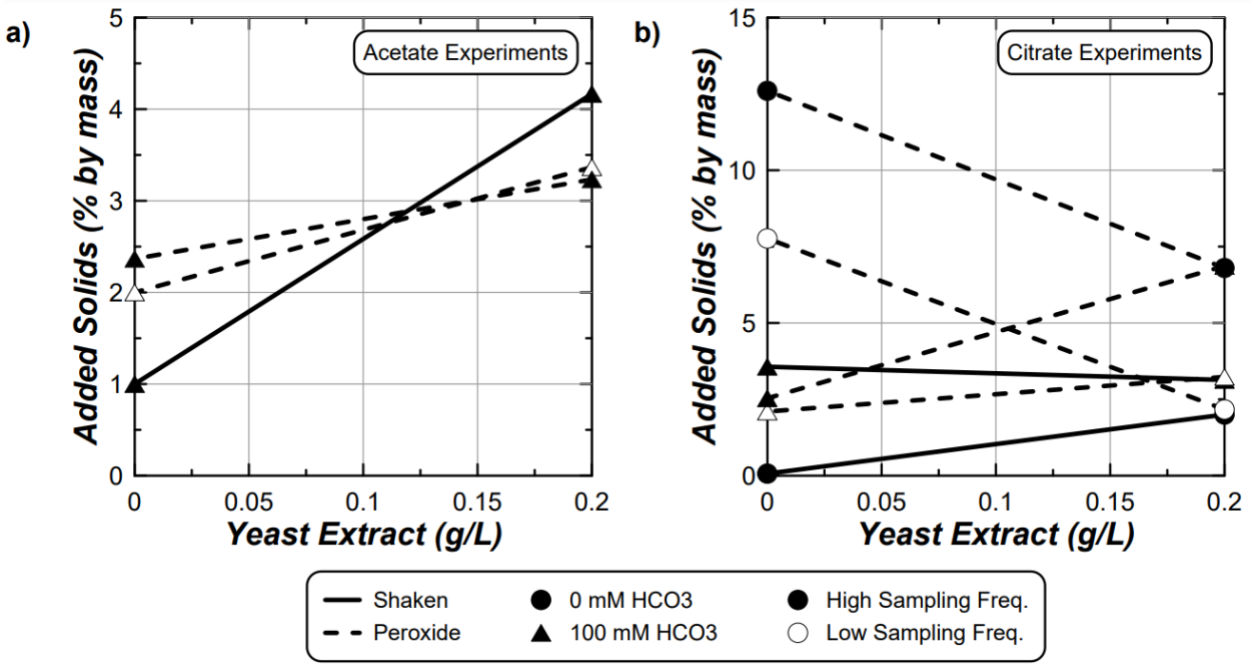

Figure 2.5 Comparisons of calcium carbonate contents (in % by mass) versus supplied yeast extract concentrations for all **(a)** acetate and **(b)** citrate oxidation batch experiments.

Chapter 3: ACETATE & CITRATE OXIDATION SOIL COLUMN EXPERIMENTS

3.1 Introduction

Previous batch experiments were performed to examine the ability of microbial acetate and citrate oxidation to enable the precipitation of calcium carbonate-based biocementation. These experiments demonstrated that when oxygen was present, supplied solutions containing 25 mM calcium, 50 mM acetate, 100 mM bicarbonate, and 0.2 g/L yeast extract with an initial pH of approximately 7.35 resulted in the highest calcium carbonate precipitation magnitudes. In contrast, experiments receiving citrate-based solutions had more limited success in generating calcium carbonate minerals, however, large added masses of other mineral phases were observed and suspected to be calcium citrate. Batch experiments also considered whether or not acetate or citrate could be successfully oxidized when an oxygen releasing compound was supplied (1 mM calcium peroxide) intended to supplement dissolved oxygen concentrations. It was found that aerated experiments achieved the highest precipitation magnitudes, with peroxide containing experiments achieving mixed results. Experiments also considered the effect of sodium bicarbonate additions on precipitation magnitudes with the presence of bicarbonate resulting in increases in precipitation magnitudes for most experiments.

In order to further explore the feasibility of using microbial acetate and citrate oxidation for biocementation under conditions more representative of porous media, however, two sets of soil column experiments were performed which considered differences in applied solution compositions as well as different oxygen supply mechanisms. Soil column tests specifically allowed for the investigation of (1) process reaction kinetics under conditions more representative

of subsurface soils including much more representative soil-to-solution ratios, (2) changes in soil biogeochemical and geophysical behaviors in time, (3) the impact of repeated solution injections and changes in solution compositions including inorganic carbon additions, yeast extract additions, and different oxygen supply mechanisms, and (4) the ability to apply solutions in different phases including stimulation wherein solutions were intended to first enrich soils for native microorganisms and cementation, wherein calcium was supplied to improve soils. A total of 22 soil columns were performed, with 10 soil columns dedicated to investigating the acetate oxidation pathway and 12 soil columns dedicated to investigating the citrate oxidation pathway. Column experiments were specifically designed to further investigate the success of solutions previously employed in the earlier batch experiments.

3.2 Acetate Soil Column Experiments

Earlier batch experiments indicated that acetate-containing solutions were able to achieve detectable bacterial growth, solution pH changes, aqueous calcium degradation, and the generation of calcium carbonate ($CaCO_{3)}$ precipitation when solutions contained 25 mM calcium, 50 mM acetate, 100 mM bicarbonate, 0.2 g/L yeast extract, and were continuously aerated. Therefore, soil column experiments were designed to further explore the success of similar solutions under conditions more representative of porous media with some important differences. Experiments were specially designed to assess differences in (1) oxygen supply mechanisms through experiments that were either aerated, received no additional oxygen beyond that achieved during mixing (dissolved oxygen), or receiving oxygen release compounds (calcium peroxide), (2) the presence or absence of yeast extract intended to alter cell growth, (3) differences in treatment sequences including phased columns that received stimulation injections first followed by

cementation injections and concurrent columns that received only cementation injections, and (4) the presence or absence of sodium bicarbonate. A summary of all 10 acetate soil column experiments is provided in **Table 3.1**. As shown, all experiments were named according to the following convention: (i) the first term describes the inclusion of acetate (A), (ii) the second term describes the sodium bicarbonate (BC) concentration, (iii) the third term describes the presence (Biotic) or absence (Abiotic) of yeast extract intended to promote cell growth, (iv) the fourth term describes the supply of oxygen via either peroxide additions (Px), aeration via sparging (A), or dissolved oxygen included from equilibration with atmospheric conditions (D), and (v) the use of either phased (P) or concurrent (C) injections.

3.2.1 Materials and Methods

3.2.1.1 Soil Columns

All columns contained Monterey Sand (D_{10} of 0.55 mm, D_{30} of 0.85 mm, D_{60} of 1.4 mm), a poorly-graded clean sand that was identical to that used in previous batch experiments. Specimens were prepared in 15.2 cm tall and 7.6 cm in inner diameter hollow acrylic cylinders and Monterey Sand materials were placed to achieve an initial relative density of approximately 40% and pore volumes (PV) of approximately 250 mL using moist tamping and six lifts. Soil column specimens included PFTE caps at both ends with barbed fittings for solution exchange as well as bender element sensors and solution sampling ports. Porex plastic filter materials, with pore sizes ranging from 125 µm to 175 µm, were placed between the caps and the soil to minimize soil particulate losses during injections. Each column was subjected to a total stress of approximately 100 kPa applied through a reaction frame that exerted a vertical force onto the column's top caps. This stress was maintained throughout the experimental duration. The applied stress of 100 kPa aimed to replicate

conditions encountered within a saturated soil layer at a depth near 10 meters. Columns were treated from the bottom upwards to ensure uniform saturation and minimize heterogeneity in transport resulting from solution density differences. Three sampling ports and three bender element ports were positioned along the column height at varying distances from the injection port. The ports were located at 3.50 cm (bottom port), 8.56 cm (middle port), and 13.67 cm (top port) from the base of the columns. Bender element sensors were installed at a distance of 8.56 cm from the base of the columns. For columns requiring air sparging, a small air diffuser was connected to a tube placed 3.50 cm from the base of the columns and was connected to a small air pump (Hittop 4W 110 gal/hr. two-outlet air pump). All columns were treated using constant flow rate peristaltic pumps. The top of the columns was connected to effluent tubes that drained into solution reservoirs to prevent desaturation and the intrusion of atmospheric oxygen intrusion during and after injections. **Figure 3.1** presents an image of all acetate soil column experiments.

3.2.1.2 Treatment Solutions & Injections

Following preparation, all columns were saturated with deionized water. Prior to stimulation and cementation treatment injections each column received 1.5 PV of treatment solutions every two days at a flowrate of 11 mL/min, intended to fully replace residing pore fluids. Treatment solutions were applied in two sequences. Concurrent columns received only cementation solution injections throughout the duration of the treatment program. Phased columns however received treatment solutions in two phases consisting of stimulation injections first, which contained no calcium and were intended to enrich organic acid oxidizing microorganisms prior to cementation, followed by identical cementation solution injections as concurrent columns. All solutions contained 50 mM acetate but contained varying calcium chloride concentrations (0 mM for stimulation solutions

applied to phased columns vs. 25 mM applied for cementation solutions for both phased and concurrent columns), varying sodium bicarbonate additions (0 mM vs. 100 mM), varying yeast extract additions (0 g/L vs. 0.2 g/L), and the addition or absence of 1 mM calcium peroxide depending on the oxygen supply mechanisms considered. The considered oxygen supply mechanisms included air sparging (aeration), the inclusion of oxygen from mixing under atmospheric conditions (dissolved oxygen), and the inclusion of calcium peroxide as an oxygen release compound (peroxide). Columns receiving air sparging received air injections after applying treatment injections by pumping air through a diffuser (###dimensions###) connected to a small pump for 30 minutes immediately after each stimulation and cementation injection at a flowrate of approximately 22 mL/min. During treatments, phased columns received 4 stimulation injections once every two days intended to achieve sufficient acetate-oxidation or citrate-oxidation activity. During this same 8-day period, concurrent columns remained saturated with deionized water but received no treatment injections.

Following stimulation injections, all columns received 14 cementation injections applied once every two days in two different 7 injection sequences. During the first 7 cementation injections (referred to as “Low Cement”), applied solutions were similar to previous stimulation solutions but included the addition of 25 mM calcium. For the last 7 cementation injections (referred to as “High Cement”), however, the concentrations of included calcium chloride and sodium acetate were doubled to 50 mM and 100 mM, respectively, while all other solution additions remained the same. The rationale for doubling the concentrations of calcium chloride and sodium acetate was to investigate if higher improvement magnitudes could be achieved per injection following the establishment of sufficient microbial activity. Immediately following the last cementation

injection, all columns were rinsed with 10 PV of a $CaCO_3$-equilibrated solution to remove soluble reaction byproducts while mitigating the potential for $CaCO_3$ dissolution (Ribeiro & Gomez 2023). The $CaCO_3$ solution was prepared by equilibrating 0.2 g/L of solid reagent-grade $CaCO_3$ (≥99.0%, Thermo Fisher Scientific, Waltham, MA) with deionized water and removing all mineral solids using a 0.2-µm filter before injecting into the columns. All columns were destructively sampled immediately following rinse injections.

3.1.2.3 *Biochemical Sampling and Monitoring*

Aqueous samples were collected from the middle sampling ports at various time points during both the stimulation and cementation phases of the experiment. All samples were obtained using sterile needles and syringes (Fisher Scientific). Collected samples were used for both pH measurements completed immediately after sampling as well as calcium and acetate assay measurements. During stimulation injections, aqueous samples for pH measurements were collected immediately after each injection, 24 hours after each injection, and 48 hours after each injection. During cementation injections, aqueous samples for pH measurements were collected immediately after each injection and 48 hours after each injection. For cementation injections 1, 3, 6, 9, 12, and 14, however, pH samples were also collected 24 hours after each injection. pH samples were approximately 4 mL in volume and were measured immediately upon collection using a semi-micro pH electrode and meter system (Orion Versa Star Meter, Thermo Fisher) and then discarded. The pH meter was calibrated daily using three buffers (4.01, 7.00, and 10.01) and had an accuracy of ± 0.05 pH units. During stimulation, samples for calcium and acetate assays were collected immediately before and after each injection, 24 hours after each injection, and 48 hours after each injection. During cementation, samples for calcium and acetate assays were

collected immediately before and after each injection. For cementation injections 1, 3, 6, 9, 12, and 14, however, additional samples were collected 4 hours, 24 hours, and 48 hours after injections. **Table 3.2** provides a summary of the aqueous sampling schedule during the stimulation and cementation phases of the experiment.

Aqueous samples for calcium and acetate measurements were 1 mL in volume and were immediately acid-stabilized using 1 mL of 1M HCl to prevent further biological activity after collection. All samples were then frozen until chemical measurements were completed. To further prepare the samples for analysis, all calcium and acetate samples were clarified using 0.45-µm cellulose acetate centrifuge spin-filters. Acetate measurements were performed using a colorimetric acetate assay kit (BioAssay Systems). This kit utilizes enzyme-coupled reactions to produce a red colorized product when mixed with diluted samples. The absorbance values of these samples were measured at 570 nm using a microplate spectrophotometer. To minimize the effects of acidic solutions on enzyme-catalyzed reactions, all acetate samples were pH-adjusted to near 7 using 0.5 M NaOH. Additionally, all samples were diluted using Millipore water prior to assays to ensure that concentrations were within the range of the acetate colorimetric assay (0 to 20 mM acetate). Calcium measurements were conducted using a second colorimetric calcium assay kit (BioAssay Systems). This kit utilizes reagent-based reactions to generate a blue colorized product when mixed with diluted samples. The absorbance values of these samples were measured at 612 nm using a microplate spectrophotometer. Unlike acetate measurements, no pH adjustment was required for calcium measurements as the calcium assay reaction did not rely on enzymes. Similarly, all samples were diluted using Millipore water to achieve concentrations within the

range of the calcium colorimetric assay (0 to 5 mM calcium). **Supplemental Figure 3.13** provides example calibration data for both the calcium and acetate assays.

3.1.2.4 Geophysical Measurements

Shear wave velocity (V_s) measurements were obtained using horizontally oriented bender element pairs positioned within soil columns at the middle bender element port location (8.56 cm from column bases). V_s measurements were conducted using two bender element sensors (y-poled, Piezo Inc.) placed at known sensor spacings. To ensure sensor waterproofing, bender elements were carefully coated with epoxy, electronics max, and an insulating coating, following established procedures outlined in Gomez et al. (2017). The transmitted bender element sensors were energized with a 24V, 100 Hz square wave, and the resulting signals from the receiving bender elements were measured and recorded using an oscilloscope at a sampling frequency of 1 MHz. The arrival times of the shear waves and the corresponding signals were interpreted visually, and the V_s values were calculated based on the measured sensor spacings. Initial V_s values for all columns ranged between 120 m/s and 150 m/s prior to treatments.

3.1.2.5 Soil Calcium Carbonate ($CaCO_3$) Content Measurements

Following all treatments, all columns were destructively sampled and partitioned along their length into eight discrete sections (approximately 2 cm thick). Soil sections were then oven-dried and homogenized to yield subsamples for $CaCO_3$ content measurements. $CaCO_3$ content was quantified in accordance with ASTM D4373 by reacting $CaCO_3$ with 1M hydrochloric acid (HCl) to generate CO_2 and a corresponding increase in test chamber pressure (ASTM 2014). Calibration

relationships between expected pressure changes and known masses of $CaCO_3$ were used to determine $CaCO_3$ contents for soil samples from the observed chamber pressures. At least three measurements were completed for each soil section. **Supplemental Figure 3.13** provides example calibration curve data for soil $CaCO_3$ content measurements.

3.1.2.5 Scanning Electron Microscope (SEM) Imaging

Scanning electron microscope (SEM) images were completed with a FEI Thermo Apreo-S Scanning Electron Microscope using an acceleration voltage of 2 kV, a beam current of 13 pA, and magnifications of 100x, 200x, and 1000x. All soil specimens were oven-dried and mounted onto imaging pedestals using carbon tape.

3.1.3 Results and Discussion

Figure 3.2 presents the pH measurements in time for all acetate soil column experiments. Experiments containing 100 mM sodium bicarbonate additions are shown in **Figure 3.2a**, while those without sodium bicarbonate are presented in **Figure 3.2b**. During the stimulation phase, all aerated bicarbonate experiments exhibited significant pH increases, reflective of successful organic acid oxidation. Both aerated bicarbonate experiments with and without yeast extract additions exhibited large pH increases, suggesting that pH increases may have resulted in part from equilibration of solutions with intruded air. However, the aerated bicarbonate experiment with yeast extract demonstrated the highest pH increase observed of all columns, reaching a peak value near 9.28. When considering other biotic columns, both peroxide and dissolved oxygen experiments showed slight pH increases to peak values near 8.12 and 8.01, respectively, suggesting

that some but more minimal MOAO activity may have been present in these columns. All other column experiments exhibited minimal pH changes during stimulation, suggesting that bicarbonate additions, yeast extract additions, and aeration may be important factors required to stimulate natural sands for acetate oxidation activity. During the first 7 cementation injections, all bicarbonate containing columns experienced an immediate and significant pH drop, indicative of calcium carbonate precipitation, due to the consumption of carbonate species and the related release of hydrogen ions. As shown in **Figure 3.2a**, the phased, aerated bicarbonate experiment containing yeast extract exhibited significant pH increases on days 14, 15, and 19 (cementation injections 3 and 5), indicating a higher probability of calcium carbonate precipitation due to the higher abundance of aqueous carbonate at more alkaline pH values. During the last 7 cementation injections, wherein the concentrations of calcium and acetate were doubled to 50 mM calcium and 100 mM acetate, respectively, pH values continued to exhibit a downward trend, with only a small initial increase observed in the phased, aerated bicarbonate experiment containing yeast extract. By day 26 (cementation injection 9), all experiments showed minimal pH changes, suggesting that enriched microbial communities may not have tolerated the higher concentrations of calcium and acetate employed in the later injections.

All experiments without bicarbonate showed little change during all phases of the experiment indicating that the presence of inorganic carbon additions may be a critical towards enabling the enrichment of organic acid oxidizing bacteria and /or calcium carbonate precipitation possibly through the buffering of solution pH and the increased availability of carbonate species, among other factors. Since the bacterial communities involved in these stimulated experiments were not

characterized, the resulting effect of bicarbonate additions on these enriched microorganisms remains unknown but is hypothesized to be potentially significant.

Figure 3.3 presents measurements of solution calcium concentrations in time for all soil columns during 7 select cementation injections (CEM 1, CEM 3, CEM 6, CEM 8, CEM 9, CEM 12, and CEM 14). In all experiments, calcium degradation in time was expected to be indicative of calcium carbonate precipitation, which may have occurred through both abiotic and biomediated processes. During CEM 1, CEM 3, and CEM 6, columns received 25 mM of calcium, however, during CEM 8, CEM 9, CEM 12, and CEM 14, columns received a higher 50 mM calcium concentration. **Figure 3.3a** shows data for Column A_100 mM HCO3_Biotic_A_C which received oxygen via air sparging, did not receive any stimulation injections (concurrent), and received solutions containing both 100 mM sodium bicarbonate and yeast extract. As shown, near complete consumption of the injected calcium can be observed for all cementation injections. From CEM 1 to CEM 6 increases in the rate of precipitation can be observed with significant calcium consumed within the first hour after injections. During the transition to higher calcium concentrations in CEM 8, a large reduction in precipitation rates is observed suggesting that the activity of bacterial communities present within the column may have been reduced due to osmotic shock and/or inhibition by high calcium concentrations. However, by CEM 9 this activity largely recovered, with full consumption of calcium observed for all further injections. Similar trends are also shown for all columns in **Supplemental Figure 3.1**, which presents calcium concentration data for all columns during each cementation injection. **Figure 3.3b** presents data for Column A_100 mM HCO3_Biotic_A_Ph, which was identical to the previously discussed column (**Figure 3.3a**) with the exception that it received 4 stimulation injections prior to all cementation injections. Although

higher initial activity was expected in this phased column when compared to the previous concurrent column, both columns showed nearly identical calcium consumption trends, indicating that the addition of stimulation injections had little effect on calcium degradation behaviors. The convergence of behaviors at earlier times (i.e., CEM 1) between these columns was unexpected but suggested that some of the observed precipitation may have resulted from abiotic precipitation reactions and may not have been necessarily fully biomediated.

Figure 3.3c and 3.3d presents similar trends for Column A_100 mM HCO3_Biotic_Px_C and A_100 mM HCO3_Biotic_Px_Ph, respectively, which both contained calcium peroxide, 100 mM bicarbonate, and yeast extract but received either concurrent or phased injections. Results show similar trends to the similar aerated columns (**Figure 3.3a to 3.3b**), however, their reaction rates appeared to slow considerably for similar injections. **Figure 3.3c** showed no degradation of calcium during the residence period of last cementation injection for the concurrent column while the similar phased column (**Figure 3.3d)** experienced complete consumption of the injected calcium, suggesting that the inclusion of stimulation injections may provide a slightly benefit for peroxide receiving columns. **Figure 3.3e** presents Column A_100 mM HCO3_Biotic_D_Ph, which were similar to other bicarbonate containing biotic phased columns but received no additional oxygen other than the dissolved oxygen available within the injected solutions. Results in this column were nearly identical to is aerated counterpart shown in **Figure 3.3b** indicating that no additional oxygen may be required for degradation of calcium. Again, this suggested the possibility of significant abiotic precipitation occurring in all columns which would require the presence of bicarbonate but would be expected to be largely insensitive to differences in enrichment and oxygen availability. **Figure 3.3f** presents results for Column A_100 mM

HCO3_Abiotic_A_Ph, which served as a control for all bicarbonate containing aerated columns, receiving similar solutions without yeast extract. This abiotic column interestingly exhibited low calcium concentrations after injections as well as significant degradation of calcium during the first cementation injection and all further injections. Although unexpected, two possible mechanisms may explain the consumption of calcium observed in this abiotic control column: (1) While yeast extract was expected to provide the growth factors needed for bacterial growth, trace nutrients from the soil used may have allowed for microbial growth and activity in the absence of yeast extract; (2) The absence of yeast extract in the abiotic solutions resulted in precipitation being observed during the solution preparation process, however, similar precipitation was not observed when yeast extract was present. Thus, the large calcium reductions observed in the abiotic column may have resulted primarily from the presence of bicarbonate and calcium in the absence of yeast extract. Although not fully understood, it remains possible that abiotic reactions occurred in all bicarbonate containing columns, although the exact degree to which this influenced each condition is difficult to assess given that yeast extract may have significantly altered observed abiotic precipitation behaviors independent of microbial growth.

Figures 3.3g to 3.3j present calcium reduction trends for all soil columns that received solutions that did not contain sodium bicarbonate, intended to investigate the effect of inorganic carbon additions on the precipitation process. As shown, all columns containing yeast extract (**Figure 3.3g to 3.3i**) showed very little change in calcium during the first 7 cementation injections but more significant degradation of calcium after cementation injection 8. This suggested that the addition of bicarbonate was critical for achieving precipitation during the first 7 cementation injections either due to its role in abiotic reactions or effects on enriched microbial communities

and MOAO activity. Interestingly, when examining the abiotic control in the absence of sodium bicarbonate, almost no activity is observed until the last cementation injection. This suggested that minimal acetate oxidation likely occurred without yeast extract at a minimum when bicarbonate was not present. When considering broader trends between all columns, columns receiving similar solutions with yeast extract generally consumed greater magnitudes of injected calcium than those without the presence of yeast extract highlighting the potential role of microbial activity. When comparing differences in oxygen sources, aerated columns consumed calcium most rapidly with calcium concentrations approaching zero in most columns after the retention period. Calcium consumption rates in time were slightly slower but similar for biotic columns receiving dissolved oxygen and peroxide, however. The behaviors between the two sets of concurrent and phased columns examined were almost identical indicating that adding a stimulation phase may have little effect on calcium degradation, at a minimum when sodium bicarbonate it present. Different behaviors may have been observed, however, had phase and concurrent columns been tested without bicarbonate wherein the effect of abiotic reactions would be minimized.

Figure 3.4 presents aqueous calcium measurements and corresponding pH measurements for each column measured during cementation injections. These trends were examined in order to assess the ability of pH measurements to provide information regarding process completion. Injected solutions were expected to start at high calcium and carbonate concentrations, with reductions in calcium occurring at a near constant pH due to the consumption of carbonate species and continued alkalinity production from acetate oxidation. Once calcium was completely consumed, however, and precipitation reactions stopped, it was expected that continued acetate oxidation would result in a pH rise that might be useful to assess when precipitation reactions had been completed.

Although almost all columns showed calcium reductions from 50 mM to lower values at near neutral pH, several showed a large pH increase once calcium concentrations approached zero. In particular, Column A_100 mM HCO3_Biotic_A_Ph (**Figure 3.4b**) showed a large pH rise to near 9 once aqueous calcium approached 0 mM. Similar relationships may prove useful for practical applications to assess reaction completion using pH measurements as opposed to aqueous calcium measurements, which require significantly more resources.

Figure 3.5 presents measurements of solution acetate concentrations in time for select columns during select stimulation (when present) and cementation injections (STIM4, CEM 1, CEM 6, CEM 14). In all experiments, acetate degradation in time was reflective of MOAO activity in time and was used to evaluate the role of biological activity on observed behaviors. During STIM 4, CEM 1, CEM 6, all columns received solutions with 50 mM acetate, however, during CEM 14, columns received a higher 100 mM acetate concentration. As shown, all columns exhibited minimal acetate degradation activity during the STIM 4, with activity observed during and after CEM 1 for select columns. In particular, significant acetate degradation can be observed in Column A_100 mM HCO3_Biotic_A_C (**Figure 3.5a**) during CEM 1 and CEM 6 with lesser but some activity detected during CEM 14. The similar phased column (**Figure 3.5b**), however, exhibited minimal activity for all injections. When considering the other biotic columns with peroxide (**Figure 3.5c**) and dissolved oxygen (**Figure 3.5d**) some degradation activity is observed, although much less than the aerated concurrent column (**Figure 3.5a**). Minimal degradation was also observed in the comparable abiotic control (**Figure 3.5e**). Lastly, significant degradation was observed in Column A_0 mM HCO3_Biotic_A_Ph which did not have bicarbonate with less activity in the abiotic version A_0 mM HCO3_Abiotic_A_Ph. Similar trends are also shown for

all columns in **Supplemental Figure 3.2**, which presents acetate concentration data for all columns during each stimulation and cementation injection.

Figure 3.6 presents comparisons of corresponding aqueous calcium and acetate measurements obtained from select soil columns during cementation. When examining these trends, progressive reductions in acetate and calcium ions (Ca^{2+}) were expected in columns experiencing biomediated precipitation, with calcium reductions in the absence of acetate reductions expected to indicate largely abiotic precipitation. As shown in **Figure 3.6e**, large calcium reductions are observed in the abiotic control with bicarbonate, however, acetate concentrations remained largely unchanged, again suggesting that most precipitation occurring in this column was likely abiotic. When examining the abiotic control without bicarbonate (**Figure 3.6g**), minimal acetate and calcium changes are observed reflective of the absence of abiotic precipitation enabled by bicarbonate and the absence of MOAO activity. When looking at both biotic aerated columns, progressive decreases in calcium and acetate are observed in both columns with significantly lower concentrations observed near the end of reactions in the concurrent variation (**Figure 3.6a**) and appreciable acetate remaining at low calcium in the phased column (**Figure 3.6b**). Trends similar to the aerated phased column are also observed in the peroxide and dissolved oxygen phased columns (**Figure 3.6c**, **Figure 3.6d**). Lastly, in the biotic phased aerated column lacking bicarbonate, some small concentrations of acetate and calcium were observed, but the majority of data points existed at higher calcium and acetate concentrations indicative of more limited biomediated reactions (**Figure 3.6e**).

Figure 3.7 presents soil shear wave velocity (V_s) measurements completed for all columns during cementation injections. As shown, lower concentration cementation injections (i.e., "low cement") were applied 0 to 14 days after stimulation with higher concentration cementation injections (i.e., "high cement") applied from 14 to 28 days after stimulation. **Figure 3.7a and 3.7b** present measured V_s values while **Figures 3.7c and 3.7d** presents V_s values normalized by initial uncemented values (V_{s0}). All columns had similar initial uncemented shear wave velocities (V_{s0}) between 127 m/s and 157 m/s prior to any treatment injections with small differences attributed to stress relaxation during stimulation injections. As shown in **Figure 3.7a and 3.7c**, the phased aerated column receiving solutions with sodium bicarbonate and yeast extract exhibited the greatest increase in Vs during cementation injections, reaching a peak value of 187 m/s and a ΔVs of 43 m/s after 12 cementation injections. During the 13th cementation injection, however, a clog in the effluent tube of this column resulted in a pressure increase during injections and lower V_s values were observed immediately after, likely due to minor cementation damage. When looking at the column receiving similar concurrent injections, an almost identical V_s improvement was observed during the first 7 cementation injections, but improvement in this column was significantly less when higher concentrations were applied during the last 7 injections. This outcome suggested that the achieved bacterial communities may have been more tolerant of higher acetate and calcium concentrations due to enrichment prior to the introduction of calcium. When examining data for the concurrent and phased columns receiving solutions with peroxide, yeast extract, and bicarbonate little to no change in V_s was observed. When looking at the abiotic control for these columns which received similar injections but without yeast extract, little to no change in V_s was observed. Although previous calcium consumption and lack of acetate consumption was indicative of abiotic calcium carbonate precipitation, this result shows that this precipitation does

not increase the soils V_s at mid-height. The phased dissolved oxygen column with bicarbonate and yeast extract also showed limited change in V_s values, although this particular V_s sensor pair had less reliable signals, which may have contributed to increased measurement variability. As shown in **Figure 3.7b and 3.7d**, all columns receiving solutions without bicarbonate showed no significant increases in V_s. This result was consistent with the limited calcium and acetate consumption observed in these columns and may suggest that limited microbial activity was achieved in columns without bicarbonate and / or the majority of reactions observed in the bicarbonate containing experiments were abiotic and induced by the presence of bicarbonate in the treatment solution. While V_s improvements in all columns were relatively small, recent studies have shown that even small V_s increases resulting from cementation can dramatically improve soil liquefaction triggering resistances and small-strain behaviors (Lee et. al. 2022).

Figure 3.8 presents measured soil $CaCO_3$ contents along column lengths for all columns. Each measurement represents the average of three soil $CaCO_3$ content measurements, however, included error bars indicate ± one standard deviation for measurements. As shown, for all columns the majority of $CaCO_3$ precipitation occurred in the bottom 5 cm of the column near the injection source. As shown, all columns receiving solutions containing bicarbonate achieved higher soil $CaCO_3$ contents than columns receiving solutions without bicarbonate, consistent with V_s trends. Similar to the V_s data, both aerated columns receiving solutions containing bicarbonate and yeast extract achieved the highest $CaCO_3$ contents, which were near 2% and 1.5% by mass in the concurrent and phased columns at the base and decreased to near 0.25% by mass after a distance of 6 cm from the injection source and larger distances. Interestingly, the phased column receiving solutions with bicarbonate but without yeast extract achieved some measurable $CaCO_3$ at the base

near 0.75% by mass with values quickly decreasing to near 0.25% by mass after a distance of 3 cm. This is consistent with the lack of significant V_s increases in this column, which were measured at mid-height. This outcome may have resulted from greater precipitation of $CaCO_3$ during solution mixing for this column when compared to the biotic counterparts. Conversely, the difference between the abiotic and biotic variations may support the presence of greater microbial activity in the columns receiving solutions with yeast extract, although this activity may have been localized near the injection location. For all columns, this localization of improvement at the base of columns may explain the limited V_s increase observed in all columns which was measured at mid-height (distance of 8.56 cm from the injection source).

Figure 3.9 presents relationships between the final shear wave velocities (V_s) as well as normalized shear wave velocities (Vsf/Vs0) and corresponding average and mid-port soil $CaCO_3$ contents. Comparisons with final V_s values are shown in **Figure 3.9 and 3.9b** with normalized V_s values shown in **Figure 3.9c and 3.9d**. Since the spatial distribution of $CaCO_3$ content was non-uniform, Vs values were compared with both average $CaCO_3$ contents for entire columns (**Figure 3.9a and 3.9b**) as well as the specific $CaCO_3$ content values present at the bender element locations (**Figure 3.9c and 3.9d**). **Figure 3.9d** perhaps presents the most meaningful comparison of values, with soil $CaCO_3$ contents measured at the bender element sensor location compared with normalized Vs measurements. As shown, increases in normalized V_s are observed with increases in soil $CaCO_3$ contents with an improvement near 30% observed at a soil $CaCO_3$ contents near 0.25% by mass. This was similar to improvements observed by Lee et. al. (2022) wherein a V_s increase near 30 m/s was observed near a calcite content of 0.25%. Data from **Figure 3.9** also illustrates the importance of solution composition including the presence of yeast extract and

bicarbonate additions in treatment solutions. All columns receiving solutions without yeast extract and bicarbonate exhibited lower $CaCO_3$ contents and consequently obtained lower final V_s values. **Supplemental Figure 3.3** further presents the relationship between $CaCO_3$ precipitation magnitudes and supplied yeast extract and bicarbonate and **Supplemental Figure 3.4** presents the relationship between final V_s measurements and supplied yeast extract and bicarbonate.

Figure 3.10 presents SEM images of materials obtained from the bottom 2 cm of select acetate column specimens. $CaCO_3$ contents at the bottom layers of the columns ranged from 0% to 2% by mass depending on the column's yeast extract and bicarbonate conditions. **Figure 3.10a** shows images of specimens from Column A_100 mM BC_Biotic_A_Ph. As shown, some small and poorly formed crystals can be observed on particle surfaces. **Figure 3.10b to 3.10d** present images of specimens from Columns A_100 mM BC_Biotic_Px_Ph, A_100 mM BC_Biotic_D_Ph, and A_100 mM BC_Abiotic_A_Ph wherein much less crystals are observed, consistent with the lower soil $CaCO_3$ contents measured in this column. In contrast, images from Columns A_0 mM BC_Biotic_A_Ph and A_0 mM BC_Abiotic_A_Ph (**Figure 3.10e to 3.10f)** illustrated the presence of clean particle surfaces with no clear presence of $CaCO_3$ crystals, consistent with the minimal soil $CaCO_3$ measured in these columns. **Supplemental Figure 3.5** presents images of particle surfaces from similar columns at higher magnifications. In these images some bacterial impressions can be observed on crystal surfaces in all specimens that received solutions containing yeast extract. Some impressions could also be observed in specimens receiving solutions without yeast extract, albeit at a much lower frequency. Columns receiving solutions without bicarbonate also exhibited bacterial impressions, indicating the presence of bacterial growth despite more minimal $CaCO_3$ precipitation. **Supplemental Figure 3.6** presents images of specimens obtained

from the top 2 cm of select columns. As shown, almost no precipitated crystals can be observed, consistent with the low measured $CaCO_3$ values at this location. Bacterial impressions can still be observed in specimens containing yeast extract, however, suggesting the presence of thin mineral coatings may have still existed on particle surfaces. **Figure 3.11** presents images of all acetate columns after treatments. As shown, all columns showed little change visually; however, consistent with SEM images, some visible $CaCO_3$ precipitation can be observed at the base of Column A_100 mM BC_Biotic_A_Ph (**Figure 3.11a)**.

3.1.3 Conclusions

A series of soil column experiments were performed to up-scale treatment strategies developed in earlier acetate batch experiments. Column experiments allowed for examination of trends observed in batch experiments regarding the influence of treatment strategy, treatment solution conditions, oxygen source, microbial nutrients, and inorganic carbon. The use of soil columns also allowed for investigation of non-destructive monitoring of geophysical and biochemical changes with repeated treatment injections. In all experiments, solutions were designed to enrich native bacteria and were either phased to allow for stimulation injections prior to cementation or applied concurrently wherein cementation was initiated immediately without prior enrichment. Experiments provided mixed results, with columns receiving solutions with bicarbonate and yeast extract achieving appreciable calcium carbonate and some detectable microbial activity, while columns receiving solutions lacking bicarbonate and yeast extract achieved much less precipitation. Results suggest that aerated columns achieved greater improvement than similar columns receiving oxygen via peroxide additions and dissolved oxygen in solutions, however, the magnitudes of precipitation reactions attributable to abiotically-induced reactions versus

biomediated reactions remained somewhat unclear. The most improved column received concurrent injections with bicarbonate and yeast extract additions (A_100 mM BC_Biotic_A_C) and achieved a V_s increase of 43 m/s at mid-height and a maximum soil $CaCO_3$ content near 2% by mass at the column base after 36 days, although improvement appeared to be highly non-uniform. It should be noted that similar V_s improvements at mid-height could likely be achieved following a single 250 mM Ca^{2+} ureolytic MICP treatment (DeJong 2022), suggesting that this process produced significantly less $CaCO_3$ even when accounting for the much lower supplied Ca^{2+} concentrations. Despite this, results from these columns suggest that microbial acetate oxidation may be feasible pathway for generating $CaCO_3$, although further work needs to be performed to truly understand the benefits afforded by the biomediated process when compared to similar abiotic columns. In particular, the presence of some bacterial growth and abiotic precipitation during mixing in columns lacking adding yeast extract obfuscated these results and made the contribution of biological activity less definitive in the most improved biotic aerated columns. Despite these insights, limited improvement in all acetate columns suggested that further work may be needed to refine this process, particularly when attempting to enrich native microorganisms and that precipitation reactions resulting from the oxidation of other organic acids might also be further considered.

3.2 Citrate Soil Column Experiment

3.2.1 Introduction

Previous batch experiments illustrated that microbial citrate oxidation may provide the ability to generate CaCO3 and other minerals, however, this mechanism had not yet been investigated in more representative porous media. Following the earlier acetate oxidation soil columns which achieved mixed results and lower improvement levels than expected, it was unclear if the citrate oxidation pathway could possibly achieve greater improvement magnitudes due to the precipitation of other minerals such as calcium citrate in addition to $CaCO_3$. Earlier batch experiments suggested that solutions containing 25 mM calcium, 50 mM citrate, 100 mM bicarbonate, and 0.2 g/L yeast extract with an initial pH of approximately 7.35 resulted in the greatest precipitation magnitudes and this was used as a baseline treatment solution for soil columns. Similar to acetate oxidation soil columns, citrate oxidation soil column experiments were designed to further explore the success of similar solutions under conditions more representative of porous media with some important differences. Experiments were specially designed to assess differences in (1) oxygen supply mechanisms through experiments that were either aerated, received no additional oxygen beyond that achieved during mixing (dissolved oxygen), or receiving oxygen release compounds (calcium peroxide), (2) the presence or absence of yeast extract intended to alter cell growth, (3) differences in treatment sequences including phased columns that received stimulation injections first followed by cementation injections and concurrent columns that received only cementation injections, and (4) the presence or absence of sodium bicarbonate. A summary of all 12 citrate soil column experiments is provided in **Table 3.3**. As shown, all experiments were named according to the following convention: (i) the first term describes the inclusion of citrate at either a lower 50 mM (C1) or higher 100 mM initial concentrations (C2), (ii) the second term describes the sodium bicarbonate (BC) concentration, (iii)

the third term describes the presence (Biotic) or absence (Abiotic) of yeast extract intended to promote cell growth, (iv) the fourth term describes the supply of oxygen via either peroxide additions (Px), aeration via air sparging (A), or dissolved oxygen included from equilibration with atmospheric conditions (D), and (v) the use of either phased (Ph) or concurrent (C) injections.

3.2.2 Materials and Methods

3.2.2.1 Soil Columns

All columns contained Monterey Sand (D_{10} of 0.55 mm, D_{30} of 0.85 mm, D_{60} of 1.4 mm), a poorly-graded clean sand that was identical to that used in previous batch experiments. Specimens were prepared in 15.2 cm tall and 7.6 cm in inner diameter hollow acrylic cylinders and Monterey Sand materials were placed to achieve an initial relative density of approximately 40% and pore volumes (PV) of approximately 250 mL using moist tamping and six lifts. Soil column specimens included PFTE caps at both ends with barbed fittings for solution exchange as well as bender element sensors and solution sampling ports. Porex plastic filter materials, with pore sizes ranging from 125 µm to 175 µm, were placed between the caps and the soil to minimize soil particulate losses during injections. Each column was subjected to a total stress of approximately 100 kPa applied through a reaction frame that exerted a vertical force onto the column's top caps. This stress was maintained throughout the experimental duration. The applied stress of 100 kPa aimed to replicate conditions encountered within a saturated soil layer at a depth near 10 meters. Columns were treated from the bottom upwards to ensure uniform saturation and minimize heterogeneity in transport resulting from solution density differences. Three sampling ports and three bender element ports were positioned along the column height at varying distances from the injection port. The ports were located at 3.50 cm (bottom port), 8.56 cm (middle port), and 13.67 cm (top port)

from the base of the columns. Bender element sensors were installed at a distance of 8.56 cm from the base of the columns. For columns requiring air sparging, a small air diffuser was connected to a tube placed 3.50 cm from the base of the columns and was connected to a small air pump (Hittop 4W 110 gal/hr. two-outlet air pump). All columns were treated using constant flow rate peristaltic pumps. The top of the columns was connected to effluent tubes that drained into solution reservoirs to prevent desaturation and the intrusion of atmospheric oxygen intrusion during and after injections. **Figure 3.12** presents an image of the citrate soil column experiments.

3.2.2.2 Treatment Solutions & Injections

Following preparation, all columns were saturated with deionized water. Prior to stimulation and cementation treatment injections each column received 1.5 PV of treatment solutions every two days at a flowrate of 11 mL/min, intended to fully replace residing pore fluids. Following results from the earlier acetate oxidation columns, all columns received phased treatments wherein solutions were applied in two phases. In all columns, 4 stimulation injections were applied once every two days (8 days total), contained no calcium, and were intended to enrich organic acid oxidizing microorganisms prior to cementation. Following stimulation, all columns then received 14 cementation solution injections once every two days (28 days total) wherein solutions were first applied at lower calcium and citrate concentrations for the first 7 injections (i.e., “low cement”) and were then increased for the last 7 injections (i.e., “high cement”). Ten columns received stimulation solutions with 50 mM sodium citrate, low cementation solutions with 50 mM sodium citrate and 25 mM calcium chloride, and high cementation solutions with 100 mM sodium citrate and 50 mM calcium chloride along with varying yeast extract additions (0 g/L vs. 0.2 g/L), varying sodium bicarbonate additions (0 mM vs. 100 mM), and the addition or absence of 1 mM calcium

peroxide depending on the oxygen supply mechanisms considered. Columns receiving these lower initial concentrations are designated with “C1”. Two other columns received stimulation solutions with 100 mM sodium citrate, low cementation solutions with 100 mM sodium citrate and 50 mM calcium chloride, and high cementation solutions with 200 mM sodium citrate and 100 mM calcium chloride along with varying yeast extract additions (0 g/L vs. 0.2 g/L), varying sodium bicarbonate additions (0 mM vs. 100 mM), and the addition or absence of 1 mM calcium peroxide depending on the oxygen supply mechanisms considered. Columns receiving these higher initial concentrations are designated with “C2”. Similar to acetate columns, the considered oxygen supply mechanisms included air sparging (aeration), the inclusion of oxygen from mixing under atmospheric conditions (dissolved oxygen), and the inclusion of calcium peroxide as an oxygen release compound (peroxide). Columns receiving air sparging received air injections after applying treatment injections by pumping air through a diffuser (39.3 mm diameter, 15 mm thick) connected to a small pump for 30 minutes immediately after each stimulation and cementation injection at a flowrate of approximately 22 mL/min.

During treatments, all columns received 4 stimulation injections once every two days intended to achieve sufficient citrate-oxidation activity. Following stimulation injections, all columns received 14 cementation injections applied once every two days in two different 7 injection sequences. During the first 7 cementation injections (referred to as “Low Cement”), applied solutions were similar to previous stimulation solutions but included the addition of either 25 mM (C1 columns) or 50 mM (C2 columns) calcium. For the last 7 cementation injections (referred to as “High Cement”), concentrations of included calcium chloride and sodium acetate were doubled while all other solution additions remained the same (100 mM citrate and 50 mM calcium in C1

columns, 200 mM citrate and 100 mM calcium in C2 columns). The rationale for doubling the concentrations of calcium chloride and sodium acetate was to investigate if higher improvement magnitudes could be achieved per injection following the establishment of sufficient microbial activity. Immediately following the last cementation injection, all columns were rinsed with 10 PV of a $CaCO_3$-equilibrated solution to remove soluble reaction byproducts while mitigating the potential for $CaCO_3$ dissolution. The $CaCO_3$ solution was prepared by equilibrating 0.2 g/L of solid reagent-grade $CaCO_3$ (≥99.0%, Thermo Fisher Scientific, Waltham, MA) with deionized water and removing all mineral solids using a 0.2-µm filter before injecting into the columns. All columns were destructively sampled immediately following rinse injections.

3.2.2.3 Biochemical Sampling and Monitoring

Aqueous samples were collected from the middle sampling ports at various time points during both the stimulation and cementation phases of the experiment. All samples were obtained using sterile needles and syringes (Fisher Scientific). Collected samples were used for both pH measurements completed immediately after sampling as well as calcium and acetate assay measurements. During stimulation injections, aqueous samples for pH measurements were collected immediately after each injection, 24 hours after each injection, and 48 hours after each injection. During cementation injections, aqueous samples for pH measurements were collected immediately after each injection and 48 hours after each injection. For cementation injections 1, 3, 6, 9, 12, and 14, however, pH samples were also collected 24 hours after each injection. pH samples were approximately 4 mL in volume and were measured immediately upon collection using a semi-micro pH electrode and meter system (Orion Versa Star Meter, Thermo Fisher) and then discarded. The pH meter was calibrated daily using three buffers (4.01, 7.00, and 10.01) and

had an accuracy of ± 0.05 pH units. During stimulation, samples for calcium and citrate assays were collected immediately before and after each injection, 24 hours after each injection, and 48 hours after each injection. During cementation, samples for calcium and citrate assays were collected immediately before and after each injection. For cementation injections 1, 3, 6, 9, 12, and 14, however, additional samples were collected 4 hours, 24 hours, and 48 hours after injections. **Table 3.4** provides a summary of the aqueous sampling schedule during the stimulation and cementation phases of the experiment.

Aqueous samples for calcium and citrate measurements were 1 mL in volume and were immediately acid-stabilized using 1 mL of 1M HCl to prevent further biological activity after collection. All samples were then frozen until chemical measurements were completed. To further prepare the samples for analysis, all calcium and citrate samples were clarified using 0.45-µm cellulose acetate centrifuge spin-filters. Citrate measurements were performed using a colorimetric citrate assay kit (BioAssay Systems). This kit utilizes enzyme-coupled reactions to produce a red colorized product when mixed with diluted samples. The absorbance values of these samples were measured at 570 nm using a microplate spectrophotometer. To minimize the effects of acidic solutions on enzyme-catalyzed reactions, all acetate samples were pH-adjusted to near 7 using 0.5 M NaOH. Additionally, all samples were diluted using Millipore water prior to assays to ensure that concentrations were within the range of the citrate colorimetric assay (0 to 400 µM citrate). Calcium measurements were conducted using a second colorimetric calcium assay kit (BioAssay Systems). This kit utilizes reagent-based reactions to generate a blue colorized product when mixed with diluted samples. The absorbance values of these samples were measured at 612 nm using a microplate spectrophotometer. Unlike citrate and acetate measurements, no pH adjustment

was required for calcium measurements as the calcium assay reaction did not rely on enzymes. Similarly, all samples were diluted using Millipore water to achieve concentrations within the range of the calcium colorimetric assay (0 to 5 mM calcium). **Supplemental Figure 3.13** presents example calibration data for both the calcium and citrate assays.

3.2.2.4 Geophysical Measurements

Shear wave velocity (V_s) measurements were obtained using horizontally oriented bender element pairs positioned within soil columns at the middle bender element port location (8.56 cm from column bases). V_s measurements were conducted using two bender element sensors (y-poled, Piezo Inc.) placed at known sensor spacings. To ensure sensor waterproofing, bender elements were carefully coated with epoxy, electronics max, and an insulating coating, following established procedures outlined in Gomez et al. (2017). The transmitted bender element sensors were energized with a 24V, 100 Hz square wave, and the resulting signals from the receiving bender elements were measured and recorded using an oscilloscope at a sampling frequency of 1 MHz. The arrival times of the shear waves and the corresponding signals were interpreted visually, and the V_s values were calculated based on the measured sensor spacings. Initial V_s values for all columns ranged between 130 m/s and 159 m/s prior to treatments.

3.2.2.5 Soil Calcium Carbonate ($CaCO_3$) Content Measurements

Following all treatments, all columns were destructively sampled and partitioned along their length into eight discrete sections (approximately 2 cm thick). Soil sections were then oven-dried and homogenized to yield subsamples for $CaCO_3$ content measurements. Soil $CaCO_3$ content was

quantified in accordance with ASTM D4373 by reacting $CaCO_3$ with 1M hydrochloric acid (HCl) to generate CO_2 and a corresponding increase in test chamber pressure (ASTM, 2014). Calibration relationships between expected pressure changes and known masses of $CaCO_3$ were used to determine $CaCO_3$ contents for soil samples from the observed chamber pressures. At least three measurements were completed for each soil section. Although present, $CaCO_3$ content measurements were unable to quantify other non-carbonate mineral quantities such as calcium citrate which were present in these experiments.

3.2.2.6 Scanning Electron Microscope (SEM) Imaging

Scanning electron microscope (SEM) images were completed with a FEI Thermo Apreo-S Scanning Electron Microscope using an acceleration voltage of 2 kV, a beam current of 13 pA, and magnifications of 100x, 200x, and 1000x. All soil specimens were oven-dried and mounted onto imaging pedestals using carbon tape prior to imaging.

3.2.3 Results and Discussion

Figure 3.13 presents pH measurements in time for all citrate soil column experiments. Responses for experiments receiving solutions containing sodium bicarbonate are shown in **Figure 3.13a**, while those receiving solutions without bicarbonate are presented in **Figure 3.13b**. During the stimulation phase, the aerated bicarbonate experiment without yeast extract exhibited the highest pH values with measurements after 48 hours indicating values as large as 8.5 to 9. Coupled with insights from earlier batch experiments, these large pH values suggested that biological activity may have been present in this column despite the absence of yeast extract. In all other columns,

pH values remained between 7 and 8 during stimulation with the exception of the peroxide and dissolved oxygen experiments containing bicarbonate which achieved larger pH values near 8.7 immediately after the first stimulation injection. Once columns were transitioned to cementation injections, similar pH values between 7 and 8 were observed in all columns with cyclic changes in pH values indicating pH decreases after injections and gradual pH rises throughout the 48 hour residence periods. When comparing responses between columns with and without yeast extract, interestingly similar pH behaviors were observed without YE with higher pH values over the course of treatment in some cases. Furthermore, experiments lacking bicarbonate also exhibited similar pH rise during stimulation injections as experiments containing bicarbonate and comparable pH values during cementation between 6.5 and 7.5. Although pH trends are influenced by other citrate oxidation and calcium carbonate precipitation, pH increases during stimulation and cyclic changes in pH during cementation suggested that citrate oxidizing bacteria may have been enriched in some columns prior to cementation with the possibility for calcium carbonate precipitation during cementation injections. Limited differences between experiments containing and lacking yeast extract were also consistent with the earlier batch experiment results and suggested the possibility that microbial activity may have been present in columns that did not receive yeast extract.

Figure 3.14 presents the calcium concentration measurements in time for all citrate soil columns during select cementation injections (CEM 1, CEM 3, CEM 6, CEM 8, CEM 9, CEM 12, and CEM 14). Calcium degradation in time was expected to indicate calcium carbonate mineral formation; however, the precipitation of other non-carbonate minerals such as calcium citrate could have also resulted in some appreciable calcium consumption during these experiments. As

shown, during CEM 1, CEM 3, and CEM 6, columns received solutions with initial calcium concentrations of either 25 mM or 50 mM and during CEM 8, CEM 9, CEM 12, and CEM 14, columns received solutions with initial calcium concentrations of either 50 mM or 100 mM. Although differences in the initial concentrations were observed due to different applied concentrations and reactions occurring during injections, low calcium concentrations below 10 mM indicative of reaction completion were only observed in columns C1_100 mM HCO_3_Biotic_Px_Ph, C1_100 mM HCO_3_Biotic_D_Ph, and C1_100 mM HCO_3_Biotic_A_Ph all which contained both yeast extract and bicarbonate.

Column C1_100 mM BC_Biotic_Px_Ph received solutions with yeast extract, bicarbonate, and peroxide and showed detectable calcium degradation during cementation (**Figure 3.14a**). However, the reaction rate in this column appeared to reduce with subsequent injections at higher concentrations with more limited reactions occurring during CEM 14. Column C1_100 mM BC_Biotic_D_Ph received solutions with bicarbonate and yeast extract and used dissolved oxygen as its only oxygen source and was able to consistently degrade calcium to near zero (**Figure 3.14c**). Column C1_0 mM BC_Biotic_Px_Ph (**Figure 3.14e**) was similar to the column shown in **Figure 3.14a** but received solutions that included no sodium bicarbonate. As shown, some small calcium degradation can be observed, however, calcium consumption is much less than the similar column with sodium bicarbonate. Similarly, Column C1_0 mM BC_Biotic_D_Ph which received solutions with yeast extract, no bicarbonate, and dissolved oxygen as its only oxygen source (**Figure 3.14g**) also exhibited little change in calcium whereas its bicarbonate-containing counterpart (Figure **3.14c**) had much greater calcium consumption. Column C2_100 mM BC_Biotic_Px_Ph (**Figure 3.14i**) receiving solutions with higher calcium concentrations of 50

mM (first 7 injections) and 100 mM (last 7 injections), as well as correspondingly higher citrate concentrations and yeast extract, bicarbonate, and peroxide showed appreciable calcium consumption; however, only ~50% of the injected calcium was utilized within 48 hours. The reaction rate in this column also significantly slowed down by the 14th cementation injection (CEM14). Column C1_100 mM BC_Biotic_A_Ph (**Figure 3.14k**) received solutions containing yeast extract and bicarbonate and received oxygen via aeration and was shown to be able to fully degrade the supplied calcium after 48 hours with the exception of Cementation 8 during which activity may have been inhibited by the increase in applied citrate and calcium concentrations.

Supplemental Figure 3.7 presents similar data with calcium concentrations in time for all columns plotted together for respective cementation injections. As shown, all columns receiving solutions without yeast extract showed minimal calcium degradation, suggesting that yeast extract may provide key nutrients needed for enrichment and growth of citrate oxidizing bacteria. When comparing different oxygen sources, the aerated and dissolved oxygen columns generally achieved more rapid calcium consumption followed by columns receiving peroxide amended solutions. This outcome was surprising and suggested that sufficient dissolved oxygen may be present in solutions after mixing and that additional oxygen supplementation may not be necessary at least when bicarbonate is present. It is important to acknowledge the potential contribution of abiotic precipitation reactions in these systems, however, which may not have required that citrate be fully consumed in order to achieve full consumption of the supplied calcium.

Figure 3.15 presents aqueous calcium concentrations for select columns versus corresponding solution pH measurements for select cementation injections. It was expected that decreases in calcium would occur at near constant pH due to buffer of solutions by carbonate species, but that increases in pH may result at near zero calcium concentrations due to continued citrate oxidation in the presence of precipitation. As shown all columns, showed minimal changes in pH with calcium reductions. In columns achieving near complete precipitation, only Column C1_100 mM BC_Biotic_Px_Ph exhibited a pH increase at near zero calcium, with minimal pH changes in other Columns such as C1_100 mM BC_Biotic_D_Ph and C1_100 mM BC_Biotic_A_Ph, which also contained yeast extract and achieved low calcium concentrations. These results suggested that although pH may provide an effective monitoring metric for acetate oxidation, monitoring pH changes during cementation may provide a less meaningful metric for monitoring of the citrate oxidation process.

Figure 3.16 presents measurements of solution citrate concentrations in time for select columns during specific stimulation and cementation injections (STIM4, CEM 1, CEM 3, CEM 6, CEM 9, CEM 12, and CEM 14). In all experiments, citrate concentration reductions in time were expected to be reflective of microbial citrate oxidation, but also reflected possible reductions related to calcium citrate precipitation. During STIM 4, CEM 1, CEM 3, and CEM 6, columns received solutions with initial citrate concentrations of either 50 mM or 100 mM and during CEM 9, CEM 12, and CEM 14, columns received solutions with initial citrate concentrations of either 100 mM or 200 mM. As shown, all columns that received solutions containing yeast extract and 100 mM bicarbonate (**Figure 3.16a, 3.16c, 3.16k)** were shown to exhibit appreciable citrate degradation with the rate of degradation in all of these columns, with the exception of the aerated column,

slowing down during the last cementation injection (CEM 14). When comparing degradation rates, the aerated column (C1_100 mM BC_Biotic_D_Ph) shown in **Figure 3.16k** exhibited the highest citrate degradation rates, followed closely by dissolved oxygen column (**Figure 3.16c)** and peroxide columns (**Figure 3.16a, 3.16e)**. The biotic peroxide column receiving solutions with either 100 mM or 200 mM citrate (**Figure 3.16i**) was also able to rapidly degrade the 100 mM citrate initially but slowed down significantly by the last injection which contained 200 mM citrate. Columns with yeast extract but without bicarbonate (**Figure 3.16e and 3.16g**) were also able to degrade citrate although these citrate reductions appeared to result in more limited calcium consumption (**Figure 3.14e and 3.14g)**. All columns without yeast extract showed minimal changes in citrate with the exception of the aerated column (**Figure 3.16l**), however, the reaction rate and magnitude of citrate degradation observed in this column was significantly lower than its yeast extract containing counterpart (**Figure 3.16k)**. All columns receiving solutions containing yeast extract experienced reductions in reaction rates during the last cementation injection, which may have resulted from the higher citrate and calcium concentrations applied in later injections. Overall, these results indicated that yeast extract was required to achieve citrate oxidation and that citrate consumption from abiotic calcium citrate precipitation was likely minimal. While bicarbonate is not be required to enable citrate degradation, for most cases citrate was degraded more quickly in the presence of bicarbonate when compared to similar columns without bicarbonate. Finally, the aerated column appeared to achieve the most rapid citrate oxidation, however, oxidation using peroxide additions and dissolved oxygen was still shown to be viable. Similar results are also presented in **Supplemental Figure 3.8** wherein citrate concentrations in time for all columns were plotted together for select injections.

Figure 3.17 presents corresponding aqueous calcium and citrate concentrations measured in select columns during select cementation injections. In biotic columns it was expected that progressive reductions in citrate would result in corresponding reductions in calcium, whereas abiotic columns with bicarbonate may experience calcium reductions without citrate degradation related to abiotic precipitation reactions. As shown in **Figure 3.17**, biotic columns with bicarbonate experienced progressive calcium and citrate reductions, however, with near full degradation of the supplied calcium and citrate achieved in most cases. Biotic columns without bicarbonate, however, showed some ability to degrade citrate but exhibited minimal changes in supplied calcium concentrations. Abiotic columns without yeast extract showed minimal trends for all cases suggesting that yeast extract is needed to enable cell growth and citrate oxidation activity. However, citrate oxidation activity only appears to result in appreciable precipitation when bicarbonate is present.

Figure 3.18 presents soil shear wave velocity (V_s) measurements in time following stimulation for all columns during cementation injections. **Figures 3.18a and 3.18b** presents measured V_s values, however, **Figures 3.18c and 3.18d** present V_s values which were normalized by initial uncemented values (V_{s0}). All columns had initial shear wave velocities (V_{s0}) between 130 m/s and 159 m/s prior to any treatment injections (**Supplemental Figure 3.2**) and comparable values at the start of cementation injections. As shown in **Figure 3.18a and 3.18c**, the dissolved oxygen column containing yeast extract and bicarbonate (C1_100 mM BC_Biotic_D_Ph) achieved a significantly higher final V_s value of 278 m/s and higher final normalized V_s ratio (V_s / V_{s0}) near 2.2 when compared to all other columns. Interestingly, its aerated counterpart (C1_100 mM BC_Biotic_A_Ph), which exhibited the greatest citrate oxidation activity achieved a small final V_s of 171 m/s with a final normalized V_s ratio (V_s/ V_{s0}) near 1.7. This was unexpected; however, it

was hypothesized that the process of aerating columns may have disturbed the formation of interparticle bonds each injection. All other columns showed no significant increases in V_s indicating that oxygen sources, yeast extract additions, and bicarbonate additions are important considerations during treatment solution design. Although the larger V_s improvements observed in the aerated and dissolved oxygen columns receiving solutions with yeast extract and bicarbonate were encouraging, further characterization of the cementation distributions were needed in order to more fully understand the extent and magnitudes of improvements within all columns.

Figure 3.19 presents measured soil $CaCO_3$ contents along column lengths for all columns. Each measurement represents the average of three soil $CaCO_3$ content measurements, however, included error bars indicate ± one standard deviation for measurement. As shown, soil $CaCO_3$ precipitation was relatively uniform in all columns with only small decreases in $CaCO_3$ contents with increasing distance from the injection ports for columns with detectable $CaCO_3$. Only four columns achieved measurable $CaCO_3$, while all other columns had soil $CaCO_3$ content measurements that were below the detection limit (< 0.1% $CaCO_3$ by mass). Vs and $CaCO_3$ are closely related as an increase in $CaCO_3$ typically result in an increase in Vs. Consistent with the earlier V_s data, the dissolved oxygen column containing bicarbonate and yeast extract achieved the highest soil $CaCO_3$ contents between 0.6% and 0.3% by mass at all locations. In contrast, all columns without yeast extract or bicarbonate showed no measurable $CaCO_3$ contents at all locations. Interestingly, the aerated column containing yeast extract and bicarbonate achieved lower $CaCO_3$ values than its dissolved oxygen counterpart near 0.3% at all locations. This was unexpected as the greater abundance of oxygen in the aerated column and greater citrate oxidation was expected to achieve greater $CaCO_3$ precipitation. That being said, this significant difference may have also altered enriched microbial

communities aside from differences in citrate oxidation and precipitation conditions. While surprising, this outcome was consistent with the earlier V_s trends, however, and suggested that the disturbance of interparticle bonds from aeration may have been more minimal than initially expected. Regardless, this data, paired with the earlier geophysical and biogeochemical data, indicates that bicarbonate and yeast extract are important factors in the citrate precipitation process and no additional oxygen sources may be required to enable citrate oxidation beyond the dissolved oxygen introduced into solutions during the solution mixing process.

Figure 3.20 presents relationships between the final shear wave velocities (V_{sf}) and corresponding soil $CaCO_3$ contents. Final Vs values are shown in **Figure 3.20a and 3.20b** and final normalized V_s values are shown in **Figure 3.20c and 3.20d**. Trends versus average $CaCO_3$ contents for each column are presented in **Figure 3.20a and 3.20b** and trends versus soil $CaCO_3$ contents at mid-height are presented in **Figure 3.20c and 3.20d**. As shown, increases in $CaCO_3$ resulted in a near linear increase in soil shear wave velocities. **Figure 3.20d** compares soil $CaCO_3$ contents and V_s values measured at the mid-height location. In this plot, a trend of increasing V_s with increasing $CaCO_3$ is observed as expected and but V_s improvements in the most highly cemented column exceed those observed in previous studies for the same $CaCO_3$ content. For example, a ΔVs of 171 m/s was shown to correlate to a soil $CaCO_3$ content near 1.2% by mass (Lee et al. 2023), while the dissolved oxygen citrate column achieved this same improvement at a lower soil $CaCO_3$ content near 0.4% by mass. While unexpected, it is hypothesized that a greater ΔVs improvement may have resulted from a lower soil $CaCO_3$ content in the citrate column due to the possible presence of other minerals such as calcium citrate or calcium oxalate which may have been generated and cemented soils, but would not have been accounted for during soil $CaCO_3$ content measurements.

Figure 3.20 also shows the importance of including yeast extract and bicarbonate additions in treatment solutions with all columns receiving solutions without yeast extract and bicarbonate exhibiting lower $CaCO_3$ contents and consequently lower V_s improvements. This trend is also highlighted in **Supplemental Figure 3.9** which presents the relationship between increased soil $CaCO_3$ contents and supplied yeast extract and bicarbonate concentrations. Additionally **Supplemental Figure 3.10** presents the relationship between final V_s values and supplied yeast extract and bicarbonate concentrations.

Figure 3.21 presents SEM images of specimens obtained from the bottom 2 cm of all citrate columns. As shown previously, soil $CaCO_3$ contents at the base of all columns ranged from 0% to 0.62% by mass depending on treatment strategy. As shown in the most highly cemented Column C1_100 mM BC_Biotic_D_Ph (**Figure 3.21c**) an abundance of small elongated crystals were observed on particle surfaces, which appeared to be more similar to morphologies expected for calcium citrate as opposed to calcium carbonate. When considering differences between all columns, precipitate crystals were generally only observed when yeast extract and bicarbonate were present, with the exception of the higher concentration Column C2_100 mM BC_Abiotic_Px_Ph, which exhibited some surficial precipitation despite the lack of yeast extract. Similar images of particle surfaces at higher magnifications are presented in **Supplemental Figure 3.11** wherein differences in crystal morphologies between specimens can be more clearly distinguished. In these images, some bacterial impressions can be observed on crystals present in soil specimens receiving solutions containing yeast extract while no bacterial impressions are present in the absence of yeast extract. Interestingly, precipitates observed in columns receiving solutions without bicarbonate still exhibited some bacterial impressions despite limited $CaCO_3$

precipitation being present in these columns. Images of specimens obtained from the top 2 cm of select columns are also shown in **Supplemental Figure 3.12**. When comparing images of the top and bottom location, more minimal precipitates can be observed consistent with soil $CaCO_3$ content measurements. However, bacterial impressions can still be observed on particle surfaces in specimens containing yeast extract. **Figure 3.22** presents images of the final condition for all citrate columns. All columns containing yeast extract showed visible signs of precipitation with the highest concentration column C2_100 mM BC_Biotic_Px_Ph showing the most visible precipitation from the outside of the columns (**Figure 20i**). Some columns appeared to show greater localization of precipitation near the bottom of the column (i.e., Columns C1_100 mM BC_Biotic_D_Ph and C1_0 mM BC_Biotic_Px_Ph) which was unexpected considering the rather uniform soil $CaCO_3$ contents observed earlier (**Figure 3.19**). The spatial uniformity of other precipitates such as calcium citrate, however, were not quantified and may have suggested greater non-uniformity for non-carbonate precipitates if such phases had been characterized. Similar to SEM images, all columns receiving solutions without yeast extract showed no visible signs of precipitation with the exception of the highest concentration column (**Figure 22j**) and the aerated abiotic column (**Figure 22l)**. It is likely that the presence of higher chemical concentrations and air injections in these columns may have accelerated abiotic precipitation, despite the lack of appreciable microbial growth and activity.

3.2.3 Conclusions

A series of soil column experiments were performed to investigate citrate oxidation treatment strategies considered in earlier batch experiments. Column experiments allowed for further examination of trends observed in batch experiments including the influence of treatment

strategies, treatment solution compositions, oxygen sources, microbial nutrients, and inorganic carbon. The use of soil columns also allowed for the investigation of geophysical and biogeochemical changes resulting from repeated treatment injections. In all experiments, solutions were designed to enrich native citrate oxidizing bacteria and enable calcium carbonate precipitation using citrate oxidation activity. Results demonstrated that the microbial oxidation of citrate can be used to mediate calcium carbonate precipitation and improve soils. Columns receiving solutions with dissolved oxygen, citrate, calcium chloride, bicarbonate, and yeast extract achieved the highest levels of improvement followed by similar columns receiving aeration. These responses reflected both the enrichment of citrate oxidizing bacteria, abiotic precipitation events, as well as biocementation mediated by microbial citrate oxidation. Improvements assessed using V_s measurements and soil $CaCO_3$ contents indicated that citrate oxidation resulted in greater improvements than that obtained with acetate oxidation strategies as well as the precipitation of other non-carbonate minerals expected to be calcium citrate. Future work remains needed, however, to characterize the enriched microbial communities resulting from these treatment strategies, better quantify and identify the unknown mineral phases that may be present, understand the contribution of abiotic precipitation and citrate oxidation on observed precipitation magnitudes, and further explore why greater improvement was observed in the biotic column receiving dissolved oxygen when compared to the similar aerated column, wherein oxygen was more abundant.

Table 3.1. Summary of acetate soil column experiments including solution chemical compositions, presence or absence biological activity, oxygen source, and injection sequence.

	Solution Chemical Composition							
Specimen Name	**Sodium Acetate (mM)[1]**	**Calcium Chloride (mM)[1,2]**	**Sodium Bicarbonate (mM)**	**Yeast Extract (g/L)**	**Calcium Peroxide (mM)**	**Biotic/Abiotic**	**Oxygen Source**	**Injection Sequence[3, 4]**
A_100 mM BC_Biotic_A_C	50 (100)	25 (50)	100	0.2		Biotic	Aerated (A)	Concurrent (C)
A_100 mM BC_Biotic_A_Ph	50 (100)	25 (50)	100	0.2		Biotic	Aerated (A)	Phased (Ph)
A_100 mM BC_Biotic_Px_C	50 (100)	25 (50)	100	0.2	1	Biotic	Peroxide (Px)	Concurrent (C)
A_100 mM BC_Biotic_Px_Ph	50 (100)	25 (50)	100	0.2	1	Biotic	Peroxide (Px)	Phased (Ph)
A_100 mM BC_Biotic_D_Ph	50 (100)	25 (50)	100	0.2		Biotic	Dissolved Oxygen (D)	Phased (Ph)
A_100 mM BC_Abiotic_A_Ph	50 (100)	25 (50)	100			Abiotic	Aerated (A)	Phased (Ph)
A_0 mM BC_Biotic_A_Ph	50 (100)	25 (50)		0.2		Biotic	Aerated (A)	Phased (Ph)
A_0 mM BC_Biotic_Px_Ph	50 (100)	25 (50)		0.2	1	Biotic	Peroxide (Px)	Phased (Ph)
A_0 mM BC_Biotic_D_Ph	50 (100)	25 (50)		0.2		Biotic	Dissolved Oxygen (D)	Phased (Ph)
A_0 mM BC_Abiotic_A_Ph	50 (100)	25 (50)				Abiotic	Aerated (A)	Phased (Ph)

[1] First values present concentrations present in first 7 "low cement" cementation injections. Values in parenthesis present concentrations present in last 7 "high cement" cementation injections.

[2] Calcium chloride was included only during the 14 cementation injections and not during stimulation injections (when present).

[3] Concurrent columns received 14 cementation injections (7 "low cement" and 7 "high cement") over 28 days.

[4] Phased columns received 4 stimulation injections over 8 days followed by 14 cementation injections (7 "low cement" and 7 "high cement") over 28 days.

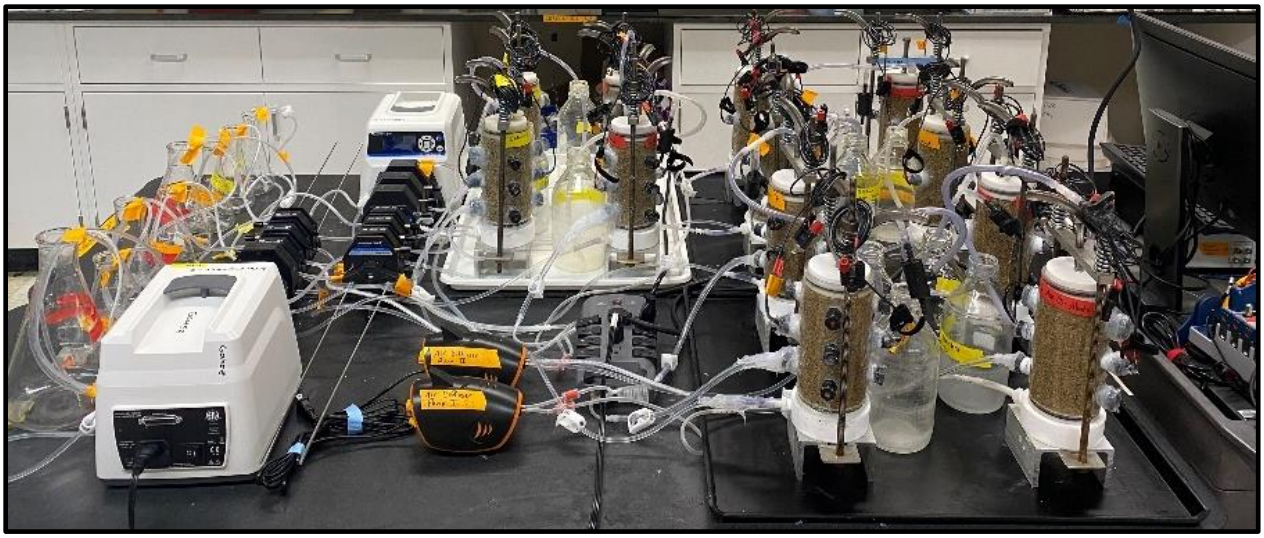

Figure 3.1. Experimental set-up for acetate oxidation soil column experiments.

Table 3.2. Summary of the aqueous sampling schedule during the stimulation and cementation phases of the acetate oxidation soil column experiment for pH, calcium, and acetate measurements.

Treatment Phase	Sampling Protocol	Experiment Days
Stimulation	pH Sampling: ~4 mL samples from middle ports immediately after injections, 24 hr. and 48 hr. after injections	All Stimulation Injections
	Acetate Sampling: 1 mL samples from middle ports before / immediately after injections, 24 hr. and 48 hr. after injections	All Stimulation Injections
Cementation	pH Sampling: ~4 mL samples from middle ports after injections and 48 hrs. after injections	All Cementation Injections
	pH Sampling: ~4 mL samples from middle ports 24 hrs. after injections	Cementation Injections 1, 3, 6, 9, 12, and 14
	Calcium / Acetate Sampling: 1 mL samples of solution from middle ports before / immediately after injections, 4 hrs., 24 hrs., and 48 hrs. after injections	Cementation Injections 1, 3, 6, 9, 12, and 14

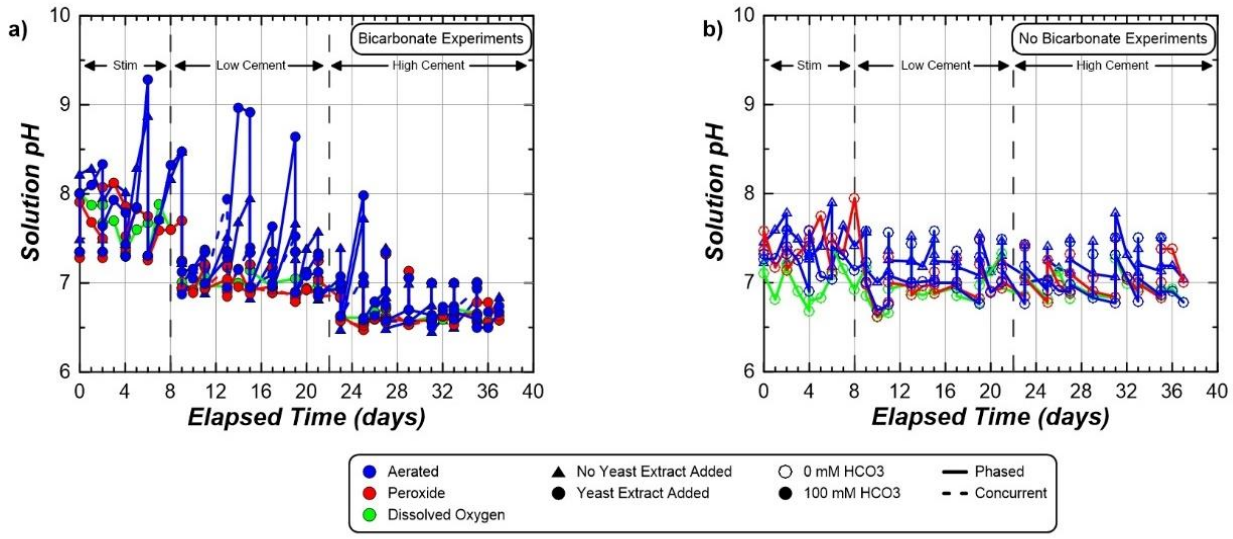

Figure 3.2 Solution pH measurements in time for all acetate oxidation soil column experiments **(a)** with bicarbonate and **(b)** without bicarbonate additions.

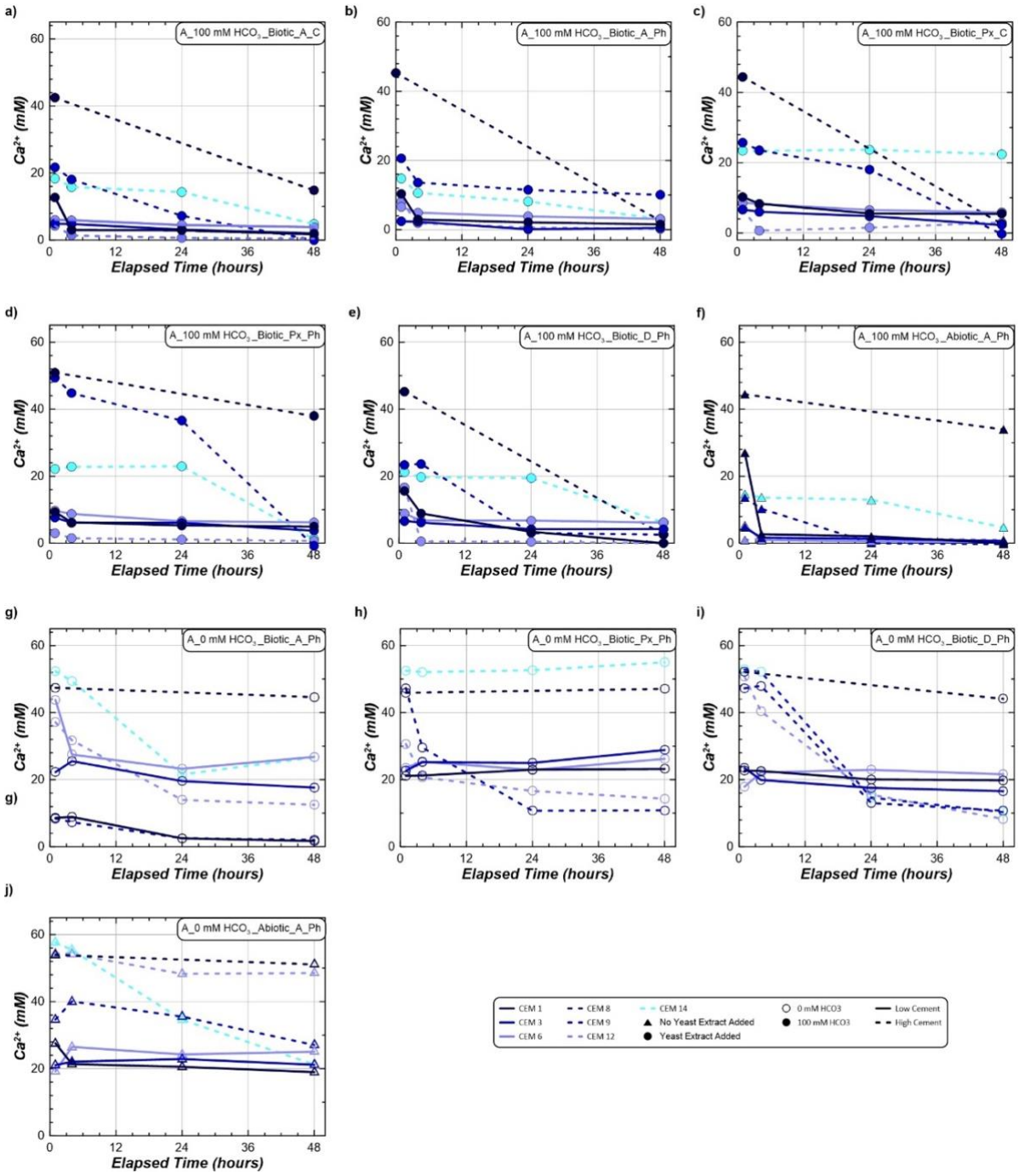

Figure 3.3. Aqueous calcium measurements in time for all acetate oxidation columns in time for select cementation injections. Plots present data from columns (**a)** A_100 mM BC_Biotic_A_C, **(b)** A_100 mM BC_Biotic_A_Ph, **(c)** A_100 mM BC_Biotic_Px_C, **(d)**, A_100 mM BC_Biotic_Px_Ph, **(e)** A_100 mM BC_Biotic_D_Ph, **(f)** A_100 mM BC_Abiotic_A_Ph, **(g)** A_0 mM BC_Biotic_A_Ph, **(h)** A_0 mM BC_Biotic_Px_Ph, **(i)** A_0 mM BC_Biotic_D_Ph, and **(j)** A_0 mM BC_Abiotic_A_Ph .

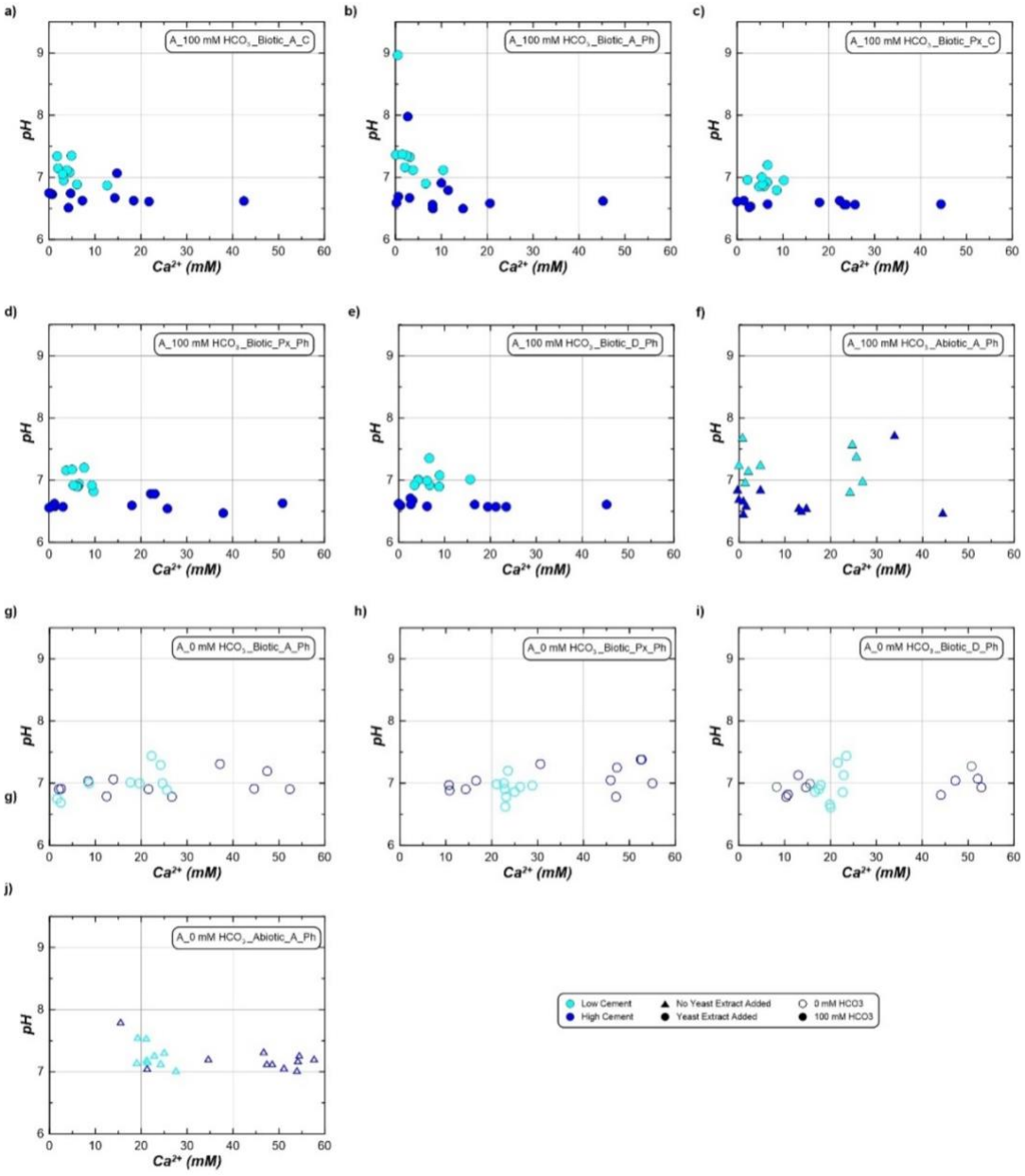

Figure 3.4. Comparison of aqueous calcium measurements versus corresponding pH measurements for all acetate columns in time for select cementation injections. Plots present data from columns (**a)** A_100 mM BC_Biotic_A_C, **(b)** A_100 mM BC_Biotic_A_Ph, **(c)** A_100 mM BC_Biotic_Px_C, **(d)**, A_100 mM BC_Biotic_Px_Ph, **(e)** A_100 mM BC_Biotic_D_Ph, **(f)** A_100 mM BC_Abiotic_A_Ph, **(g)** A_0 mM BC_Biotic_A_Ph, **(h)** A_0 mM BC_Biotic_Px_Ph, **(i)** A_0 mM BC_Biotic_D_Ph, and **(j)** A_0 mM BC_Abiotic_A_Ph .

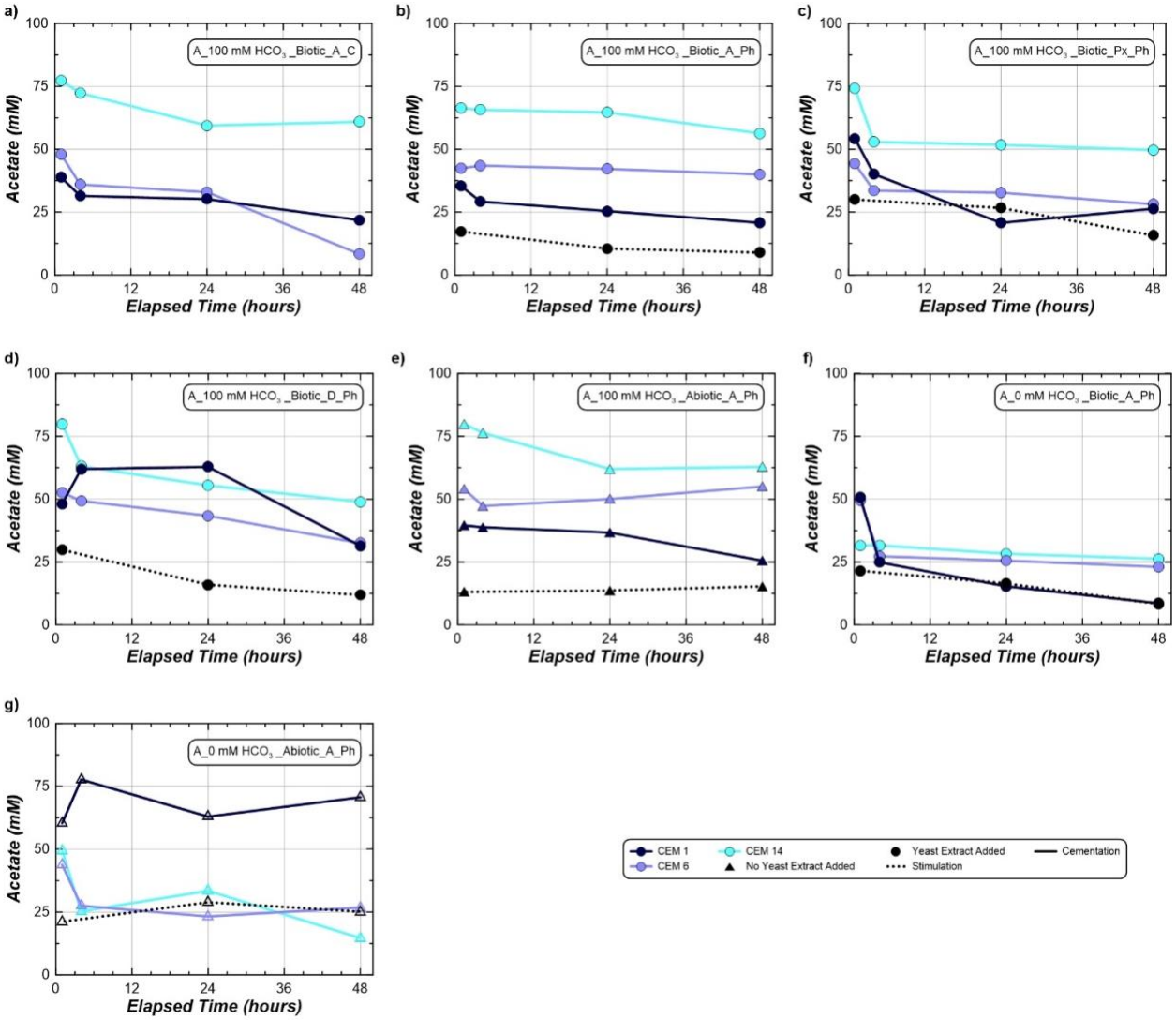

Figure 3.5. Acetate measurements in time for select acetate oxidation columns during select cementation injections. Plots present data from columns: **(a)** A_100 mM BC_Biotic_A_C, **(b)** A_100 mM BC_Biotic_A_Ph, **(c)** A_100 mM BC_Biotic_Px_Ph,, **(d)** A_100 mM BC_Biotic_D_Ph, **(e)** A_100 mM BC_Abiotic_A_Ph, **(f)** A_0 mM BC_Biotic_A_Ph, and **(g)** A_0 mM BC_Abiotic_A_Ph.

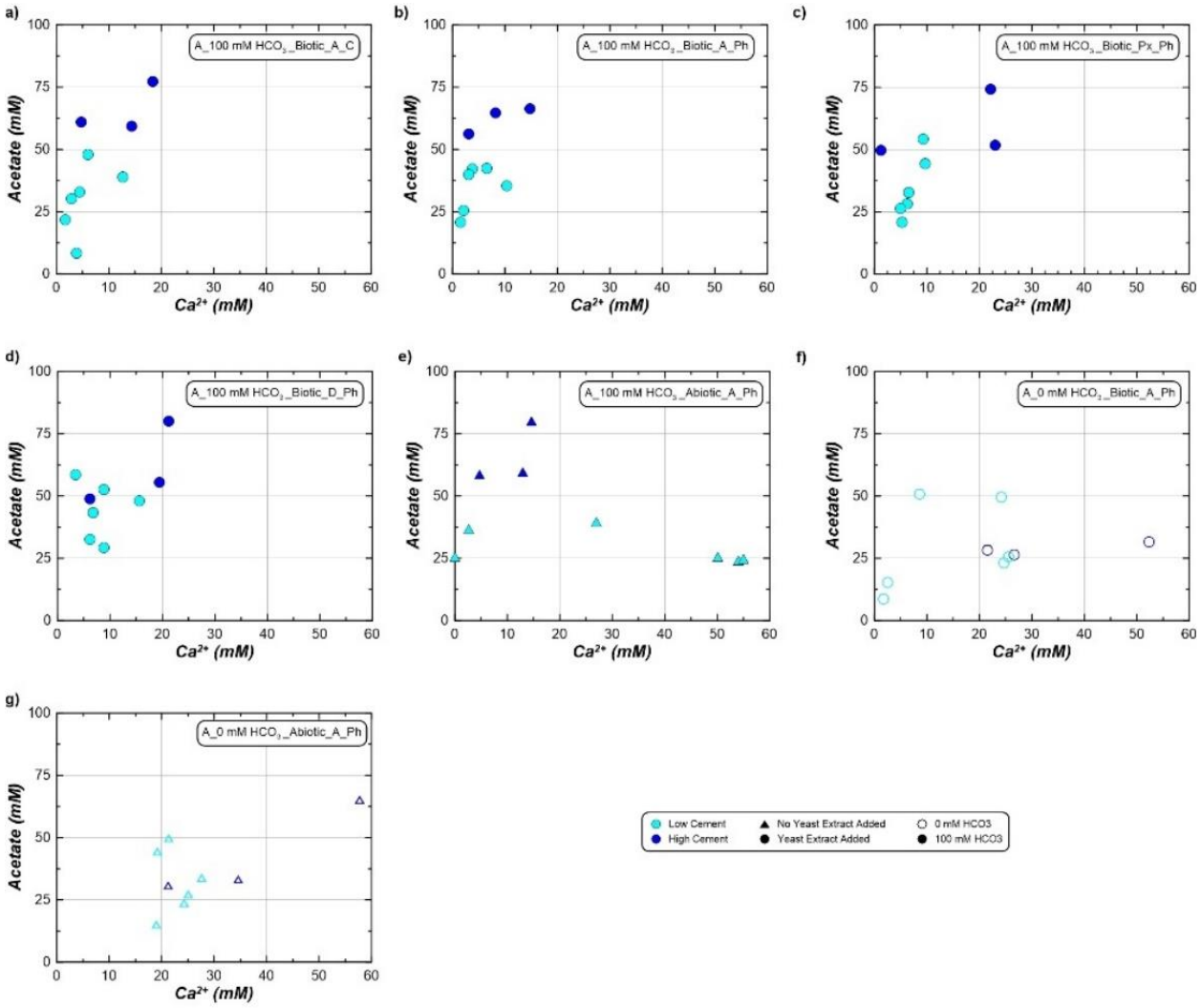

Figure 3.6. Comparison of aqueous calcium and acetate measurements for select acetate oxidation columns for select cementation injections. Plots present data from columns: **(a)** A_100 mM BC_Biotic_A_C, **(b)** A_100 mM BC_Biotic_A_Ph, **(c)** A_100 mM BC_Biotic_Px_Ph, **(d)** A_100 mM BC_Biotic_D_Ph, **(e)** A_100 mM BC_Abiotic_A_Ph, **(f)** A_0 mM BC_Biotic_A_Ph, and **(g)** A_0 mM BC_Abiotic_A_Ph

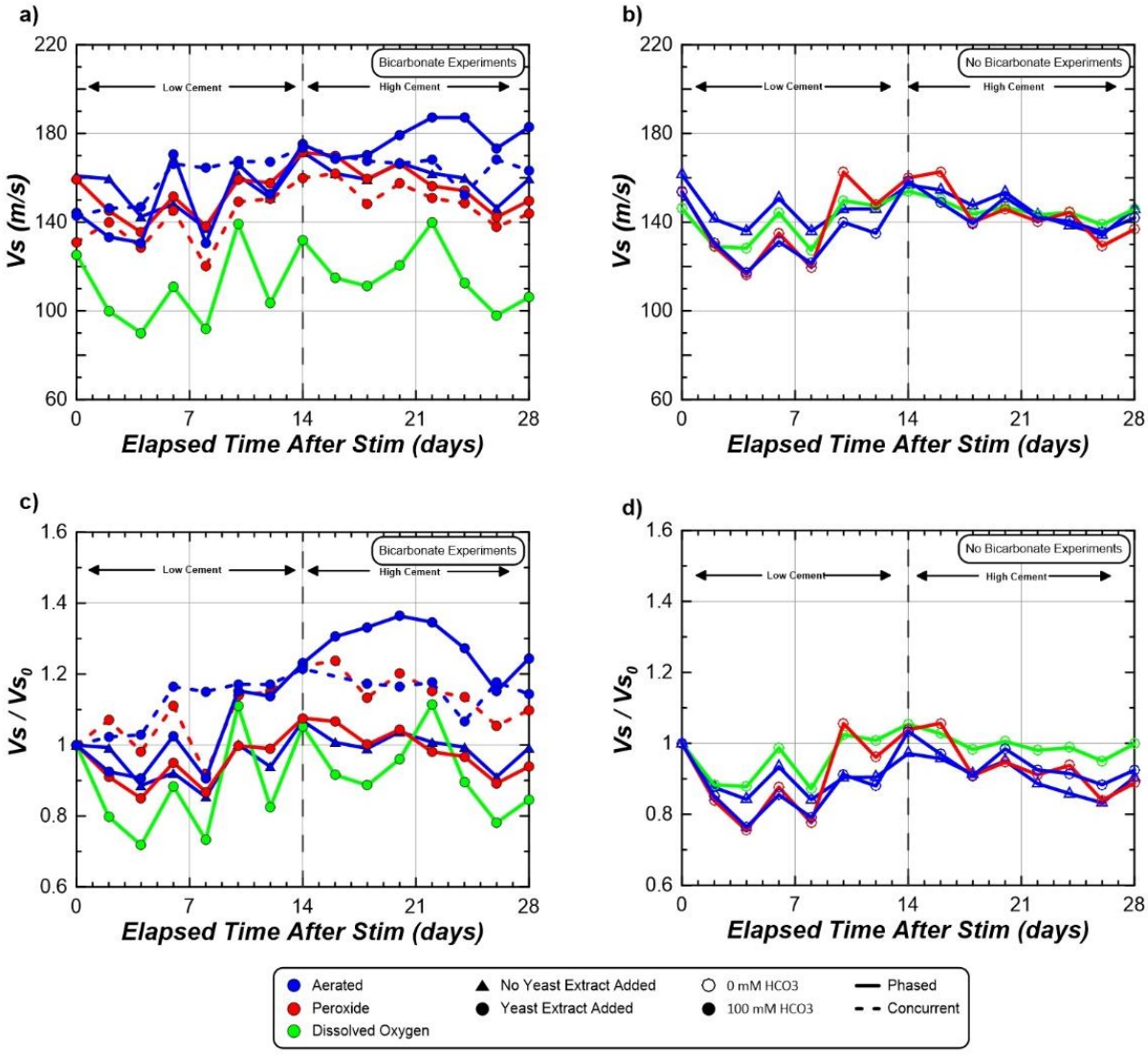

Figure 3.7. Comparisons of **(a, b)** soil shear wave velocities (Vs) and **(c, d)** normalized soil shear wave velocity (Vs/Vs0) versus time after stimulation for all acetate oxidation soil columns. Plots present data for all columns receiving solutions **(a, c)** with 100 mM sodium bicarbonate and **(b, d)** without sodium bicarbonate separately.

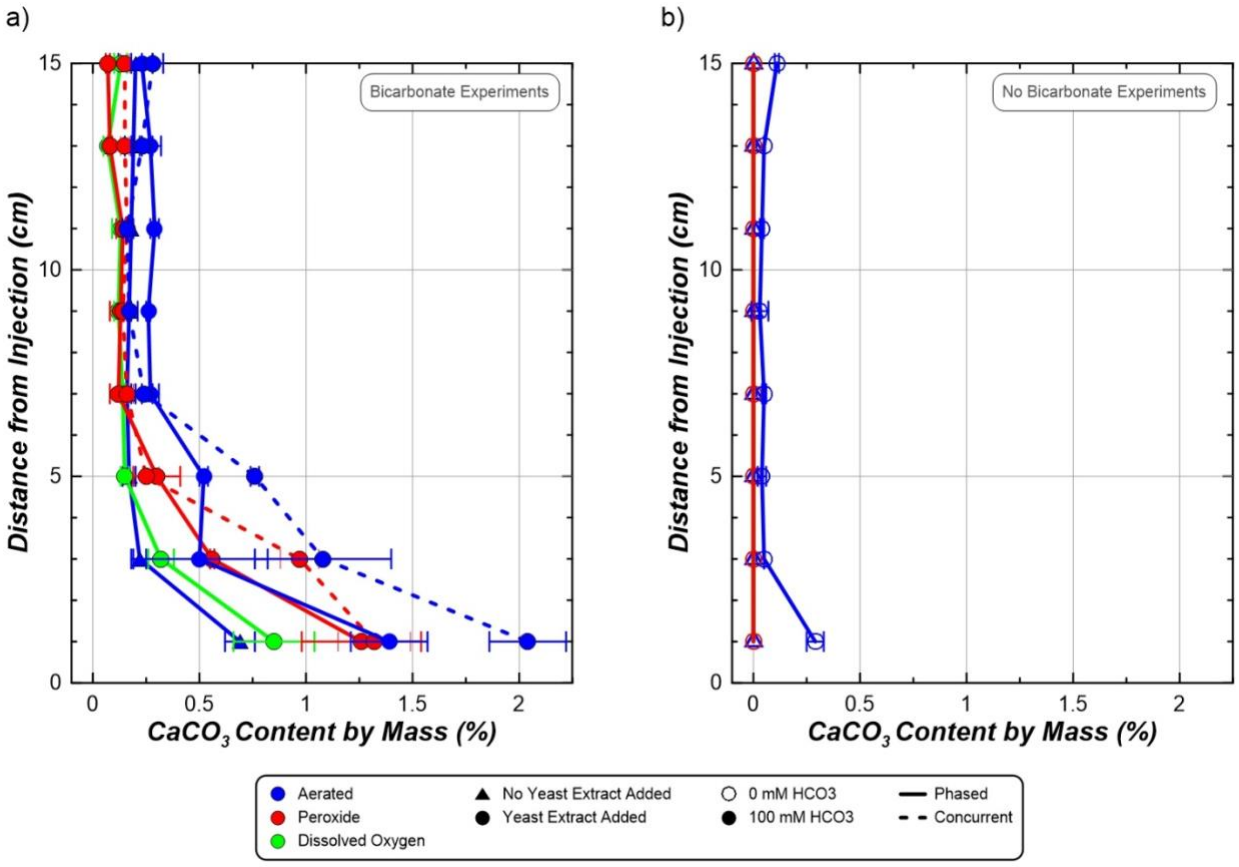

Figure 3.8. Comparisons of soil CaCO3 contents (in % by mass) versus distance from the injection source along all columns receiving solutions **(a)** with 100 mM sodium bicarbonate and **(b)** without sodium bicarbonate. Values indicate the average of three soil $CaCO_3$ content measurements for each location with error bars indicating ± one standard deviation for measurements.

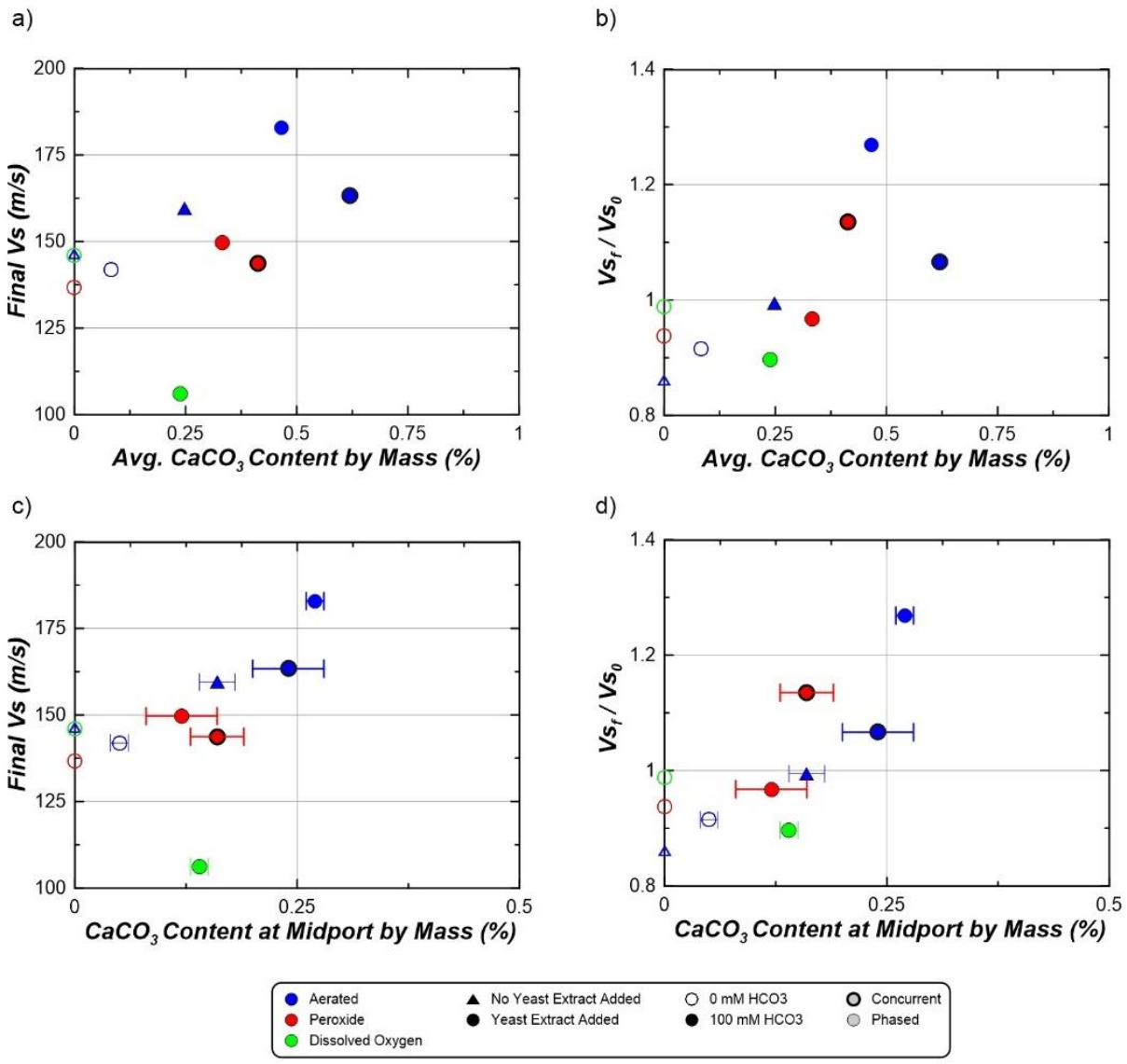

Figure 3.9. Relationships between soil CaCO3 contents and final Vs measurements for all acetate oxidation columns. Comparisons present **(a)** final Vs values versus average CaCO3 contents for entire columns**(b)** normalized final V_s ratios compared to average $CaCO_3$ contents for entire columns , **(c)** final V_s values versus soil $CaCO_3$ contents at the mid-port bender locations for each column, and **(d)** normalized final V_s ratios versus soil $CaCO_3$ contents at the mid-port bender locations for each column.

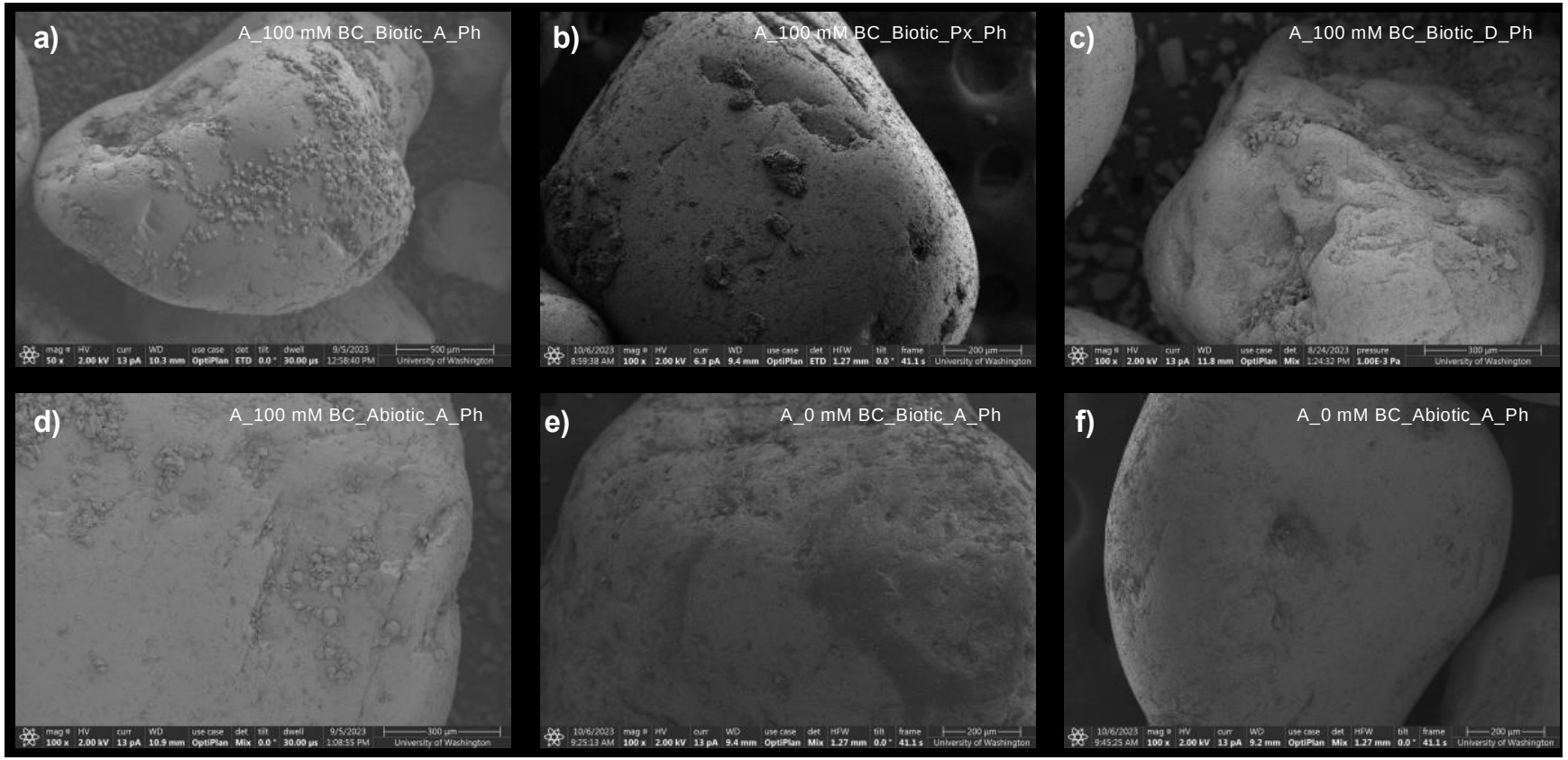

Figure 3.10. Scanning Electron Microscope (SEM) images of specimens obtained from the bottom 2 cm of select acetate oxidation columns. Images are presented for columns: **(a)** Column A_100 mM BC_Biotic_A_C, **(b)** Column A_100 mM BC_Biotic_A_Ph, **(c)** Column A_100 mM BC_Biotic_Px_Ph,, **(d)**, Column A_100 mM BC_Biotic_D_Ph, **(e)** Column A_100 mM BC_Abiotic_A_Ph, **(f)** Column A_0 mM BC_Biotic_A_Ph, and **(g)** Column A_0 mM BC_Abiotic_A_Ph.

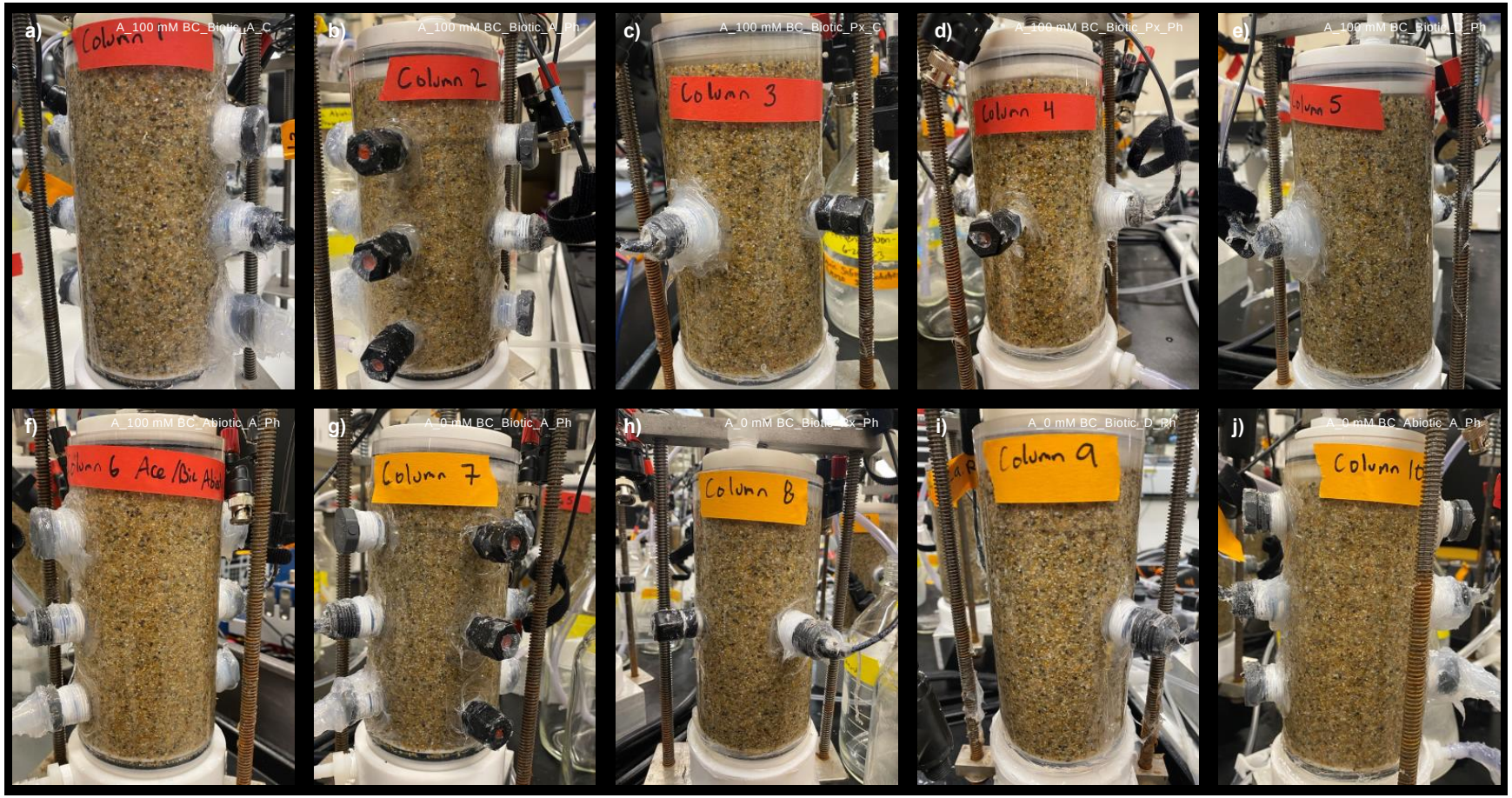

Figure 3.11. Images of the final conditions for all acetate oxidation columns. Images are presented for columns: **(a)** A_100 mM BC_Biotic_A_C, **(b)** A_100 mM BC_Biotic_A_Ph, **(c)** A_100 mM BC_Biotic_Px_C, **(d)** A_100 mM BC_Biotic_Px_Ph, **(e)** A_100 mM BC_Biotic_D_Ph, **(f)** A_100 mM BC_Abiotic_A_Ph, **(g)** A_0 mM BC_Biotic_A_Ph, **(h)** A_0 mM BC_Biotic_Px_Ph, **(i)** A_0 mM BC_Biotic_D_Ph, and **(j)** A_0 mM BC_Abiotic_A_Ph.

Table 3.3. Summary of citrate soil column experiments including solution chemical compositions, presence or absence biological activity, oxygen source, and injection sequence.

	Solution Chemical Composition							
Specimen Name[1]	**Sodium Acetate (mM)[2]**	**Calcium Chloride (mM)[2],,[3]**	**Sodium Bicarbonate (mM)**	**Yeast Extract (g/L)**	**Calcium Peroxide (mM)**	**Biotic/Abiotic**	**Oxygen Source**	**Injection Sequence[4]**
C1_100 mM BC_Biotic_A_Ph	50 (100)	25 (50)	100	0.2		Biotic	Aerated (A)	Phased (Ph)
C1_100 mM BC_Abiotic_A_Ph	50 (100)	25 (50)	100			Abiotic	Aerated (A)	Phased (Ph)
C1_100 mM BC_Biotic_Px_Ph	50 (100)	25 (50)	100	0.2	1	Biotic	Peroxide (Px)	Phased (Ph)
C1_100 mM BC_Abiotic_Px_Ph	50 (100)	25 (50)	100		1	Abiotic	Peroxide (Px)	Phased (Ph)
C1_100 mM BC_Biotic_D_Ph	50 (100)	25 (50)	100	0.2		Biotic	Dissolved Oxygen (D)	Phased (Ph)
C1_100 mM BC_Abiotic_D_Ph	50 (100)	25 (50)	100			Abiotic	Dissolved Oxygen (D)	Phased (Ph)
C1_0 mM BC_Biotic_Px_Ph	50 (100)	25 (50)		0.2	1	Biotic	Peroxide (Px)	Phased (Ph)
C1_0 mM BC_Abiotic_Px_Ph	50 (100)	25 (50)			1	Abiotic	Peroxide (Px)	Phased (Ph)
C1_0 mM BC_Biotic_D_Ph	50 (100)	25 (50)		0.2		Biotic	Dissolved Oxygen (D)	Phased (Ph)
C1_0 mM BC_Abiotic_D_Ph	50 (100)	25 (50)				Abiotic	Dissolved Oxygen (D)	Phased (Ph)
C2_100 mM BC_Biotic_Px_Ph	100 (200)	50 (100)	100	0.2	1	Biotic	Peroxide (Px)	Phased (Ph)
C2_100 mM BC_Abiotic_Px_Ph	100 (200)	50 (100)	100		1	Abiotic	Peroxide (Px)	Phased (Ph)

[1] C1 describes columns with lower initial sodium acetate and calcium concentrations while C2 describes columns with higher initial concentrations.

[2] First values present concentrations present in first 7 "low cement" cementation injections. Values in parenthesis present concentrations present in last 7 "high cement" cementation injections.

[3] Calcium chloride was included only during the 14 cementation injections and not during stimulation injections (when present).

[4] Phased columns received 4 stimulation injections over 8 days followed by 14 cementation injections (7 "low cement" and 7 "high cement") over 28 days.

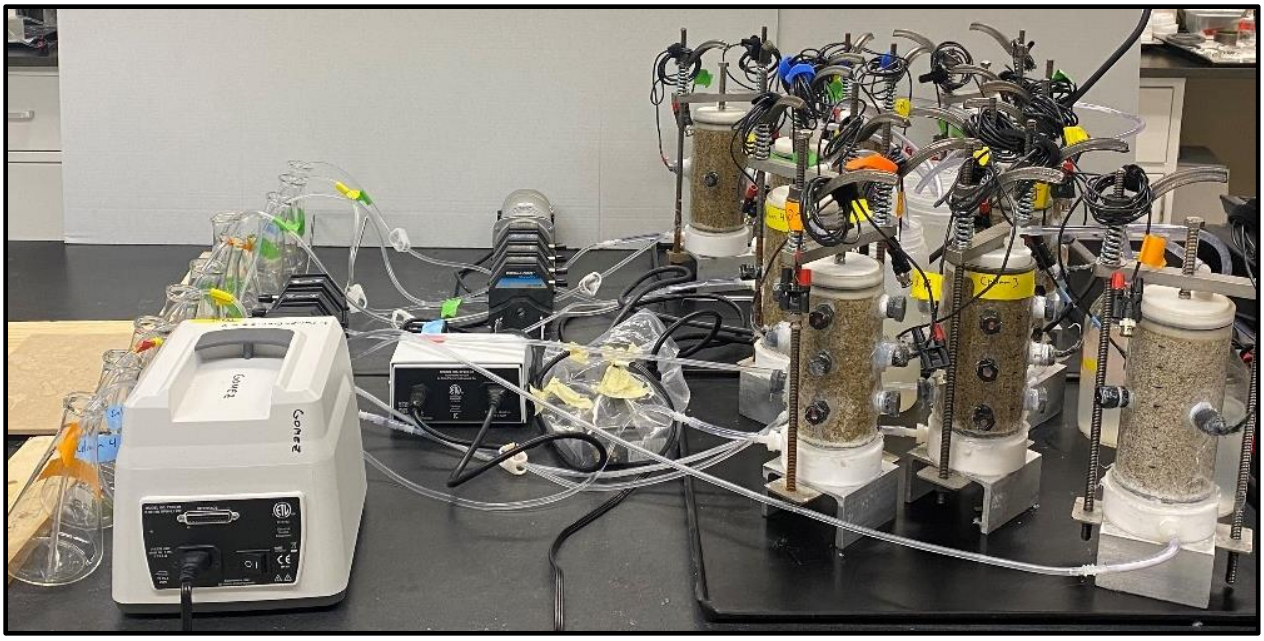

Figure 3.12. Experimental set-up for citrate oxidation soil column experiments.

Table 3.4. Summary of the aqueous sampling schedule during the stimulation and cementation phases of the citrate oxidation soil column experiment for pH, calcium, and citrate measurements.

Treatment Phase	Sampling Protocol	Experiment Days
Stimulation	pH Sampling: ~4 mL samples from middle ports immediately after injections, 24 hr. and 48 hr. after injections	All Stimulation Injections
	Citrate Sampling: 1 mL samples from middle ports before / immediately after injections, 24 hr. and 48 hr. after injections	All Stimulation Injections
Cementation	pH Sampling: ~4 mL samples from middle ports after injections and 48 hrs. after injections	All Cementation Injections
	pH Sampling: ~4 mL samples from middle ports 24 hrs. after injections	Cementation Injections 1, 3, 6, 9, 12, and 14
	Calcium / Citrate Sampling: 1 mL samples of solution from middle ports before / immediately after injections, 4 hrs., 24 hrs., and 48 hrs. after injections	Cementation Injections 1, 3, 6, 9, 12, and 14

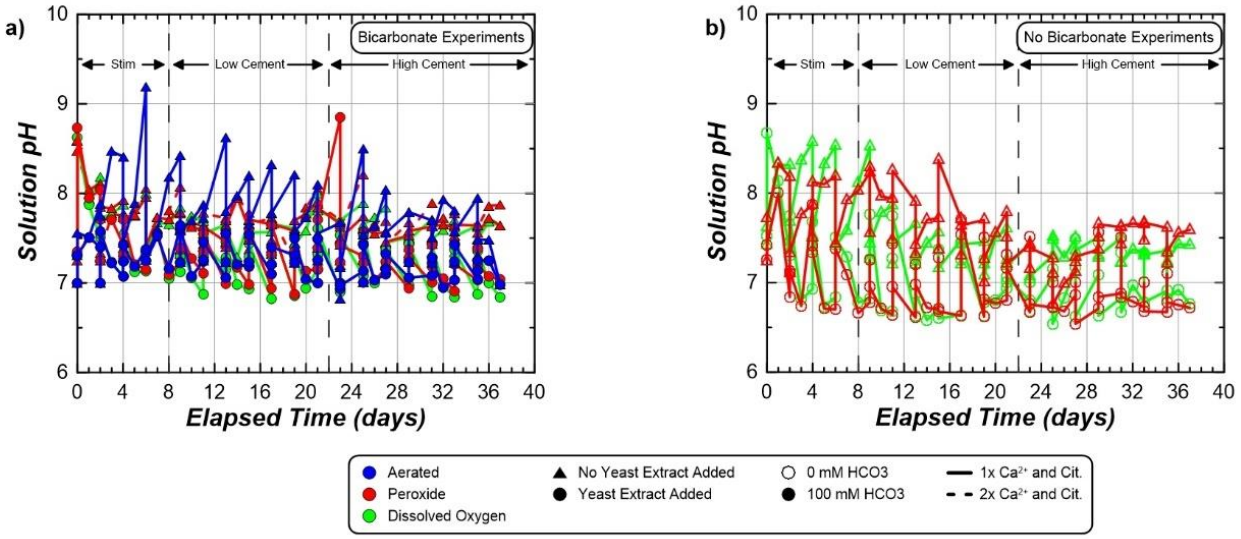

Figure 3.13. Solution pH measurements in time for all citrate oxidation soil column experiments receiving solutions **(a)** with bicarbonate and **(b)** without bicarbonate additions.

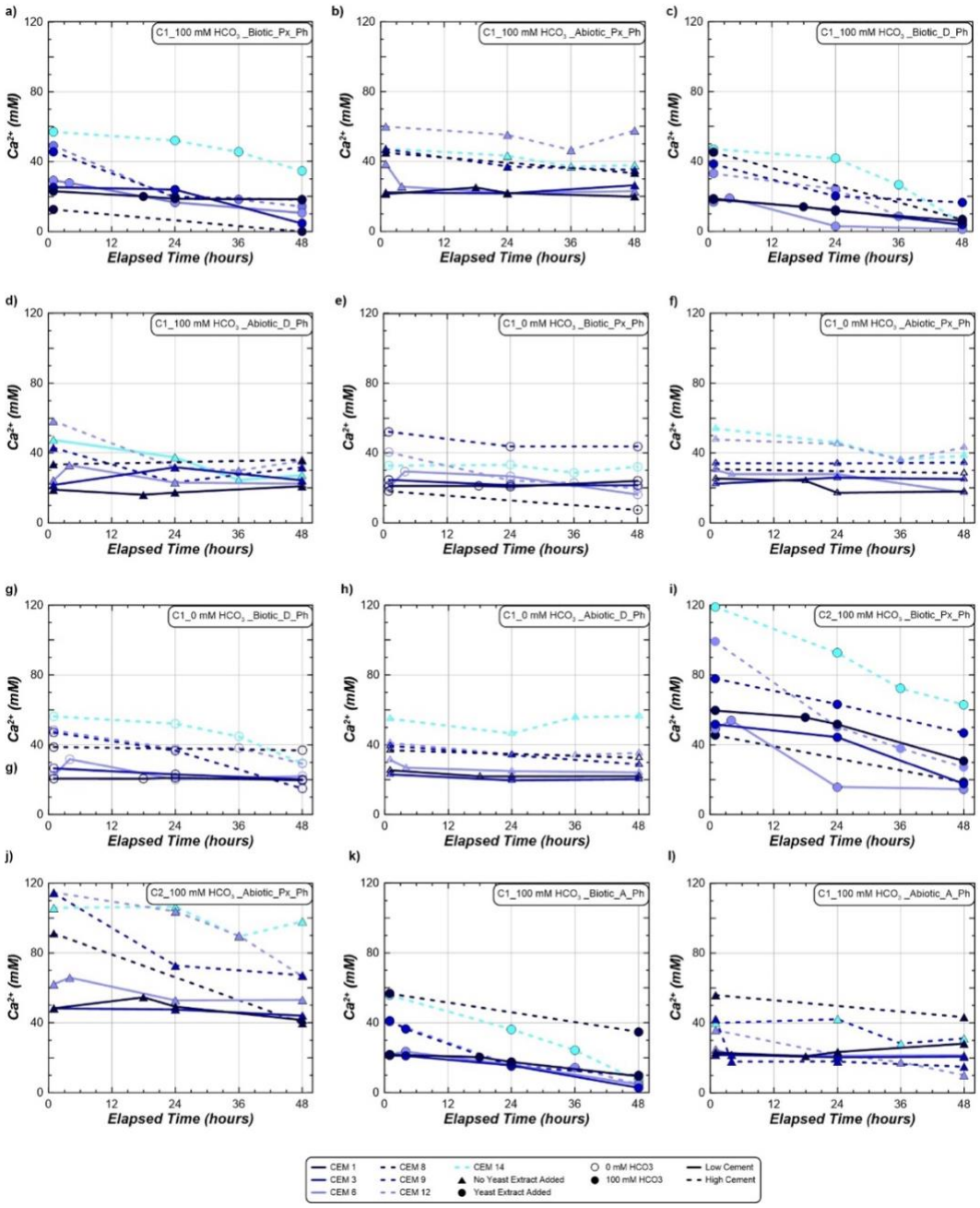

Figure 3.14. Aqueous calcium measurements in time for all citrate oxidation columns in time for select cementation injections. Plots present data from columns: **(a)** C1_100 mM BC_Biotic_Px_Ph, **(b)** C1_100 mM BC_Abiotic_Px_Ph, **(c)** C1_100 mM BC_Biotic_D_Ph, **(d)** C1_100 mM BC_Abiotic_D_Ph, **(e)** C1_0 mM BC_Biotic_Px_Ph, **(f)** C1_0 mM BC_Abiotic_Px_Ph, **(g)** C1_0 mM BC_Biotic_Px_Ph, **(h)** C1_0 mM BC_Abiotic_Px_Ph, **(i)** C2_100 mM BC_Biotic_Px_Ph, **(j)** C2_100 mM BC_Abiotic_Px_Ph, **(k)** C1_100 mM BC_Biotic_A_Ph, and **(l)** C1_100 mM BC_Abiotic_A_Ph.

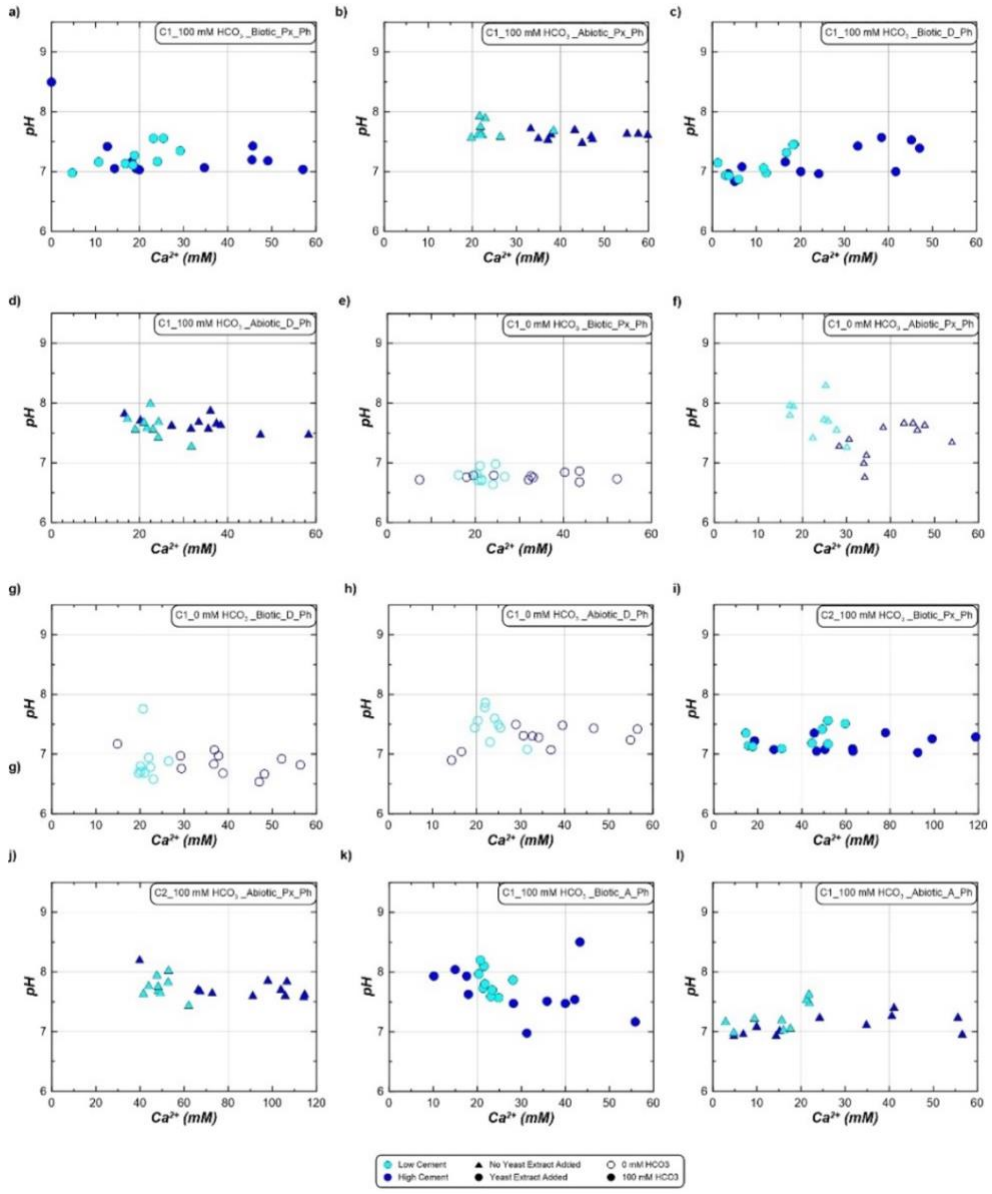

Figure 3.15. Comparison of aqueous calcium measurements versus corresponding pH measurements for all citrate oxidation columns in time for select cementation injections. Plots present data from columns **(a)** C1_100 mM BC_Biotic_Px_Ph, **(b)** C1_100 mM BC_Abiotic_Px_Ph, **(c)** C1_100 mM BC_Biotic_D_Ph, **(d)** C1_100 mM BC_Abiotic_D_Ph, **(e)** C1_0 mM BC_Biotic_Px_Ph, **(f)** C1_0 mM BC_Abiotic_Px_Ph, **(g)** C1_0 mM BC_Biotic_Px_Ph, **(h)** C1_0 mM BC_Abiotic_Px_Ph, **(i)** C2_100 mM BC_Biotic_Px_Ph, **(j)** C2_100 mM BC_Abiotic_Px_Ph, **(k)** C1_100 mM BC_Biotic_A_Ph, and **(l)** C1_100 mM BC_Abiotic_A_Ph.

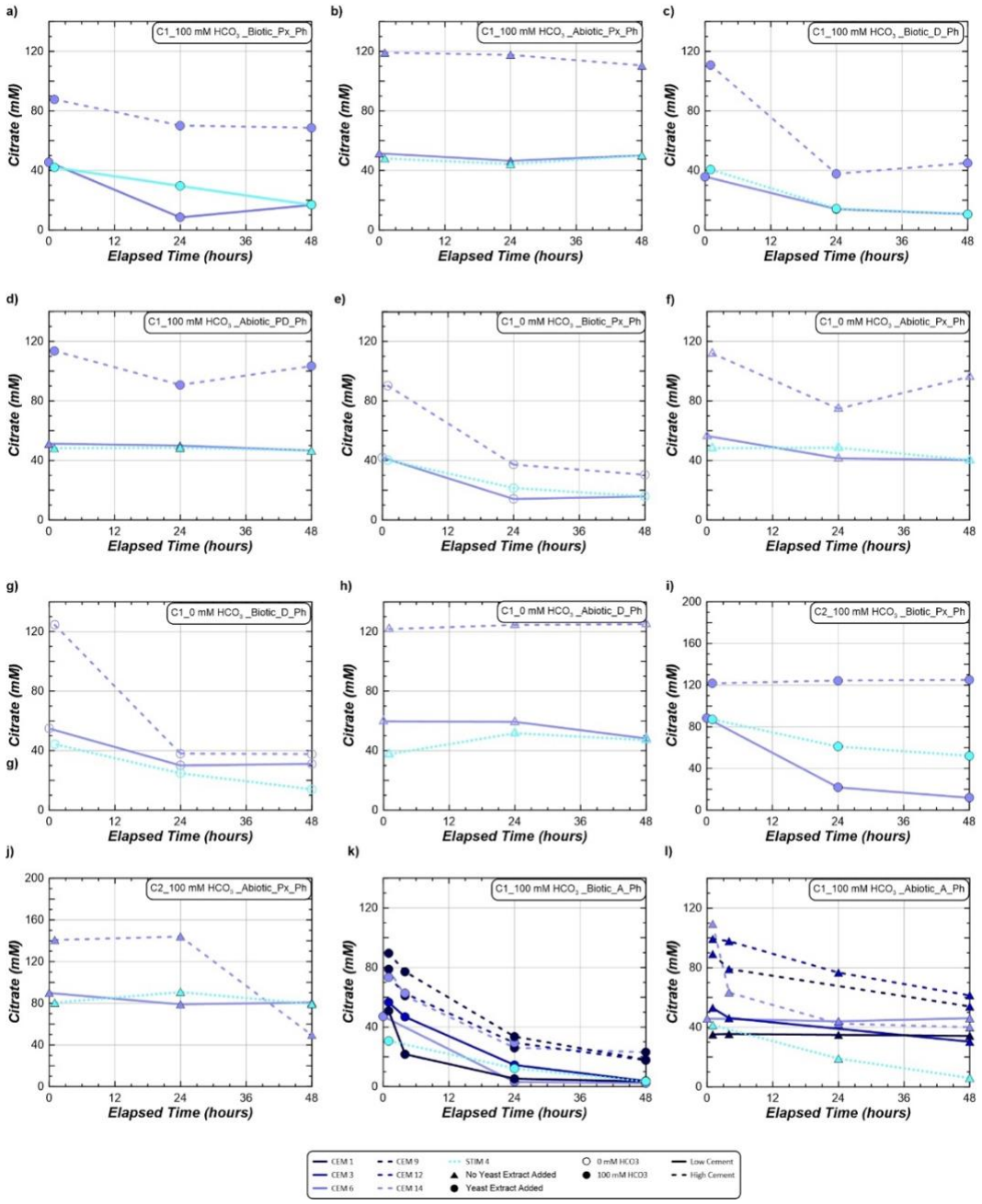

Figure 3.16. Citrate measurements in time for select citrate oxidation columns during select cementation injections. Plots present data from columns: **(a)** C1_100 mM BC_Biotic_Px_Ph, (**b)** C1_100 mM BC_Abiotic_Px_Ph, **(c)** C1_100 mM BC_Biotic_D_Ph, **(d)** C1_100 mM BC_Abiotic_D_Ph, **(e)** C1_0 mM BC_Biotic_Px_Ph, **(f)** C1_0 mM BC_Abiotic_Px_Ph, **(g)** C1_0 mM BC_Biotic_Px_Ph, **(h)** C1_0 mM BC_Abiotic_Px_Ph, **(i)** C2_100 mM BC_Biotic_Px_Ph, **(j)** C2_100 mM BC_Abiotic_Px_Ph, **(k)** C1_100 mM BC_Biotic_A_Ph, and **(l)** C1_100 mM BC_Abiotic_A_Ph.

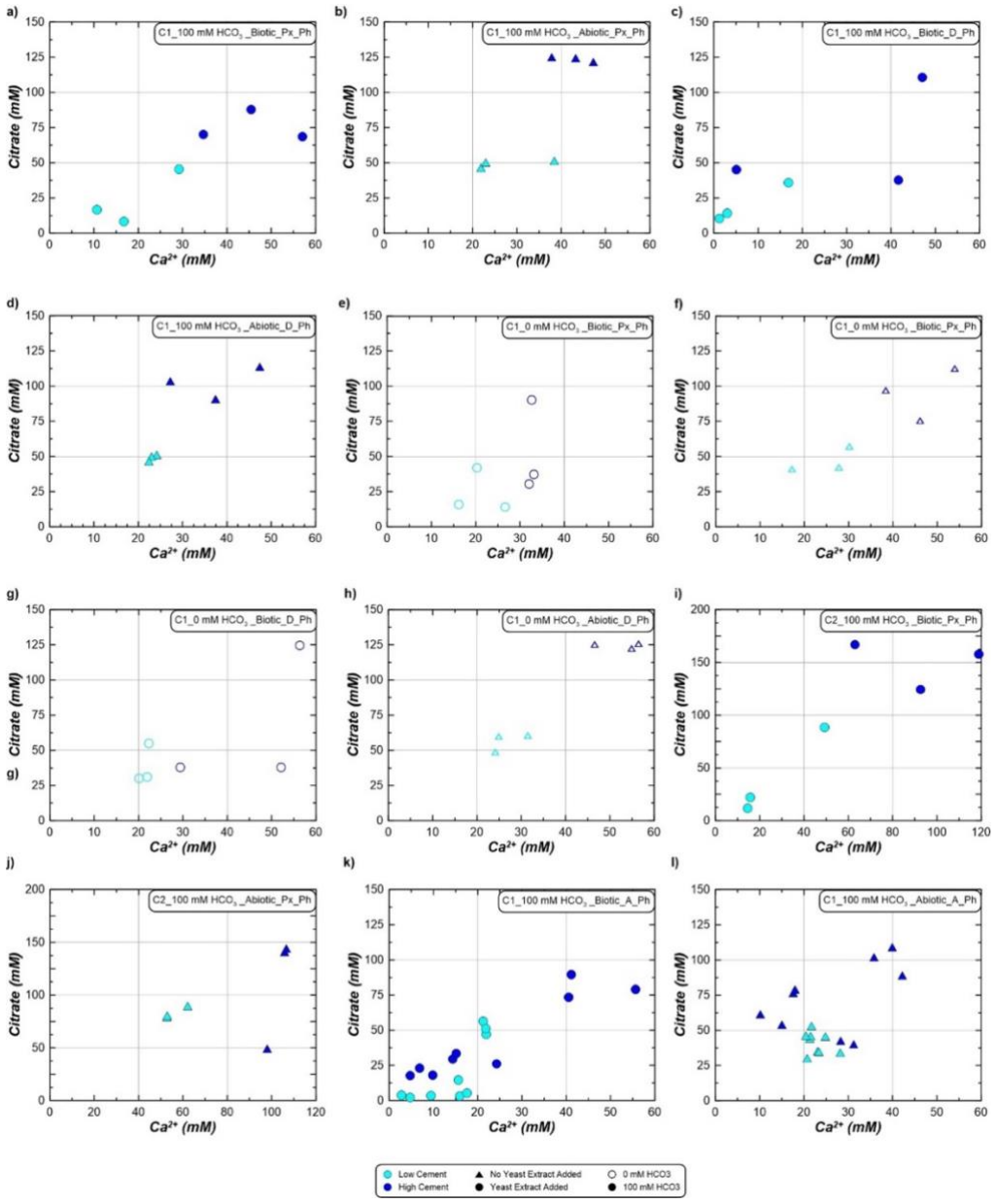

Figure 3.27. Comparison of aqueous calcium and citrate measurements for select citrate oxidation columns for select cementation injections. Plots present data from columns: **(a)** C1_100 mM BC_Biotic_Px_Ph, **(b)** C1_100 mM BC_Abiotic_Px_Ph, , **(c)** C1_100 mM BC_Biotic_D_Ph, **(d)** C1_100 mM BC_Abiotic_D_Ph, **(e)** C1_0 mM BC_Biotic_Px_Ph, **(f)** C1_0 mM BC_Abiotic_Px_Ph, **(g)** C1_0 mM BC_Biotic_Px_Ph, **(h)** C1_0 mM BC_Abiotic_Px_Ph, **(i)** C2_100 mM BC_Biotic_Px_Ph, **(j)** C2_100 mM BC_Abiotic_Px_Ph, **(k)** C1_100 mM BC_Biotic_A_Ph, and **(l)** C1_100 mM BC_Abiotic_A_Ph.

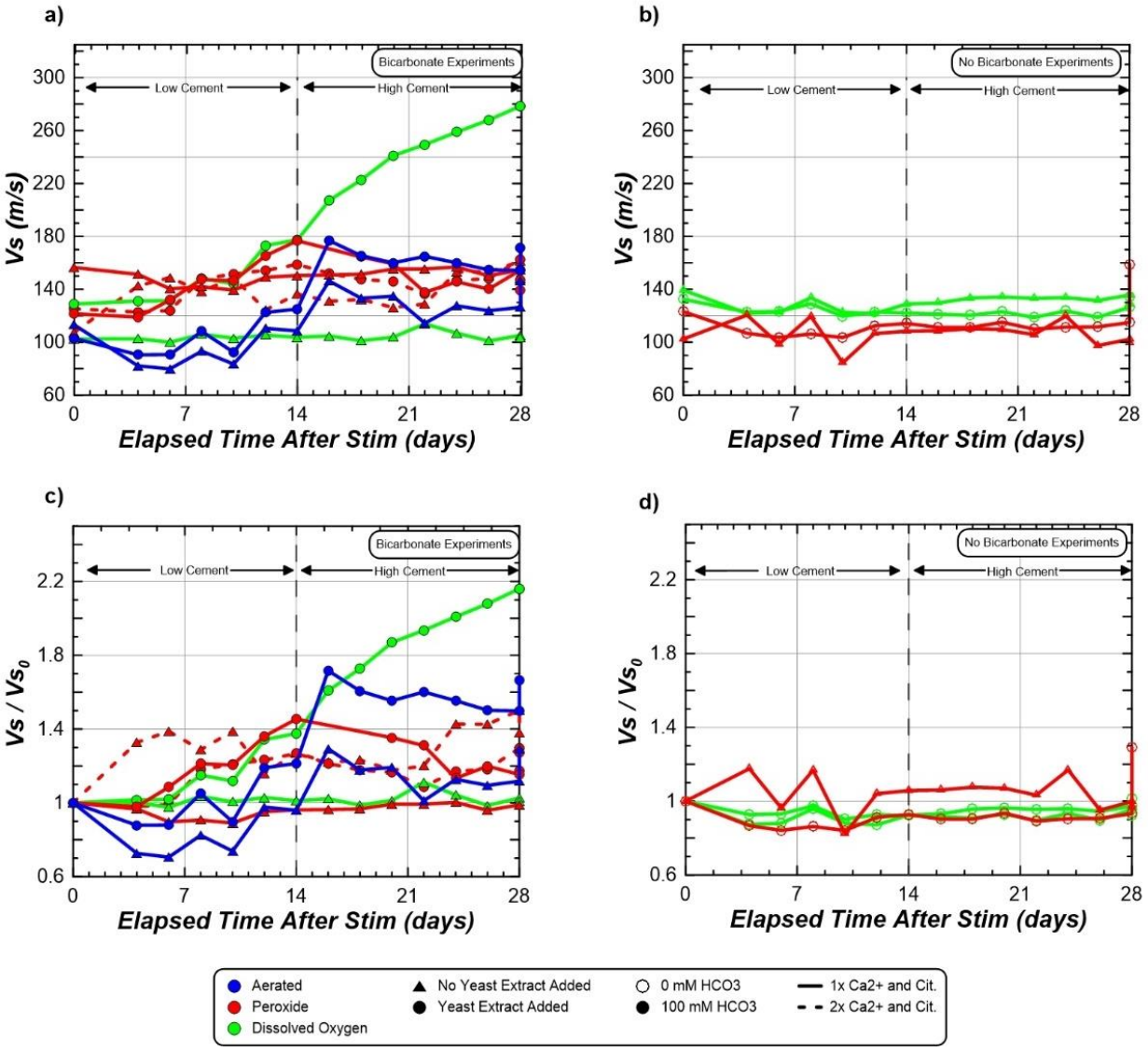

Figure 3.18. Comparisons of **(a, b)** soil shear wave velocities (Vs) and **(c, d)** normalized soil shear wave velocity (Vs/Vs0) versus time after stimulation for all citrate oxidation soil columns. Plots present data for all columns receiving solutions **(a, c)** with 100 mM sodium bicarbonate and **(b, d)** without sodium bicarbonate separately.

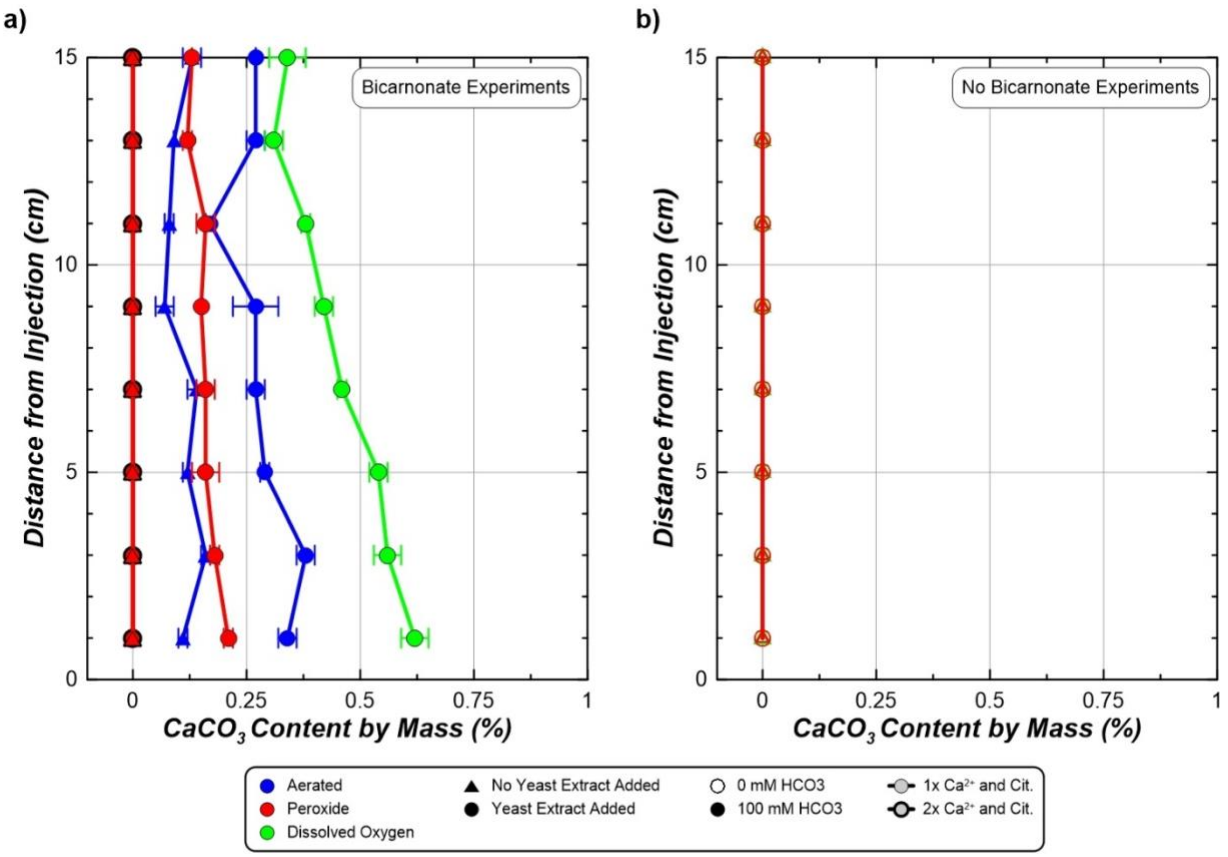

Figure 3.19. Comparisons of soil CaCO3 contents (in % by mass) versus distance from the injection source along all columns receiving solutions **(a)** with 100 mM sodium bicarbonate and **(b)** without sodium bicarbonate. Values indicate the average of three soil $CaCO_3$ content measurements for each location with error bars indicating ± one standard deviation for measurements.

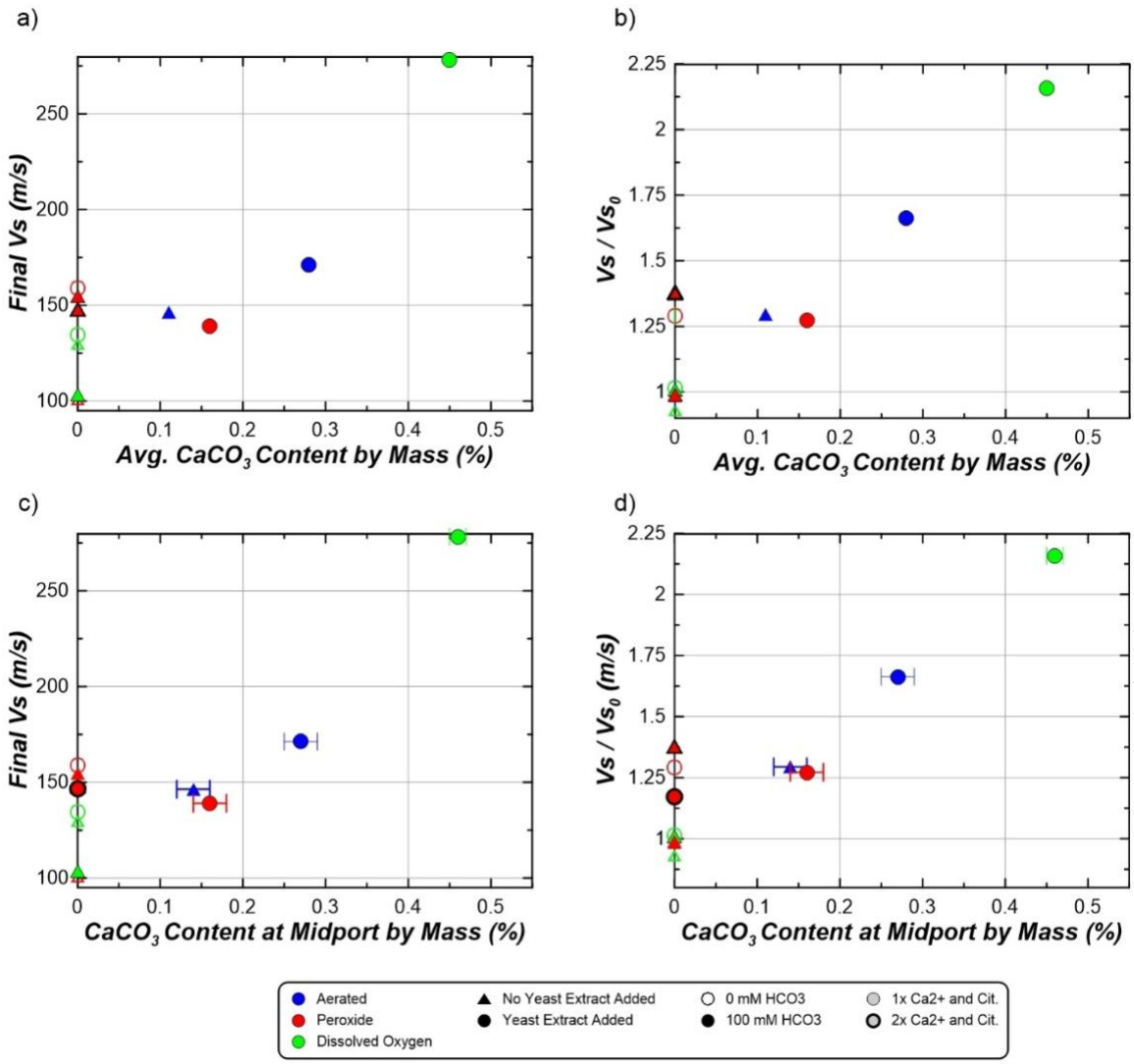

Figure 3.20. Relationships between soil CaCO3 contents and final Vs measurements for all citrate oxidation columns. Comparisons present **(a)** final Vs values versus average CaCO3 contents for entire columns, **(b)** normalized final V_s ratios compared to average $CaCO_3$ contents for entire columns, **(c)** final V_s values versus soil $CaCO_3$ contents at the mid-port bender locations for each column, and **(d)** normalized final V_s ratios versus soil $CaCO_3$ contents at the mid-port bender locations for each column.

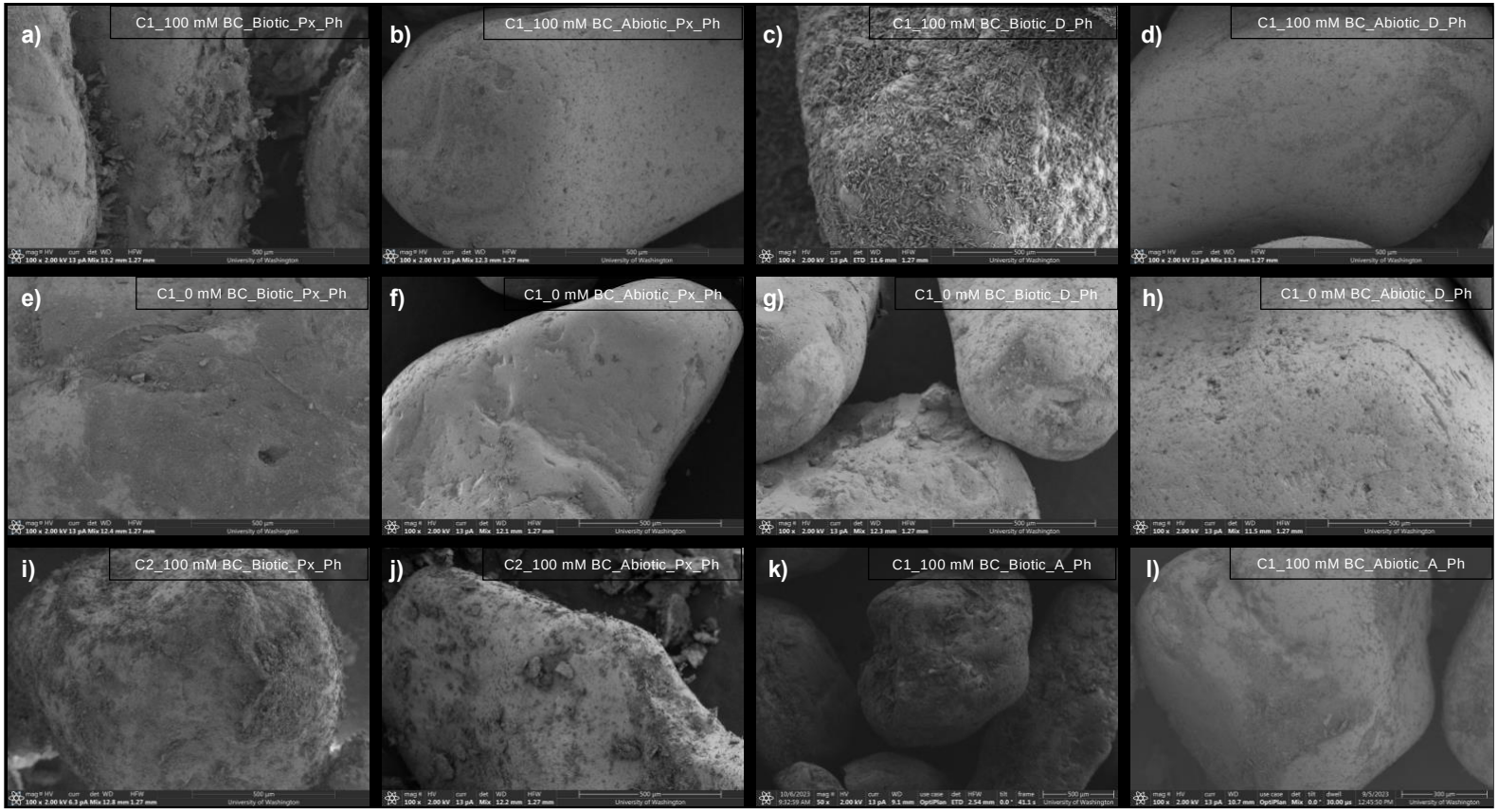

Figure 3.21. Scanning Electron Microscope (SEM) images of specimens obtained from the bottom 2 cm of all citrate oxidation columns. Images are presented for columns: **(a)** C1_100 mM BC_Biotic_Px_Ph, **(b)** C1_100 mM BC_Abiotic_Px_Ph, **(c)** C1_100 mM BC_Biotic_D_Ph, **(d)** C1_100 mM BC_Abiotic_D_Ph, **(e)** C1_0 mM BC_Biotic_Px_Ph, **(f)** C1_0 mM BC_Abiotic_Px_Ph, **(g)** C1_0 mM BC_Biotic_Px_Ph, **(h)** C1_0 mM BC_Abiotic_Px_Ph, **(i)** C2_100 mM BC_Biotic_Px_Ph, **(j)** C2_100 mM BC_Abiotic_Px_Ph, **(k)** C1_100 mM BC_Biotic_A_Ph, and **(l)** C1_100 mM BC_Abiotic_A_Ph.

Figure 3.22. Images of the final conditions for all citrate oxidation columns. Images are presented for columns: **(a)** C1_100 mM BC_Biotic_Px_Ph, **(b)** C1_100 mM BC_Abiotic_Px_Ph, **(c)** C1_100 mM BC_Biotic_D_Ph, (d) C1_100 mM BC_Abiotic_D_Ph, **(e)** C1_0 mM BC_Biotic_Px_Ph, **(f)** C1_0 mM BC_Abiotic_Px_Ph, **(g)** C1_0 mM BC_Biotic_Px_Ph, **(h)** C1_0 mM BC_Abiotic_Px_Ph, **(i)** C2_100 mM BC_Biotic_Px_Ph, **(j)** C2_100 mM BC_Abiotic_Px_Ph, **(k)** C1_100 mM BC_Biotic_A_Ph, and **(l)** C1_100 mM BC_Abiotic_A_Ph

Chapter 4: CONCLUSIONS

Microbial organic acid oxidation (MOAO) presents a promising alternative to ureolytic MICP for soil improvement, among other possible applications. The process relies on heterotrophic soil bacteria which can metabolize supplied organic acids, such as acetate or citrate, in the presence of an electron acceptor, such as oxygen, thereby generating aqueous carbonate species that can supersaturate soil solutions with respect to $CaCO_3$ when sufficient calcium is present and initiate calcium carbonate precipitation. Although MOAO was shown to require significantly longer treatment times than ureolytic MICP, owing to the much lower calcium concentrations that were applied as well as slower oxidation reactions than ureolysis, and the process is constrained by available oxygen, the pathway may offer important practical advantages by eliminating produced ammonium by-products. In this study, both batch and soil column experiments were performed to assess the potential of acetate and citrate oxidation to enable biocementation and achieved varying success. In particular, the successful generation of $CaCO_3$ was found to depend on the particular organic acids supplied, their concentrations, supplied oxygen availability, solution bicarbonate additions, and supplied solution growth factors, among other differences. From these results, the following main conclusions can be made:

- During acetate oxidation columns, the effect of both phased and concurrent injections were examined, wherein either columns received stimulation injections prior to receiving cementation injections (phased) or only cementation injections (concurrent). Although it was expected that phased columns would have higher microbial activity during all treatments due to microbial enrichment prior to cementation, observed calcium degradation,

$CaCO_3$ mineral formation, and V_s behaviors showed no significant difference between the two methods. Interestingly, Column A_100 mM HCO_3_Biotic_A_C actually showed significantly more $CaCO_3$ at the base of the column than its phased counterpart (Column A_100 mM HCO_3_Biotic_A_Ph), which was counter to the expected trend and may suggest that enrichment in the presence of calcium may be beneficial. In the citrate oxidation experiments, all columns received phased treatments and thus the effect of concurrent versus phased treatments may still merit further investigation.

- Treatment solutions employed in both the acetate and citrate oxidation soil columns were designed following earlier results from batch experiments and accordingly included similar initial concentrations of supplied calcium and citrate / acetate. When applying these same solutions to soil columns, however, only minimal improvements were observed. However, acetate / citrate and calcium concentration increases experienced by all soil column experiments during the latter phase of cementation resulted in greater improvement and suggested that applied solution concentrations may be increased above 50 mM calcium and 100 mM acetate / citrate. Such increases may have detrimental effects on enriched microbial activity over time, however, as indicated by more minimal activity observed in select columns near the end of cementation. Increasing reagent concentrations initially during cementation was also examined during citrate oxidation experiments, however, this appeared to result in more minimal $CaCO_3$ precipitation and greater abiotic precipitation of calcium citrate. Moving forward, the use of higher concentrations may merit further consideration, particularly when using microbial acetate oxidation to mediate precipitation, wherein the potential for abiotic precipitation of calcium acetate is minimal at such concentrations.

- In the performed experiments, the effect of different oxygen sources were evaluated. In general aeration appeared to enable significant MOAO activity in both citrate and acetate experiments with high activity also observed in the citrate experiments with dissolved oxygen. The addition of peroxide-based oxygen release compounds showed more variable results, however, likely due to the inhibition of microbial growth. Further work remains necessary to better understand the mechanisms responsible for the success and lack of success of select experiments receiving only dissolved oxygen or peroxide additions.
- In all columns receiving solutions containing yeast extract and achieving sufficient precipitation, the presence of bacteria was observed in SEM images wherein bacterial impressions were found on precipitate surfaces. This indicated that bacterial growth was enabled by supplied yeast extract, however, the presence of bacteria alone in these columns did not necessarily determine whether or not supplied acetate and citrate could be successfully oxidized. In acetate oxidation soil column experiments, the presence of bacterial growth only appeared to result in successful MOAO in select experiments (Column A_100 mM HCO_3_Biotic_A_C and Column A_100 mM HCO_3_Biotic_D_Ph). In citrate oxidation soil column experiments, however, citrate oxidation appeared to be present in nearly all citrate columns receiving solutions with yeast extract, with the precipitation of calcium citrate likely having only a minor effect on observed citrate degradation behaviors. While the precise role of bacterial activity in these systems is not fully understood, it is suspected that the greater improvement observed in the acetate and citrate columns receiving solutions containing both yeast extract and sodium bicarbonate may have been in part due to the presence of increased MOAO activity and related

carbonate species generation as well as the increased abundance of bacterial cells which may have served as nucleation sites for mineral formation on soil particle surfaces.

- In both acetate and citrate oxidation experiments, the addition of inorganic carbon in the form of sodium bicarbonate had a significant effect on achieved improvement as assessed by calcium degradation in time, soil $CaCO_3$ contents, and V_s increases. The presence of bicarbonate also appeared to significantly alter citrate degradation in time but had no detectable effects on acetate degradation. Although the particular mechanisms responsible for the greater improvement observed in the columns receiving solutions containing bicarbonate are not fully known, it is possible that the presence of bicarbonate may have buffered solution pH changes and promoted greater microbial activity, increased the magnitudes of abiotically-induced precipitation reactions, and/or enabled greater precipitation by MOAO activity which may have generated hydroxide increases but more minimal aqueous carbonate species. However, more minimal improvement observed in columns receiving bicarbonate-rich solutions but lacking yeast extract, suggest that at a minimum the presence of bacterial cells may play a role in the nucleation of mineral phases.
- In acetate oxidation experiments, all precipitate morphologies observed in SEM images appeared to be similar to that expected for calcium carbonate, however, crystal morphologies appeared to be more amorphous than that typically observed in ureolytic MICP-treated soils. In citrate oxidation experiments, calcium carbonate was detected, however, other unknown mineral phases were also observed which were expected to be likely calcium citrate (Zhong et. al. 2015) with needle-like morphologies. Further analysis of precipitates observed in both experiments using x-ray diffraction will likely provide

clarity regarding the specific minerals that were precipitated in these experiments and their relative abundances.

- In acetate oxidation experiments, soil column Vs values increased by up to 43 m/s, while citrate oxidation columns achieved a larger Vs increase of 171 m/s. Although these improvements are rather modest when compared to the larger improvements that can be afforded by ureolytic biocementation, these improvements may still significantly alter soil small-strain behaviors and liquefaction triggering resistances. Further investigations are needed, however, to better understand the mechanical enhancements afforded by MOAO biocementation processes, particularly at larger-strains.

While further research is needed to better understand the potential of MOAO biocementation pathways for subsurface applications, outcomes from this study suggest that the process may provide a viable alternative to ureolytic MICP when specific treatment strategies are employed. Moving forward, a more comprehensive comparison of the life cycle impacts of ureolytic and organic acid oxidation enabled MICP may provide further clarity regarding the potential advantages of the MOAO process. In particular, future research is needed to (1) better understand the enriched microbial communities present in these systems and the effect of solution composition on these enriched communities, (2) characterize the mineral phases resulting from these processes including the unknown minerals formed in the citrate oxidation experiments, (3) better understand the contribution of abiotic precipitation processes on the precipitation observed in soil columns receiving solutions with and without yeast extract, and (4) identify strategies through which a greater percentage of supplied calcium can be utilized for calcium carbonate precipitation. For example, in the best performing acetate and citrate columns it is estimated that only 53.2% and 38.6% of the supplied calcium was precipitated as calcium carbonate, respectively, providing a

significant opportunity for further optimization. Lastly, the success of experiments receiving solutions with bicarbonate additions suggests that the explored processes may present a significant opportunity to sequester carbon, while simultaneously offering an environmentally beneficial soil improvement alternative.

BIBLIOGRAPHY

ASTM (American Society for Testing and Materials). (2014). Standard test method for rapid determination of carbonate content of soils ASTM D4373-14. West Conshohocken, PA: ASTM.

Burdalski, R. J., Ribeiro, B. G. O., Gomez, M. G., and Gorman-Lewis, D. (2022). Mineralogy, morphology, and reaction kinetics of ureolytic bio-cementation in the presence of seawater ions and varying soil materials. Scientific Report, 12 (17100). https://doi.org/10.1038/s41598-022-21268-3

DeJong, J. T., M. B. Fritzges, and K. Nüsslein. (2006). Microbially induced cementation to control sand response to undrained shear. Journal of Geotechnical and Geoenvironmental Engineering, 132 (11), 1381-1392. https://doi.org/10.1061/(ASCE)1090-0241(2006)132:11(1381

DeJong, J. T., Mortensen, B. M., Martinez, B. C., & Nelson, D. C. (2010). Bio-mediated soil improvement. Ecological Engineering, 36(2), 197–210. https://doi.org/10.1016/j.ecoleng.2008.12.029

DeJong, J. T., M. G. Gomez, A. C. San Pablo, C. M. Graddy, D. C. Nelson, M. Lee, … and T. H. Kwon. (2022). "State of the Art: MICP soil improvement and its application to liquefaction hazard mitigation." *Proceedings of the 20th International Conference on Soil Mechanics and Geotechnical Engineering,* Sydney, Australia.,

El Kortbawi, M., Ziotopoulou, K., Gomez, M.G., and Lee, M. (2022). Mechanical Behaviour of Artificially Cemented Sands: Experimental and Numerical Developments. Canadian Geotechnical Journal, (Under Review).

Ersan, Y. C. (2018). Overlooked strategies in exploitation of microorganisms in the field of building materials. In Ecological Wisdom Inspired Restoration Engineering. Singapore: Springer Nature Singapore, 19-45.

Fahimizadeh, M.,P. Pasbaksh, L. S. Mae, J. B. L. Tan, and R. S. Raman. (2022). Multifunctional, sustainable, and biological non-ureolytic self-healing systems for cement-based materials. Engineering, 13. 10.1016/j.eng.2021.11.016

Ferris, F. G., Stehmeier, L. G., Kantzas, A., & Mourits, F. M. (1996). Bacteriogenic Mineral Plugging. Journal of Canadian Petroleum Technology, 35(08). https://doi.org/10.2118/96-08-06

Ganendra, G., Mercado-Garcia, D., Hernandez-Sanabria, E., Boeckx, P., Ho, A., and Boon, N. (2015). Methane biofiltration using autoclaved aerated concrete as the carrier material. Appl Microbiol Biotechnol (99), 7307-7320. https://doi.org/10.1007/s00253-015-6646-6

Graddy, C. M., M. G. Gomez, L. M. Kline, S. R. Morrill, J. T. DeJong, and D. C. Nelson. (2018). Diversity of sporosarcina-like bacterial strains obtained from meter-scale augmented and stimulated biocementation experiments. Environmental Science & Technology, 52 (7), 3997-4005. 10.1021/acs.est.7b04271

Gomez, M. G., C. M. Graddy , J. T. DeJong, D. C. Nelson, and M. Tsesarsky. (2018). Stimulation of native microorganisms for biocementation in samples recovered from field-scale treatment depths. Journal of Geotechnical and Geoenvironmental Engineering, 144 (1), 04017098. 10.1061/(ASCE)GT.1943-5606.0001804

Gomez, M. G., DeJong, J. T. & Anderson, C. M. (2018). Effect of Bio-cementation on Geophysical and Cone Penetration Measurements in Sands. Canadian Geotechnical Journal 55(11), 1632–1646. https://doi.org/10.1139/cgj-2017-0253

Gomez, M. G., & DeJong, J. T. (2017). Engineering Properties of Bio-Cementation Improved Sandy Soils Grouting. Technical Papers, ASCE, Reston, VA, 23–33 (2017). 10.1061/9780784480793.003

Hemayati, M., Nikooee, E., Habibagahi, G., Niazi, A., & Afzali, S. F. (2023). New non-ureolytic heterotrophic microbial induced carbonate precipitation for suppression of sand dune wind erosion. Scientific Reports , 13 (5845). https://doi.org/10.1038/s41598-023-33070-w

Jonkers, H. M., A. Thijssen, G. Muyzer, O. Copurogulu, and E. Schangen. (2010). Application of bacteria as self-healing agent for the development of sustainable concrete. Ecological Engineering, 36 (2), 230-235. https://doi.org/10.1016/j.ecoleng.2008.12.036

Konno K., Inoue T. A., & Nakamura M. (2014) Synergistic Defensive Function of Raphides and Protease through the Needle Effect. PLoS ONE 9(3): e91341. https://doi.org/10.1371/journal.pone.0091341

Lee, M., M. G. Gomez , A. C. San Pablo, C. M. Kolbus, C. M. Graddy, J. T. DeJong, and D. C. Nelson. (2019). Investigating ammonium by-product removal for ureolytic bio-cementation using meter-scale experiments. Scientific Reports, 9 (1), 1-15. 10.1038/s41598-019-54666-1

Lee, M., Gomez, M. G., El Kortbawi, M., & Ziotopoulou, K. (2022). Effect of Light Biocementation on the Liquefaction Triggering and Post-Triggering Behavior of Loose

Sands. Journal of Geotechnical and Geoenvironmental Engineering, 148(1), 04021170. https://escholarship.org/uc/item/00r7j9k4

Lee, M. and Gomez, M. G. (2023). Liquefaction Triggering and Post-Triggering Behavior of Biocemented Loose Sand. Canadian Geotechnical Journal, #######

Lee, M., & Gomez, M.G. (2023). Removal of Ammonium By-products Produced During Biocementation Soil Improvement Using Rinse Injection Strategies. Soil Use and Management. https://doi.org/10.1111/SUM.12984

Meyer, F. D., Bang, S., Min, S., Stetler, L. D., & Bang, S. S. (2011). Microbially-Induced Soil Stabilization: Application of Sporosarcina pasteurii for Fugitive Dust Control. In Geotechnical Special Publication (2011), 409-418. American Society of Civil Engineers. 10.1061/41165(397)409

Mitchell, J. K., and Santamarina, J. C. (2005). Biological Considerations in Geotechnical Engineering. Journal of Geotechnical and Geoenvironmental Engineering 133(10), 1222-1233. https://doi.org/10.1061/(ASCE)1090-0241(2005)131:10(122

Montoya, B. M. & DeJong, J. T. Stress-strain behavior of sands cemented by microbially induced calcite precipitation. (2015) Journal of Geotechnical and Geoenviron. Engineering 141(6), 04015019. https://doi.org/10.1061/(ASCE)GT.1943-5606.0001302

Ribeiro B.G.O., and Gomez M.G. (2023). Dissolution behavior of ureolytic bio-cementation: physical experiments and reactive transport modeling. Journal of Geotechnical and Geoenviron. Engineering 149 (9), 04023071. https://doi.org/10.1061/JGGEFK.GTENG-11275

Rütting T., Boeckx P., Müller C., and Klemedtsson L. (2011). Assessment of the importance of dissimilatory nitrate reduction to ammonium for the terrestrial nitrogen cycle. Biogeosciences 8 (7), 1779–1791. https://doi.org/10.5194/bg-8-1779-201

Stocks-Fischer, S., J. K. Galinat, and S. S. Bang. (1999). Microbiological precipitation of CaCO3. *Soil Biology and Biochemistry*, 31 (11), 1563-1571. https://doi.org/10.1016/S0038-0717(99)00082-6

Zhong, L., Li, J., Gao, Y., Cao, W., Zhang, P. and Lai, X. (2015), Preparation and characterisation of calcium citrate wires. Micro Nano Letters., 10: 419-421. https://doi.org/10.1049/mnl.2015.0090

APPENDIX A: CHAPTER 3 SUPPLEMENTARY TABLES AND FIGURES

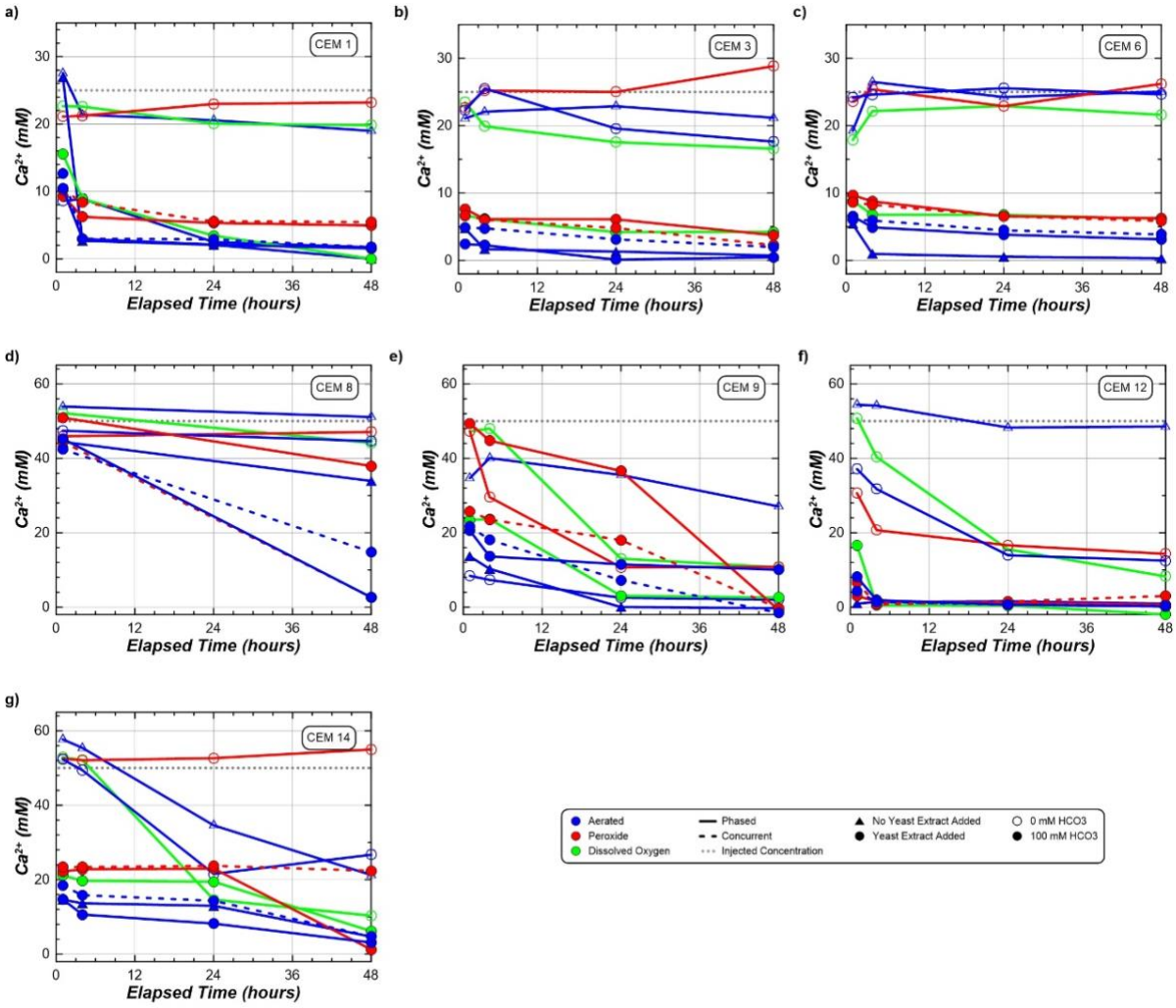

Supplemental Figure 3.1. Aqueous calcium measurements in time for all acetate oxidation columns during select cementation injections including cementation injection **(a)** 1, **(b)** 3, **(c)** 6, **(d)** 8 **(e)** 9, **(f)** 12, and **(g)** 14.

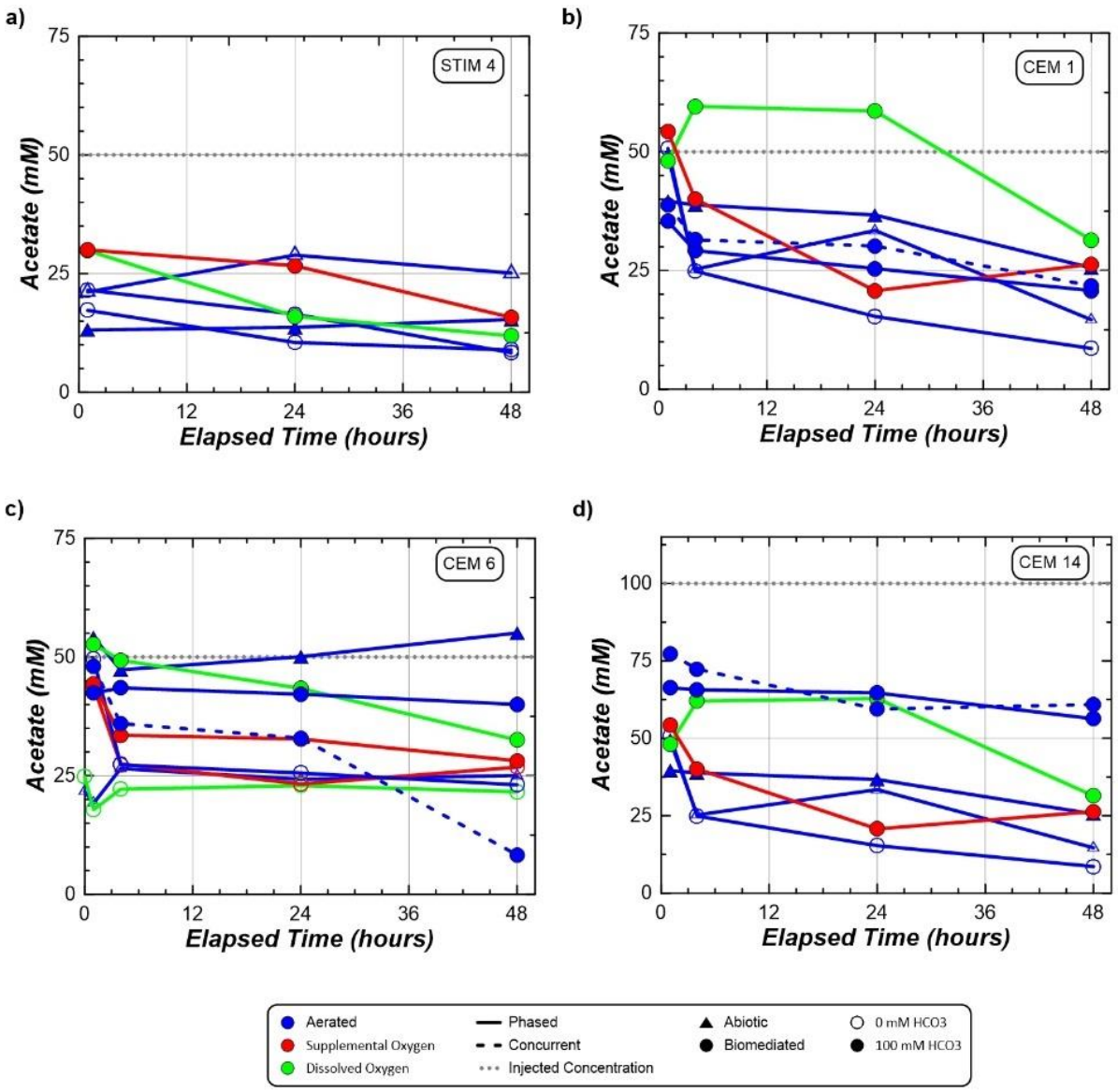

Supplemental Figure 3.2. Acetate measurements in time for select acetate oxidation columns for select treatment injections including: **(a)** stimulation injection 4 and cementation injections **(b)** 1, **(c)** 6, **(d)** and 14.

Supplemental Table 3.1. Initial shear wave velocity measurements (m/s) for all acetate oxidation soil columns prior to all treatment injections. Measurements were obtained immediately after saturation with deionized water.

Column Name	Initial Vs (m/s)
A_100 mM BC_Biotic_A_C	152.9
A_100 mM BC_Biotic_A_Ph	157.0
A_100 mM BC_Biotic_Px_C	127.5
A_100 mM BC_Biotic_Px_Ph	145.1
A_100 mM BC_Biotic_D_Ph	136.3
A_100 mM BC_Abiotic_A_Ph	147.2
A_0 mM BC_Biotic_A_Ph	146.6
A_0 mM BC_Biotic_Px_Ph	133.1
A_0 mM BC_Biotic_D_Ph	151.5
A_0 mM BC_Abiotic_A_Ph	151.4

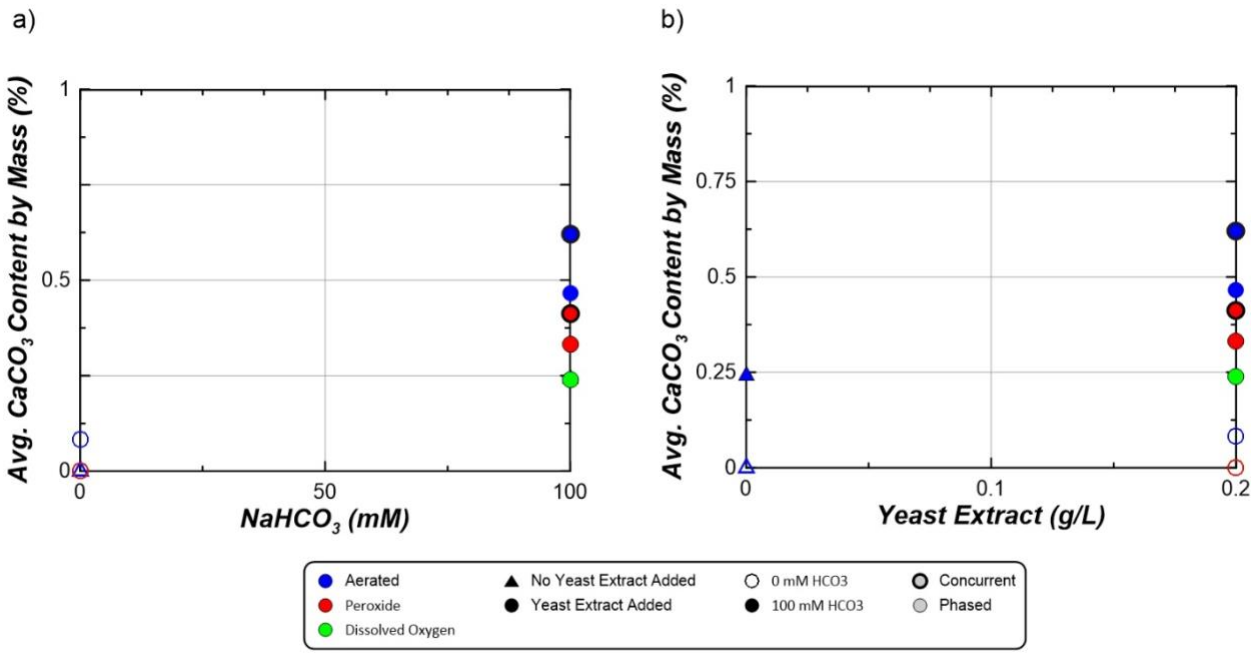

Supplemental Figure 3.3. Comparison of soil column average CaCO3 contents versus solution applied **(a)** bicarbonate concentrations (mM) and **(b)** yeast extract (g/L) for all acetate oxidation soil columns.

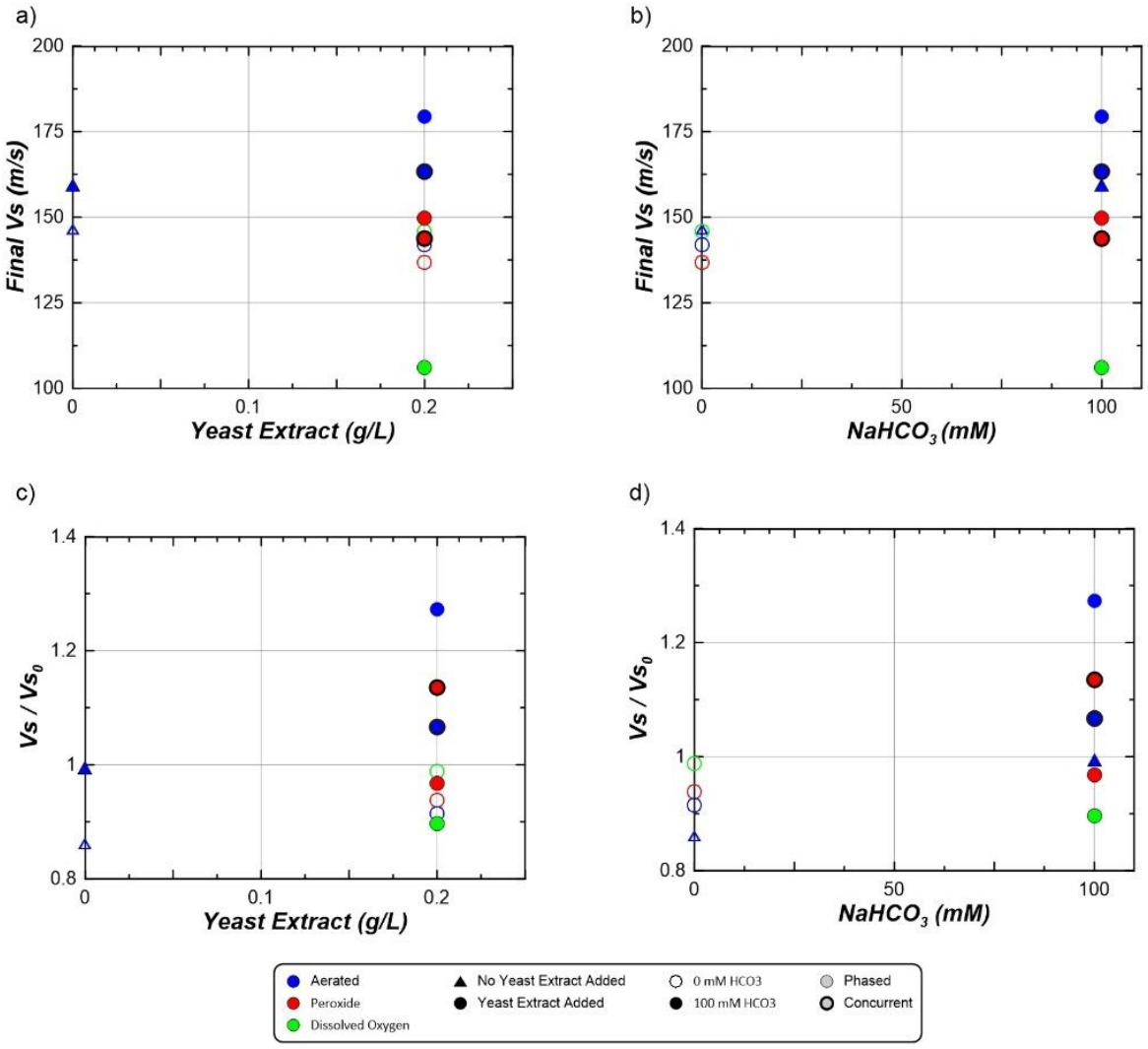

Supplemental Figure 3.4. Comparisons of **(a, b)** final shear wave velocities (Vs) and **(c, d)** normalized final Vs ratios versus applied solution **(a, c)** yeast extract and **(b, d)** bicarbonate concentrations for all acetate oxidation columns.

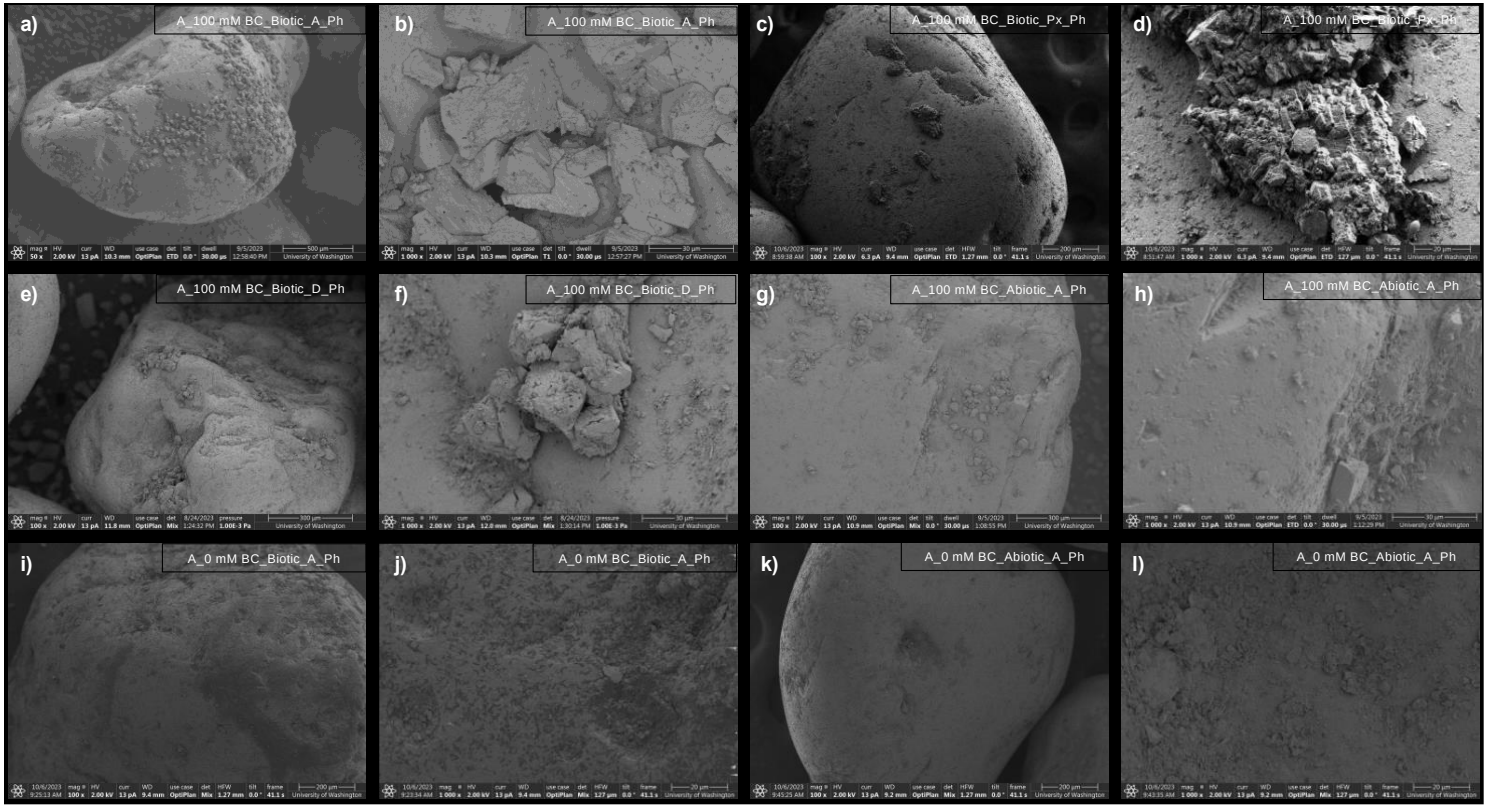

Supplemental Figure 3.5. Scanning Electron Microscope (SEM) images of specimens obtained from the bottom 2 cm of select acetate oxidation columns at various magnifications. Images are presented for columns: **(a)** A_100 mM BC_Biotic_A_Ph at 500µm scale, **(b)** A_100 mM BC_Biotic_A_Ph at 30µm scale, **(c)** A_100 mM BC_Biotic_Px_Ph at 200µm scale, **(d)** A_100 mM BC_Biotic_Px_Ph at 20µm scale, **(e)** A_100 mM BC_Biotic_D_Ph at 300µm scale, **(f)** A_100 mM BC_Biotic_D_Ph at 30µm scale, **(g)** A_100 mM BC_Abiotic_A_Ph at 300µm scale, **(h)** A_100 mM BC_Abiotic_A_Ph at 30µm scale, **(i)** A_0 mM BC_Biotic_A_Ph at 200µm scale, **(j)** A_0 mM BC_Biotic_A_Ph at 20µm scale, **(k)** A_0 mM BC_Abiotic_A_Ph at 200µm scale, and **(l)** A_0 mM BC_Abiotic_A_Ph at 20µm scale

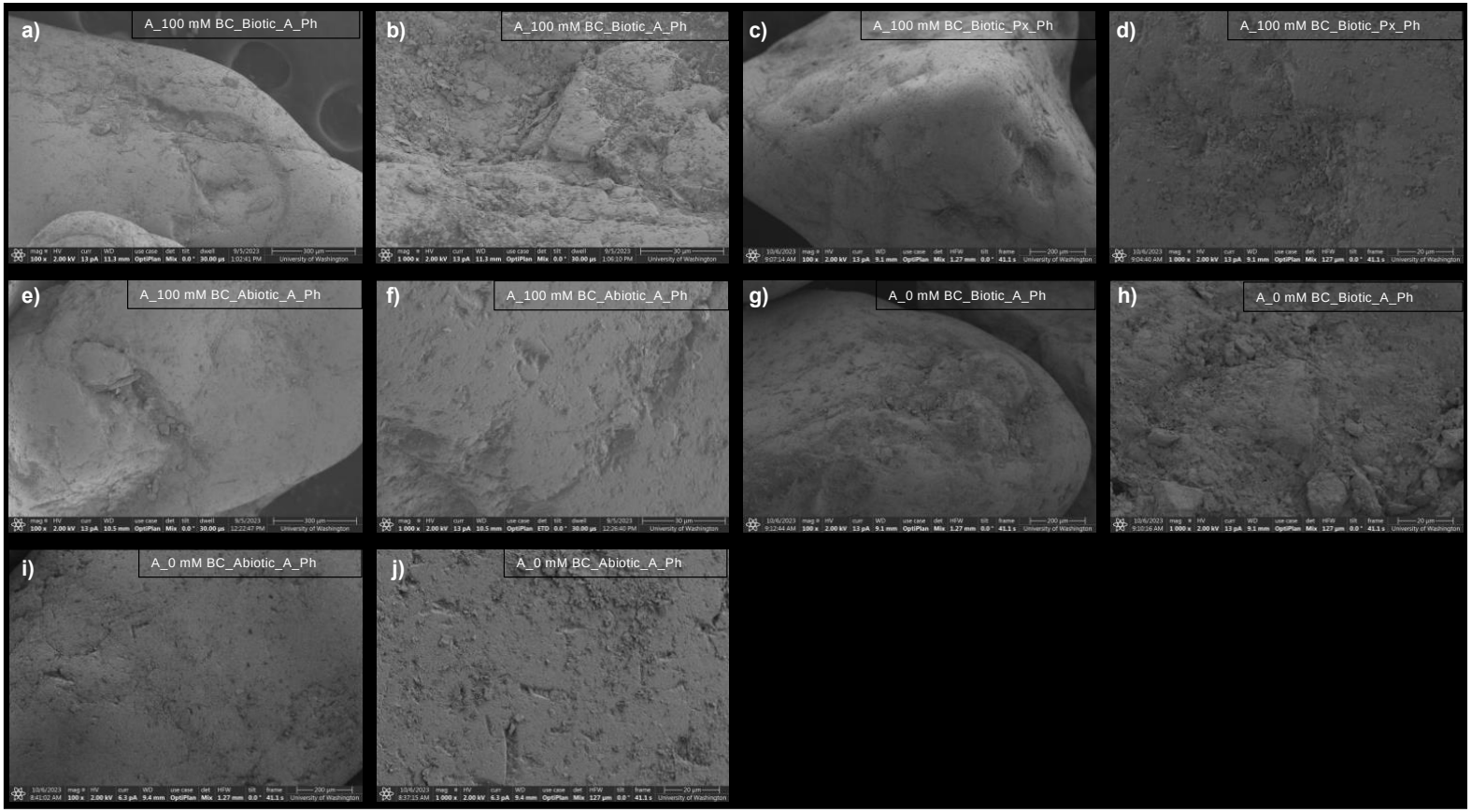

Supplemental Figure 3.6. Scanning Electron Microscope (SEM) images of specimens obtained from the top 2 cm of select acetate oxidation columns at various magnifications. Images are presented for columns: **(a)** A_100 mM BC_Biotic_A_Ph at 500µm scale, **(b)** A_100 mM BC_Biotic_A_Ph at 30µm scale, **(c)** A_100 mM BC_Biotic_Px_Ph at 200µm scale, **(d)** A_100 mM BC_Biotic_Px_Ph at 20µm scale, **(e)** A_100 mM BC_Abiotic_A_Ph at 300µm scale, **(f)** A_100 mM BC_Abiotic_A_Ph at 30µm scale, **(g)** A_0 mM BC_Biotic_A_Ph at 200µm scale, **(h)** A_0 mM BC_Biotic_A_Ph at 20µm scale, **(i)** A_0 mM BC_Abiotic_A_Ph at 200µm scale, and **(j)** A_0 mM BC_Abiotic_A_Ph at 20µm scale.

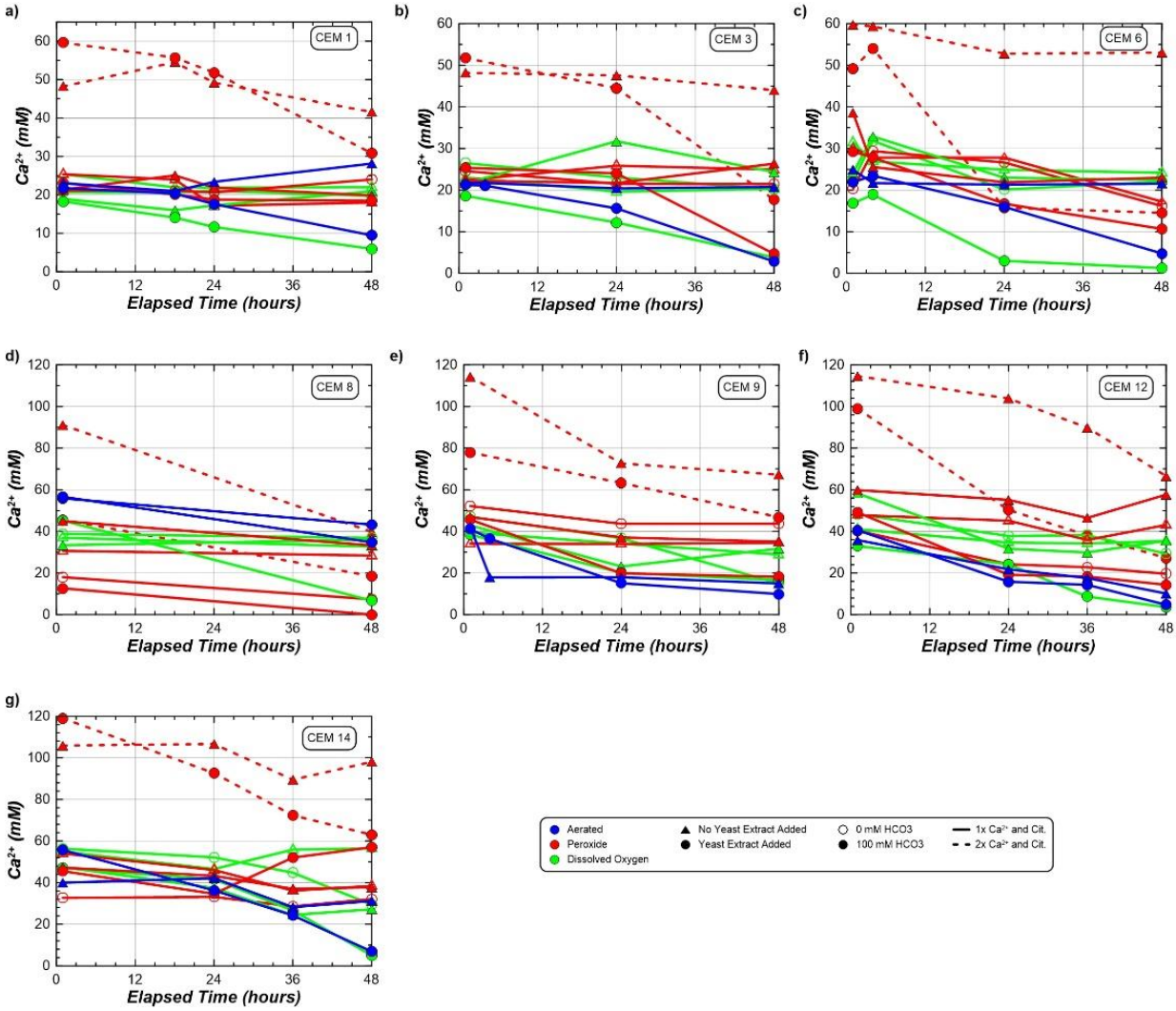

Supplemental Figure 3.7. Aqueous calcium measurements in time for all citrate oxidation columns during select cementation injections including cementation injection **(a)** 1, **(b)** 3, **(c)** 6, **(d)** 8, **(e)** 9, **(f)** 12, and **(g)** 14.

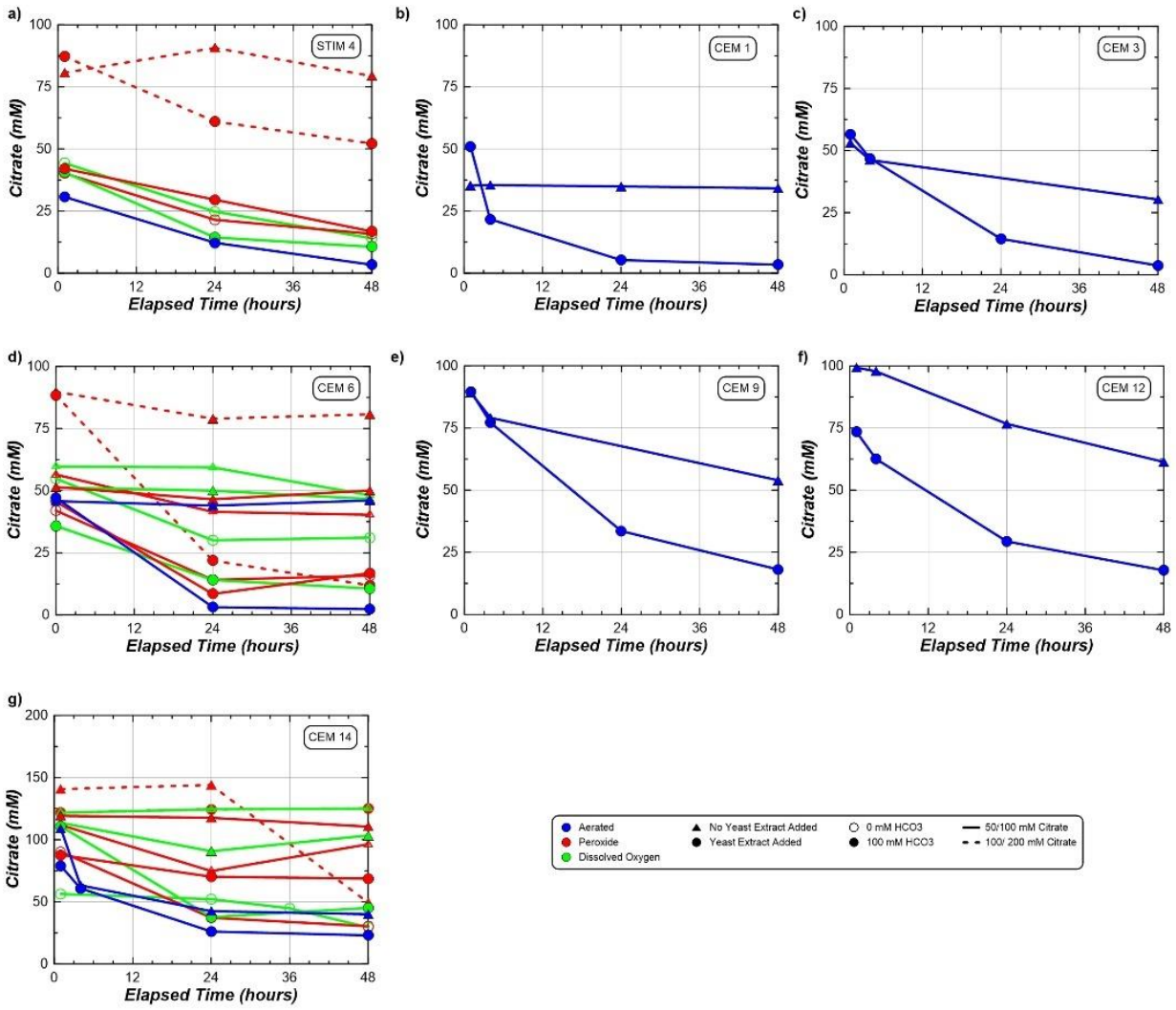

Supplemental Figure 3.8. Citrate measurements in time for select citrate oxidation columns for select treatment injections including: **(a)** stimulation injection 4 and cementation injections **(b)** 1, **(c)** 3, **(d)** 6, **(e)** 9, **(f)** 12, and **(g)** 14.

Supplemental Table 3.2. Initial shear wave velocity measurements (m/s) for all citrate oxidation soil columns prior to all treatment injections. Measurements were obtained immediately after saturation with deionized water.

Column Name	Initial Vs (m/s)
C1_100 mM BC_Biotic_A_Ph	143.2
C1_100 mM BC_Abiotic_A_Ph	145.8
C1_100 mM BC_Biotic_Px_Ph	154.4
C1_100 mM BC_Abiotic_Px_Ph	157.1
C1_100 mM BC_Biotic_D_Ph	157.8
C1_100 mM BC_Abiotic_D_Ph	142.04
C1_0 mM BC_Biotic_Px_Ph	156.55
C1_0 mM BC_Abiotic_Px_Ph	130.5
C1_0 mM BC_Biotic_D_Ph	155.5
C1_0 mM BC_Abiotic_D_Ph	142.0
C2_100 mM BC_Biotic_Px_Ph	143.1
C2_100 mM BC_Abiotic_Px_Ph	158.7

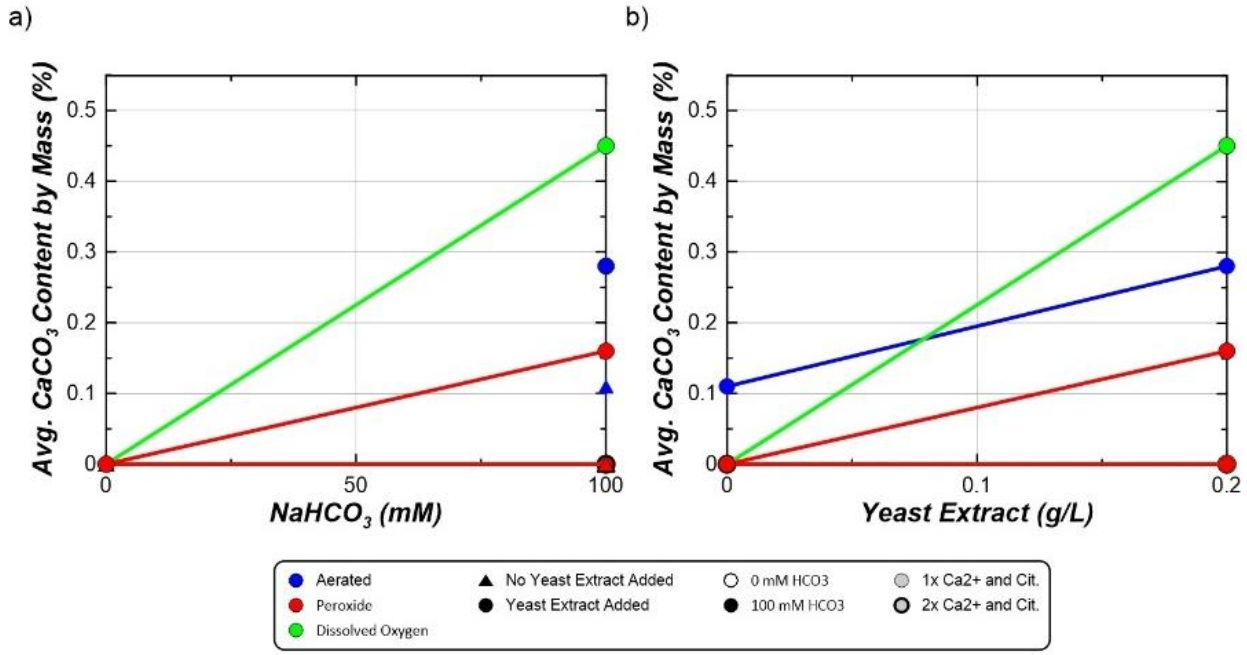

Supplemental Figure 3.9. Comparison of soil column average CaCO3 contents versus solution applied **(a)** bicarbonate concentrations (mM) and **(b)** yeast extract (g/L) for all citrate oxidation soil columns.

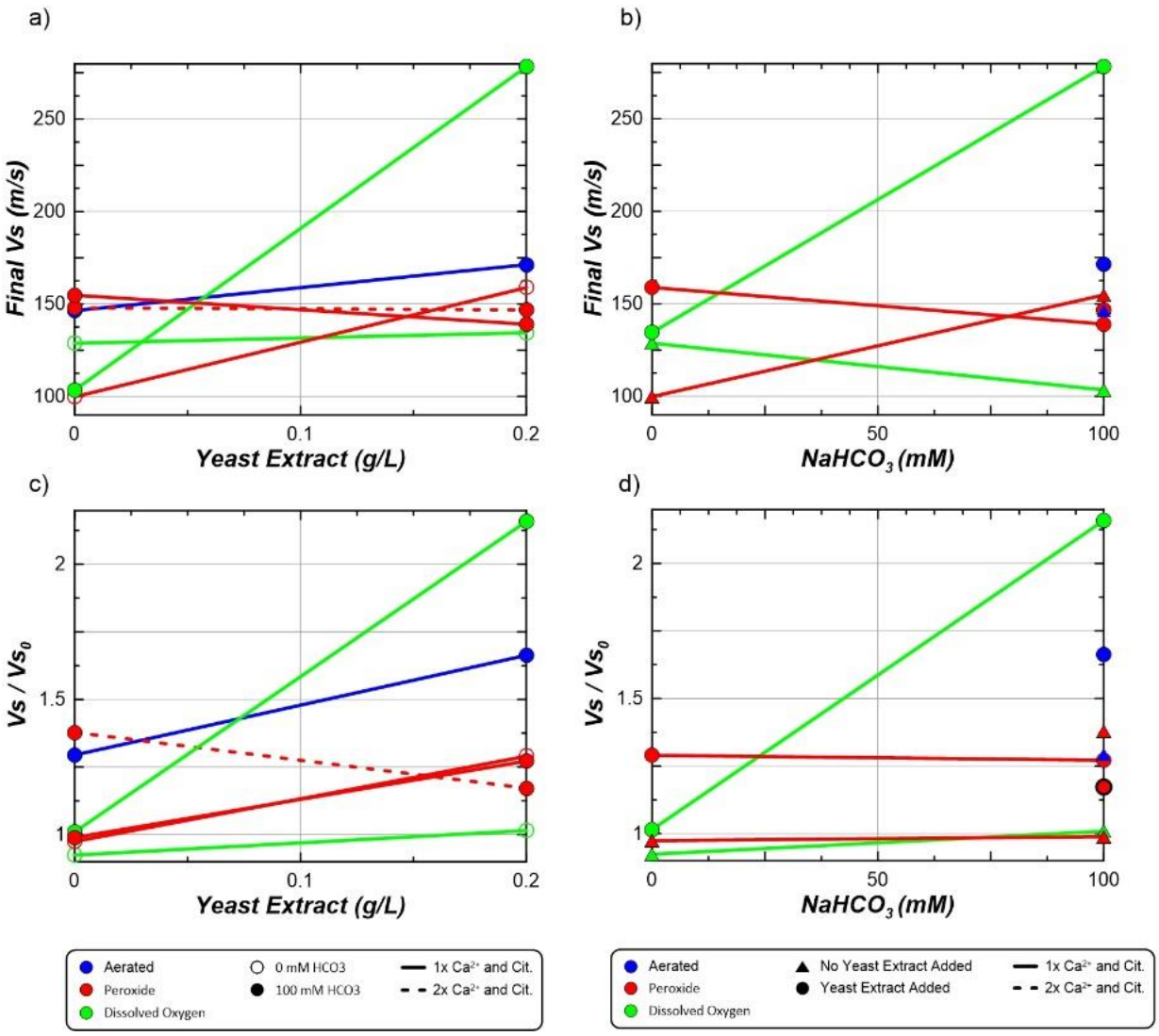

Supplemental Figure 3.10. Comparisons of **(a, b)** final shear wave velocities (Vs) and **(c, d)** normalized final Vs ratios versus applied solution **(a, c)** yeast extract and **(b, d)** bicarbonate concentrations for all citrate oxidation columns.

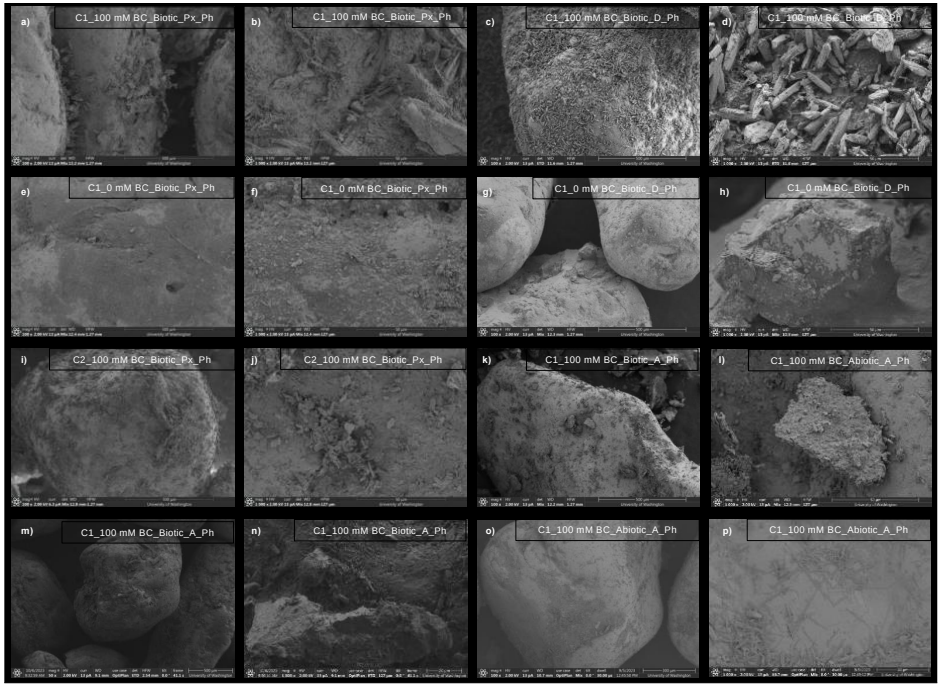

Supplemental Figure 3.11. Scanning Electron Microscope (SEM) images of specimens obtained from the bottom 2 cm of select citrate oxidation columns at various magnifications. Images are presented for columns: **(a)** C1_100 mM BC_Biotic_Px_Ph at 500µm scale, **(b)** C1_100 mM BC_Biotic_Px_Ph at 50µm scale, **(c)** C1_100 mM BC_Biotic_D_Ph at 500µm scale, **(d)** C1_100 mM BC_Biotic_D_Ph at 50µm scale, **(e)** C1_0 mM BC_Biotic_Px_Ph at 500µm scale, **(f)** C1_0 mM BC_Biotic_Px_Ph at 50µm scale, **(g)** C1_0 mM BC_Biotic_D_Ph at 500µm scale, **(h)** C1_0 mM BC_Biotic_D_Ph at 50µm scale, **(i)** C2_100 mM BC_Biotic_Px_Ph at 500µm scale, **(j)** C2_100 mM BC_Biotic_Px_Ph at 50µm scale, **(k)** C2_100 mM BC_Abiotic_Px_Ph at 500µm scale, **(l)** C2_100 mM BC_Abiotic_Px_Ph at 50µm scale, **(m)** C1_100 mM BC_Biotic_A_Ph at 500µm scale, **(n)** C1_100 mM BC_Biotic_A_Ph at 20µm scale, **(o)** C1_100 mM BC_Abiotic_A_Ph at 300µm scale, and **(p)** C1_100 mM BC_Abiotic_A_Ph at 30µm scale.

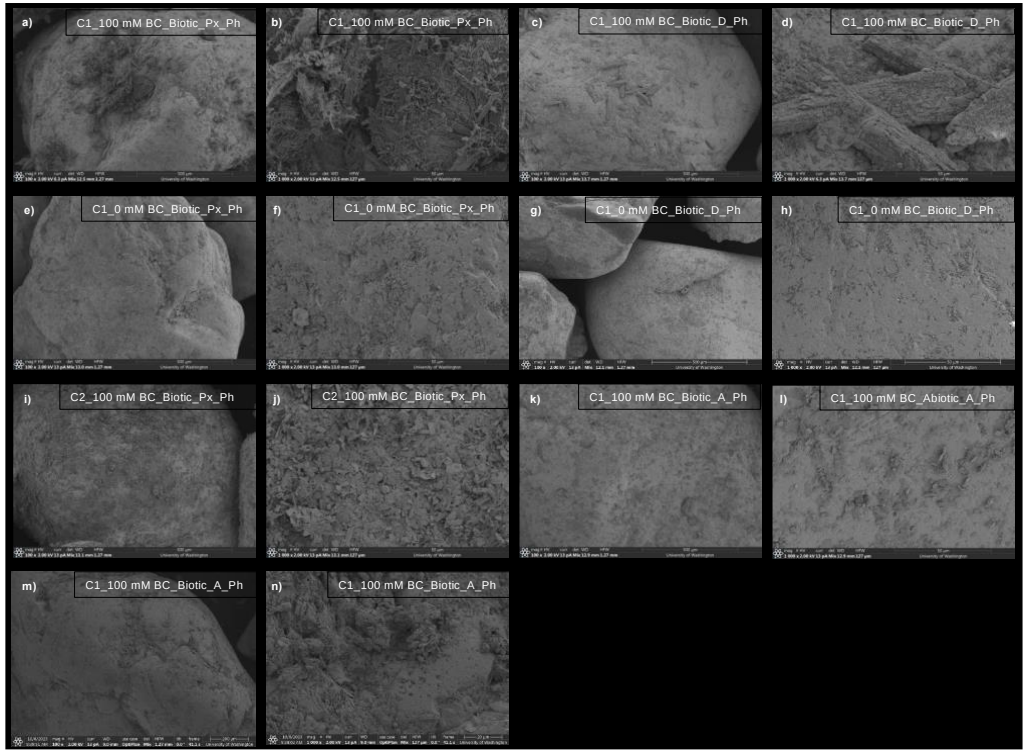

Supplemental Figure 3.12. Scanning Electron Microscope (SEM) images of specimens obtained from the top 2 cm of select citrate oxidation columns at various magnifications. Images are presented for columns: **(a)** C1_100 mM BC_Biotic_Px_Ph at 500µm scale, **(b)** C1_100 mM BC_Biotic_Px_Ph at 50µm scale, **(c)** C1_100 mM BC_Biotic_D_Ph at 500µm scale, **(d)** C1_100 mM BC_Biotic_D_Ph at 50µm scale, **(e)** C1_0 mM BC_Biotic_Px_Ph at 500µm scale, **(f)** C1_0 mM BC_Biotic_Px_Ph at 50µm scale, **(g)** C1_0 mM BC_Biotic_D_Ph at 500µm scale, **(h)** C1_0 mM BC_Biotic_D_Ph at 50µm scale, **(i)** C2_100 mM BC_Biotic_Px_Ph at 500µm scale, **(j)** C2_100 mM BC_Biotic_Px_Ph at 50µm scale, **(k)** C2_100 mM BC_Abiotic_Px_Ph at 500µm scale, **(l)** C2_100 mM BC_Abiotic_Px_Ph at 50µm scale, **(m)** C1_100 mM BC_Biotic_A_Ph at 500µm scale, and **(n)** C1_100 mM BC_Biotic_A_Ph at 20µm scale.

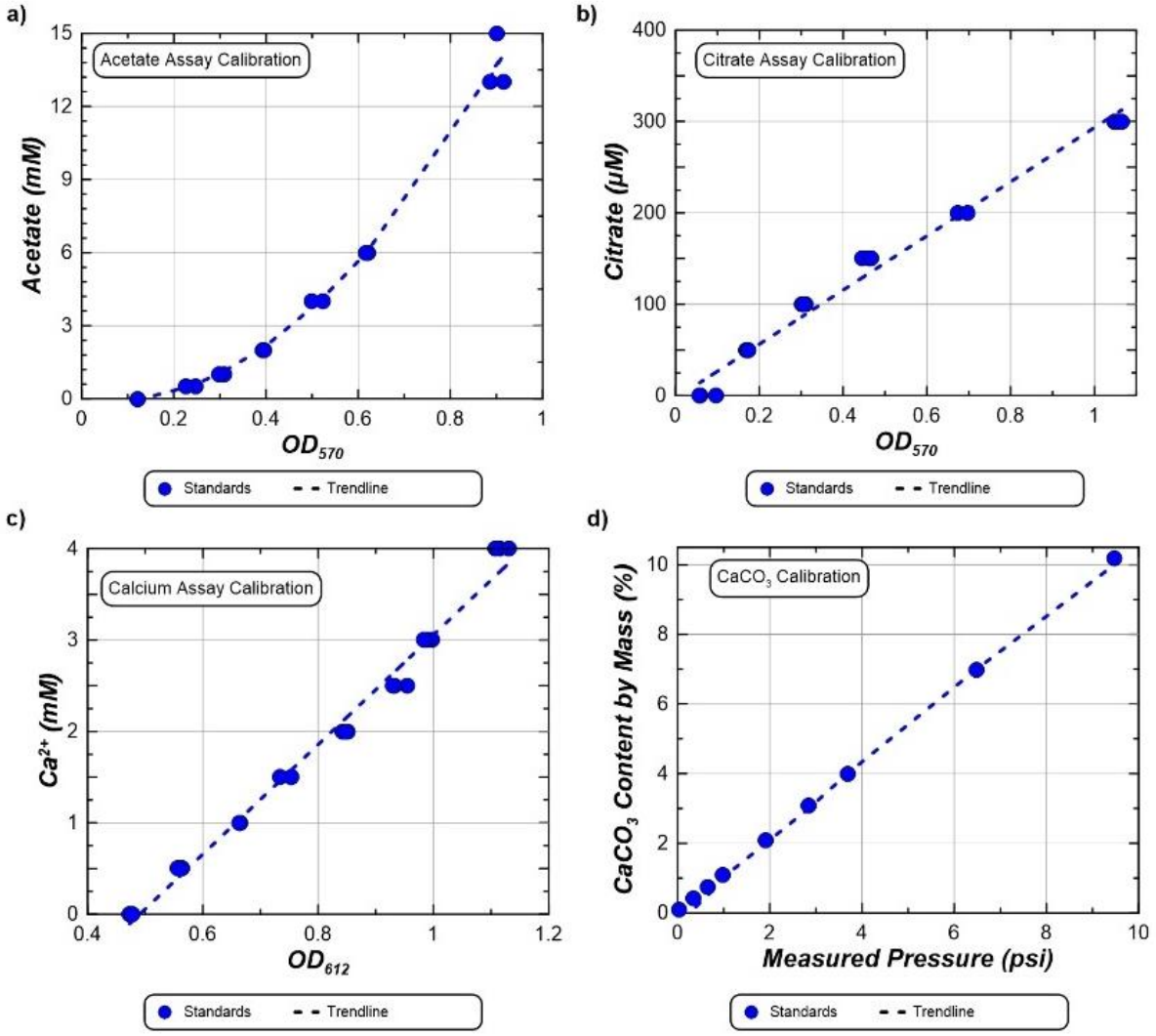

Supplemental Figure 3.13. Sample calibration curves consisting of optical density (OD) measurements versus **(a)** acetate, **(b)** citrate, and **(c)** calcium concentrations for all colorimetric assays as well as **(d)** a sample calibration curve for $CaCO_3$ content measurements consisting of soil $CaCO_3$ contents versus measured chamber pressures.